United States Department of the Interior

Geological Survey[1]

in cooperation with

Lawrence Berkeley Laboratory

University of California[2]

APPLICATION OF HEAT-FLOW TECHNIQUES TO GEOTHERMAL ENERGY EXPLORATION, LEACH HOT SPRINGS AREA, GRASS VALLEY, NEVADA

by

J. H. Sass[1], J. P. Ziagos[1], H. A. Wollenberg[2],

R. J. Munroe[1], D. E. di Somma[2], and A. H. Lachenbruch[1]

U.S. Geological Survey Open-File Report 77-762

LBL-6809

1977

Contents

Figures

Figures (continued)

Figures (continued)

Tables

Abstract

A total of 82 holes ranging in depth from 18 to 400 meters have been drilled for thermal and hydrologic studies in a 200 km^2 area of Grass Valley, Nevada, near Leach Hot Springs. Outside of the immediate area of Leach Hot Springs, heat flow ranges from 1 to 6.5 hfu with a mean of 2.4 hfu (1 hfu = 10^{-6} cal cm^2 s^{-1} = 41.8 mWm^{-2}). Within 2 km of the springs, conductive heat flow ranges between 1.6 and more than 70 hfu averaging 13.6 hfu. Besides the conspicuous thermal anomaly associated with the hot springs, two additional anomalies have been identified. One is associated with faults bounding the western margin of the Tobin Range near Panther Canyon, and the other is near the middle of Grass Valley about 5 km SSW of Leach Hot Springs. The mid-valley anomaly appears to be caused by hydrothermal circulation in a bedrock horst beneath about 375 meters of impermeable valley sediments. If the convective and conductive heat discharge within 2 km of the Leach Hot Springs is averaged over the entire hydrologic system (including areas of recharge), the combined heat flux from this part of Grass Valley is about 3 hfu, consistent with the average regional conductive heat flow in the Battle Mountain High. The hydrothermal system can be interpreted as being in a stationary stable phase sustained by high regional heat flow, and no localized crustal heat sources (other than hydrothermal convection to depths of a few kilometers) need be invoked to explain the existence of Leach Hot Springs.

INTRODUCTION

The region surrounding Leach Hot Springs in Grass Valley, Nevada (Figure 1) has been the object of a concerted geological, geochemical, and geophysical study by the Lawrence Berkeley Laboratory (LBL) of the University of California (Beyer and others, 1976; Wollenberg and others, 1975). LBL and the USGS have cooperated in studies of the geothermal and hydrologic regimes in the Leach, Kyle, and Buffalo Valley hot spring areas. Olmsted and others (1975) measured temperatures and flow rates from Leach Hot Springs, and they drilled 11 test holes within a radius of about 2 km of the springs as part of a regional hydrological appraisal of hydrothermal systems in northern Nevada. Discharge temperatures of the various spring orifices generally ranged from 70°C to greater than 90°C with some as low as ∿35°C (Olmsted and others, 1975). Source temperatures have been estimated by geochemical thermometry to be in the range 150°C to 180°C (Mariner and others, 1974), but application of the mixing-model equations of Fournier and others (1974) indicates that the source temperature may exceed 200°C (Beyer and others, 1976). Olmsted and others (1975) estimated heat fluxes from their test wells and found that heat flow decreases from >70 hfu (1 hfu = 1 heat-flow unit = 1 $\mu cal/cm^2\ s = 41.8\ mW/m^2$) near the springs to less than 2 hfu within 2 km of the springs. Sass and others (1976) measured heat flows ranging from 1.4 to 5.1 hfu in six deep (∿200 m) holes outside of the spring area, and about 9 hfu in QH-1 about 1 km from the springs (Figure 2). These

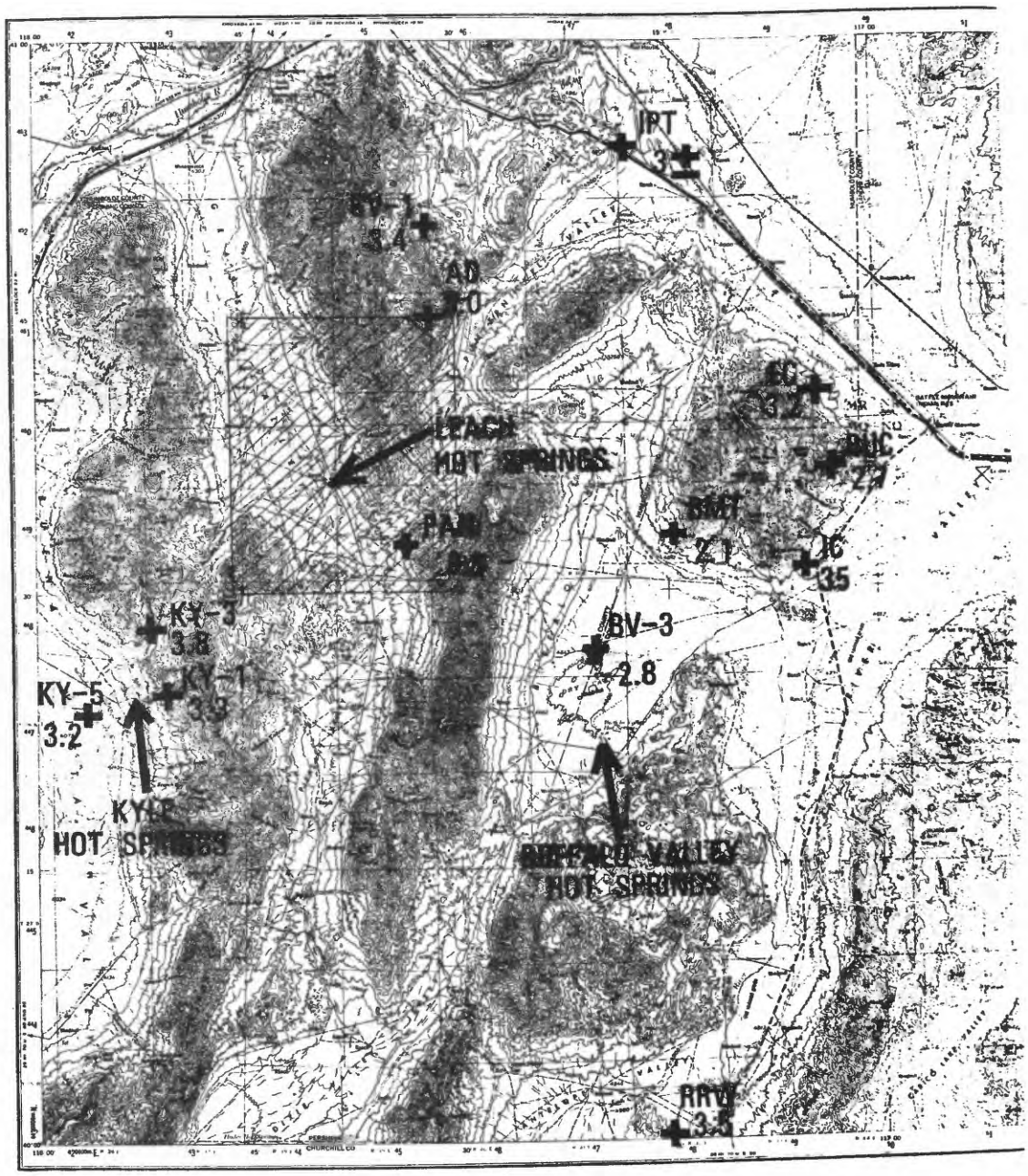

Figure 1. Topographic map showing major hot spring systems and regional heat-flow values (hfu) in relation to the Leach Hot Springs 15' quadrangle (shaded area).

results confirmed the high heat flow measured previously near Panther Canyon (PAN, Figure 1) and indicated that a complicated hydrothermal circulation system exists in Grass Valley outside of the Leach Hot Springs area itself.

The present work was undertaken to answer some of the questions posed by the earlier work of Olmsted and others (1975) and Sass and others (1976) and to delineate more fully the thermal features indicated in the earlier reconnaissance studies.

The following symbols and units are used frequently in the remainder of this report:

T, temperature °C

Γ, temperature gradient, °C/km

K, thermal conductivity, tcu, (mcal/cm s °C)

ϕ, porosity, % of voids, or fractional porosity

q, heat flow, hfu, (μcal/cm^2 s)

τ, time, s

R, coefficient of correlation, ($-1 < R < +1$)

The USGS Water Resources Division convention was used to specify site locations, i.e., 32/38-26bba represents NE 1/4, NW 1/4, NW 1/4, T32N, R38E, sec 26.

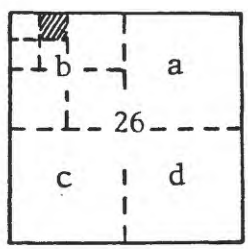

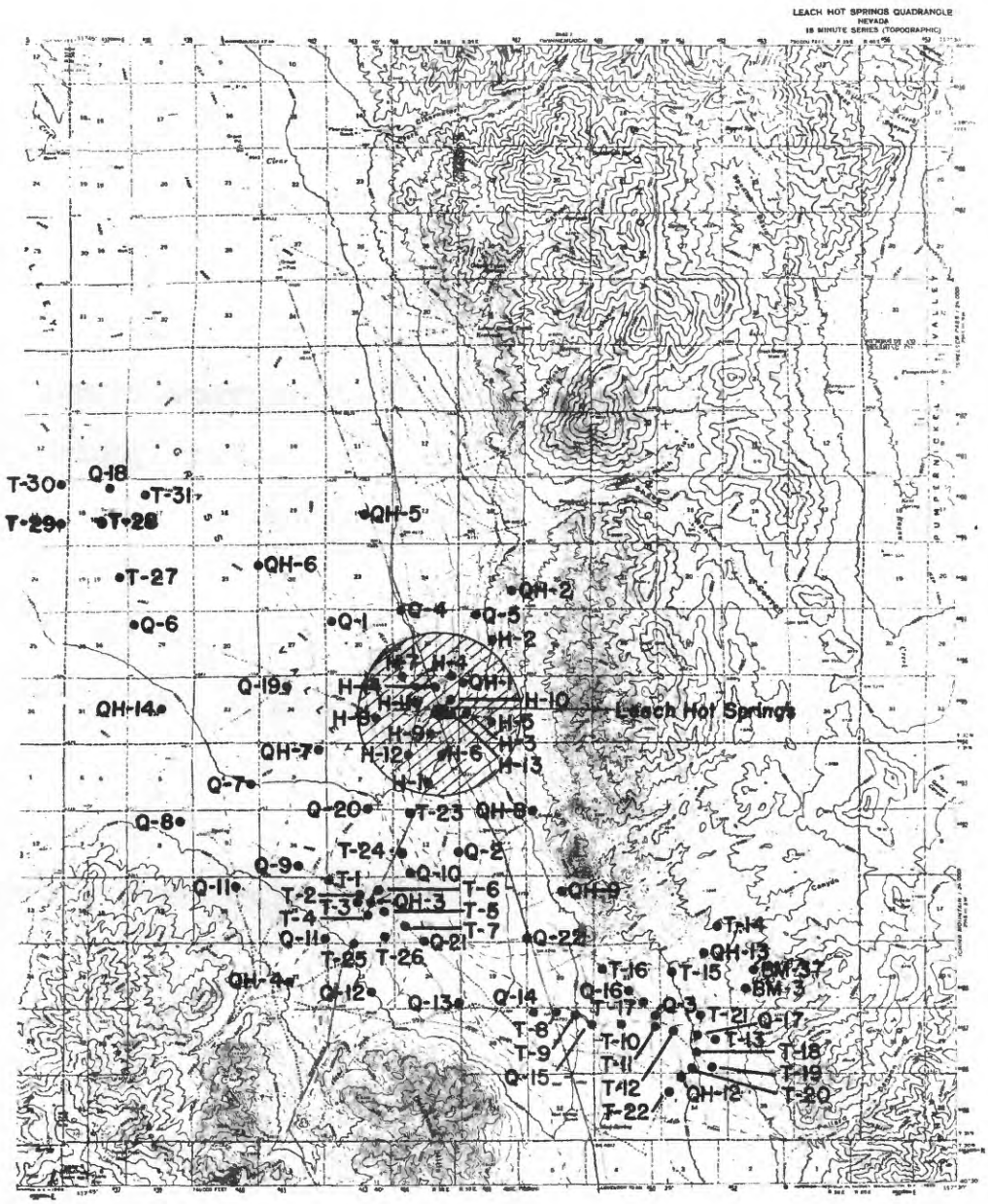

Figure 2. Leach Hot Springs 15' quadrangle showing locations of holes. Hole designations are explained in the text; shaded area outlines the area within 2 km of the springs.

GEOLOGIC SETTING

A bedrock geologic map of the Leach Hot Springs quadrangle (Figure 3) was compiled from observations by LBL personnel, reconnaissance mappings by Ferguson and others (1951), detailed mapping by Silberling (1975), Nichols (1972), and Snyder (personal communication), and air-photo interpretation by Noble (1975). Figures 4, 5, and 6 are the accompanying idealized cross sections E-E', H-H', and T-T' (see Figure 22 for locations of cross sections). Roberts and others (1958), Nichols (1972), and Silberman and McKee (1971) provided lithologic descriptions of the rock units.

Pre-Tertiary basement rocks, exposed in the Sonoma and Tobin Ranges in the eastern half of the quadrangle, and in the Goldbanks Hills in the southwestern part of the quadrangle, consist of Paleozoic eugeosynclinal and Mesozoic granitic, volcanic and migeosynclinal rocks.

Three units of Cambrian age crop out at the northern edge of the quadrangle. These are the Osgood Mountain formation, a thick, massively bedded quartzite; the Preble formation consisting of shale and micaceous shale; and the Harmony formation composed of feldspathic sandstone, arkose, and grit with some chert. The Preble and Harmony formations are in fault contact in the structurally complex Clearwater Canyon area in the northern part of the quadrangle. The Harmony formation is also exposed in the Goldbanks Hills where it is thrust over Havallah sequence rocks. The Ordovician Valmy formation also crops out in the Clearwater

Canyon area and consists of phyllitic argillite, greenstone and pure vitreous quartzite.

Most of the Sonoma and Tobin Ranges and the Goldbanks Hills are underlain by the Pennsylvanian-Permain Havallah sequence. The Havallah sequence is composed of the nearly indistinguishable Pumpernickel and Havallah formations which consist of bedded chert, siliceous argillite, greenstone, and sandstone.

The Koipato formation, of Permian-Triassic age, consists of devitrified rhyolitic and trachytic welded tuff and is exposed in parts of the Goldbanks Hills and in the Panther Canyon area between the Sonoma and Tobin Ranges. Three Triassic units are also exposed in the Panther Canyon area. These are the China Mountain formation, a conglomerate composed of chert and volcanic debris from underlying units, the Panther Canyon formation consisting of dolomite, conglomerate, mudstone, and sandstone, and the Augusta Mountain formation, a medium-thick bedded limestone with minor chert and silt.

These Paleozoic and Mesozoic units are intruded in the northern portion of the quadrangle by igneous rocks of acidic to intermediate composition and Mesozoic age. Rhyolitic and tuffaceous rocks of Tertiary age occur in scattered localities near Leach Hot Springs, in the Panther Canyon area, and at the northern boundary of the quadrangle. A sequence of sandstone, fresh water limestone, and layered tuffs, all of Tertiary age, crop out in small areas near Leach Hot Springs and underlie the Tertiary basalts in the Goldbanks Hills. The Tertiary

rhyolitic and sedimentary units are also present in the subsurface. Corase gravel of Quaternary-Tertiary age underlies the pediment to the east of Leach Hot Springs.

The intricate fault and lineament pattern in the area of Leach Hot Springs, based strongly on air-photo interpretation (Noble, 1975), is shown in Figure 29. Characteristic of hot spring systems observed in northern Nevada which are located on faults, Leach Hot Springs is located at the zone of intersection between a northeast trending fault, strongly expressed by a 10 to 15 meter high scarp, and NNW-SSE trending lineaments. Normal faulting since mid-Tertiary has offset rock units vertically several tens to several hundred meters (idealized cross section E-E', Figure 4).

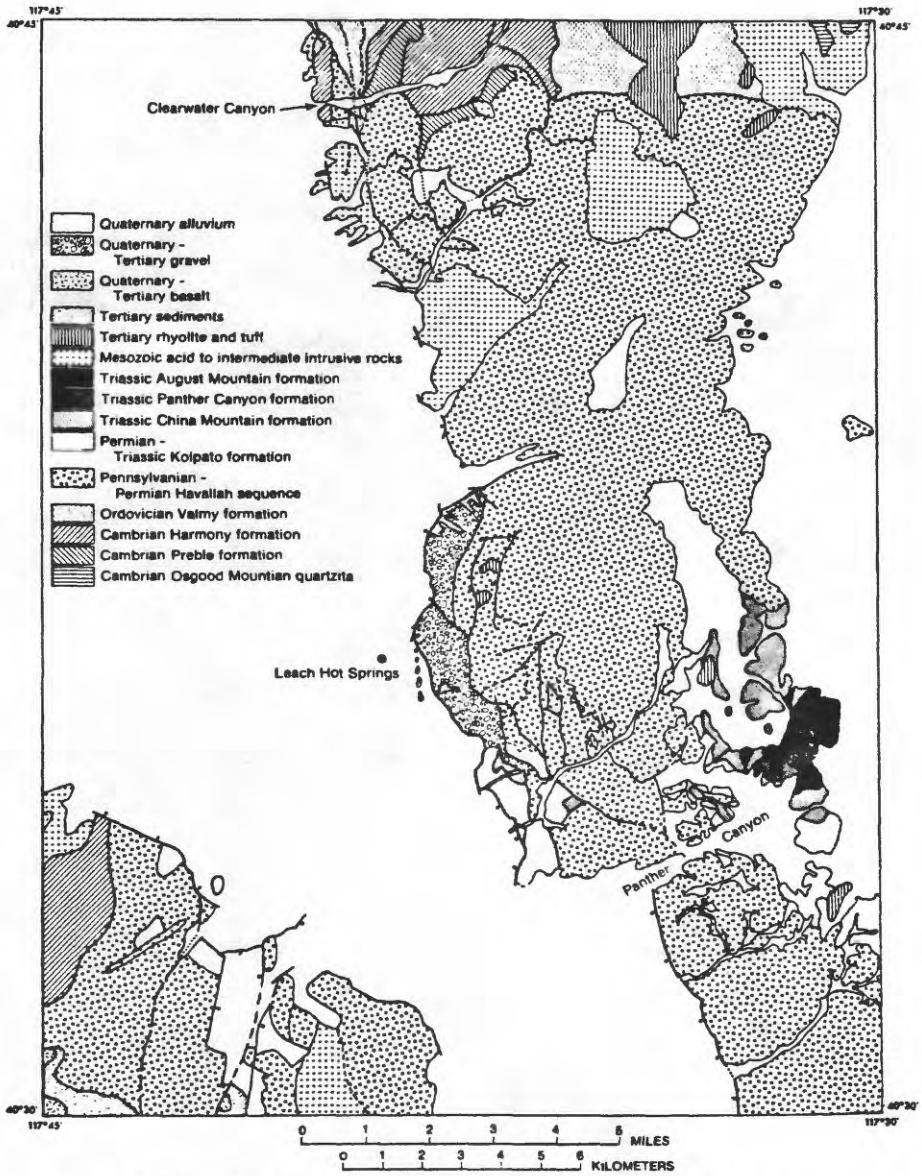

BEDROCK GEOLOGIC MAP OF LEACH HOT SPRINGS QUADRANGLE, NEVADA

XBL 778-1598

Figure 3

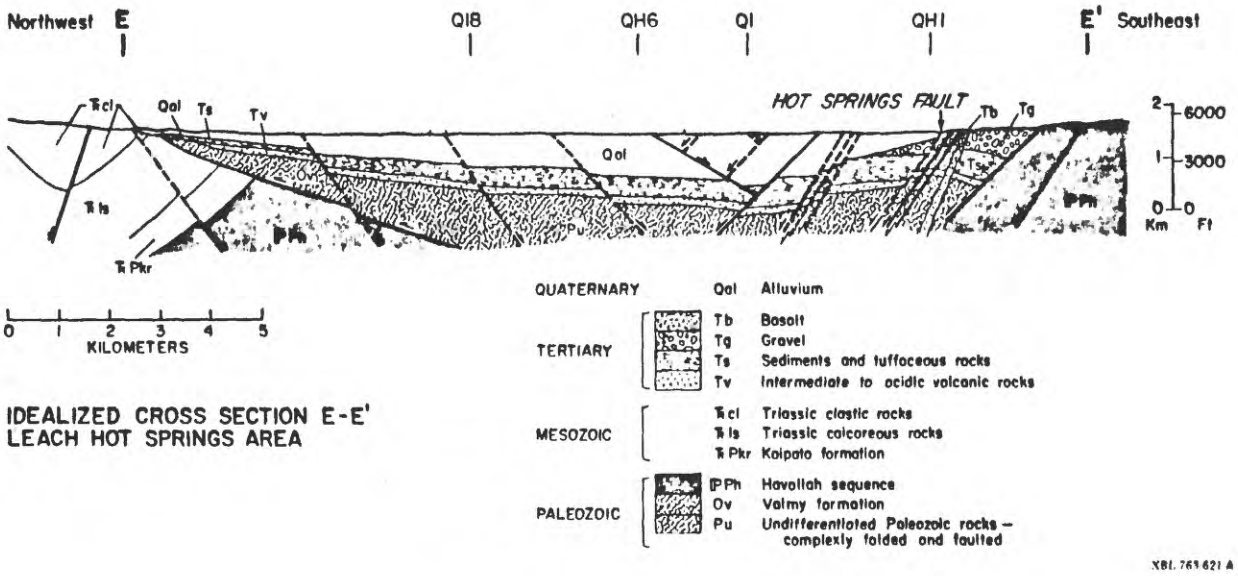

IDEALIZED CROSS SECTION E-E'
LEACH HOT SPRINGS AREA

Figure 4

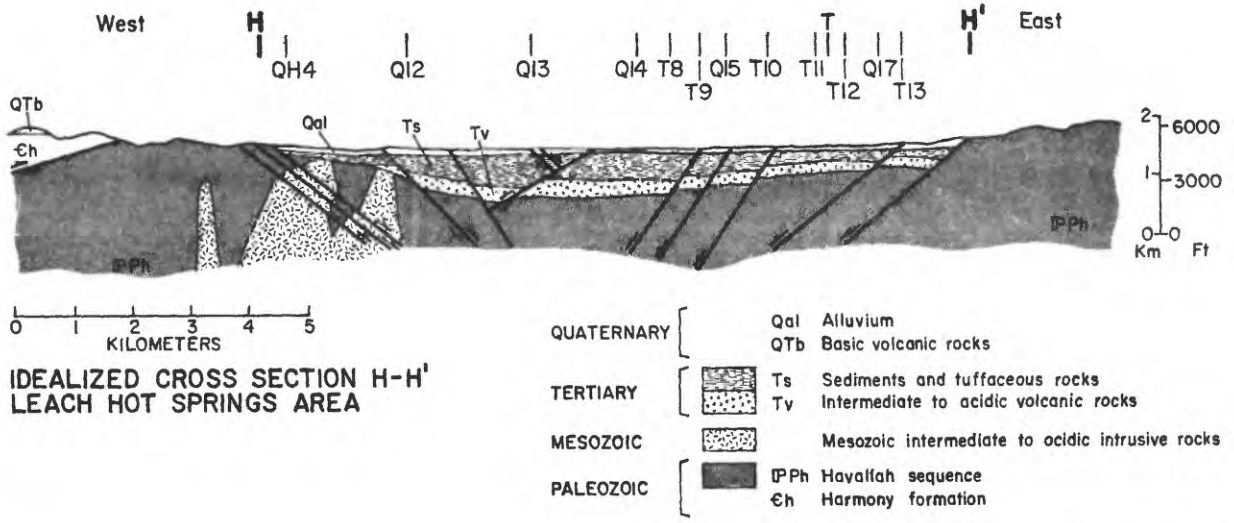

IDEALIZED CROSS SECTION H-H'
LEACH HOT SPRINGS AREA

XBL 762-2319 A

Figure 5

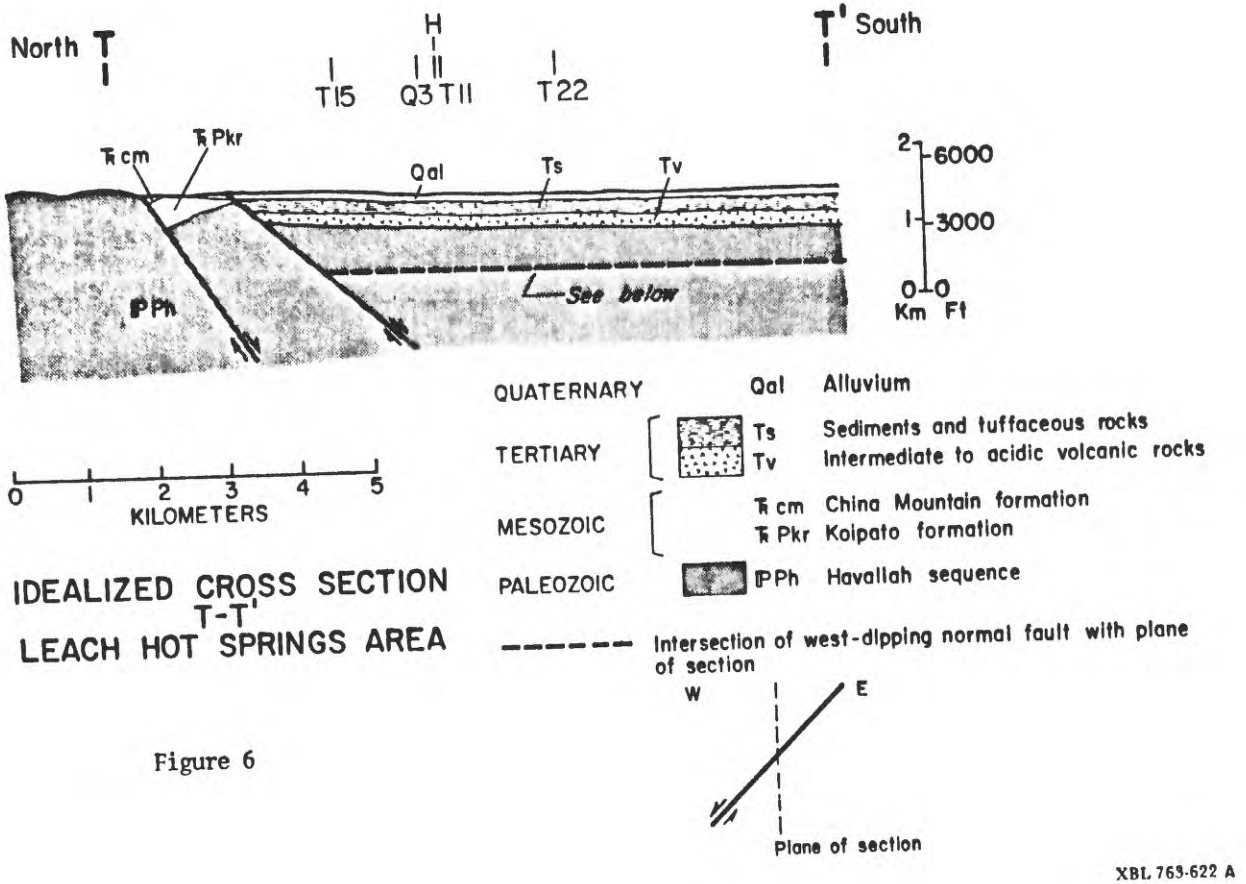
North T
H
T'
South
T15
Q3 T11
T22
Tk cm
Tk Pkr
Qal
Ts
Tv
PPh
See below
2
6000
1
3000
0
0
Km Ft
0 1 2 3 4 5
KILOMETERS
QUATERNARY
Qal
Alluvium
TERTIARY
Ts
Sediments and tuffaceous rocks
Tv
Intermediate to acidic volcanic rocks
MESOZOIC
Tk cm
China Mountain formation
Tk Pkr
Kolpato formation
PALEOZOIC
PPh
Havallah sequence
Intersection of west-dipping normal fault with plane of section
W
E
Plane of section
IDEALIZED CROSS SECTION
T-T'
LEACH HOT SPRINGS AREA
XBL 763-622 A

Figure 6

BOREHOLE TYPES

Five categories of boreholes are defined (Figure 2).

1) BM3 and BM37 were drilled through volcanic rocks and underlying basement rocks at the Big Mike Mine. Heat flows from these holes were published by Sass and others (1971b), and they formed part of the data set used to define the "Battle Mountain High."

2) Holes H-1 through H-15 are the hydrologic test wells drilled near the springs (see Olmsted and others (1975) for a detailed description of the purpose and construction of this series). Very few samples were available for thermal conductivity measurements from these wells.

3) Sites prefixed Q- were completed as heat-flow test wells. Cuttings were obtained at intervals of ∿5 m for thermal conductivity measurements and lithologic studies; in most instances, one or two cores were also obtained from each hole. A pipe, capped at the bottom and filled with water, was left in the well to allow access for later temperature measurements. The first set of Q-holes (Q-1, Q-2, and Q-3) was drilled in 1975 to depths of ∿200 m. The holes drilled in 1976 were shallower than those drilled in previous year (50-150 m) and the annulus around the casing was backfilled with drill cuttings rather than with cement, as was done previously (Sass and others, 1976).

4) The QH-holes were of dual purpose construction. (QH-1 through QH-4 were drilled in 1975 and were about 150 meters deep.) They were identical to the Q-holes as regards backfilling and sampling for thermal

conductivity and lithology (3, above), but in addition to the access pipe, a parallel pipe with a well screen at the bottom was emplaced. The annulus around the screen and for 1 or 2 m above it was packed off with gravel to protect the screen and to allow access of formation water.

5) Based on some earlier observations concerning the relation of shallow temperature to temperature gradients and heat flow at depth (to be discussed below), the T- (for temperature) series of holes was drilled to obtain detail around known anomalies or around isolated deeper holes (e.g., Q-18 region, Figure 2). These holes were only 15 to 18 meters deep (as compared with 50 to 200 meters for the Q- and QH- series) and no cores were obtained. A single sample of cuttings from the lowermost 5 m of each of the T-holes was retained.

DRILLING PROGRAM

The drilling was carried out in two distinct stages:

1) Based on the previous summer's work (Sass and others, 1976) a pattern of about 20 Q and QH holes was laid out to fill in the area west of Leach Hot Springs and to delineate the major anomalies (Panther Canyon and QH-3, Figure 2) discovered by the earlier drilling. As this part of the program neared completion, we were ahead of schedule and under budget, and additional Q and QH holes were added to increase the density of coverage.

2) Earlier work in Grass Valley indicated that the temperature just below the zone of annual temperature variation (12-15 m) was strongly dependent on the temperature gradient (and heat flow) at greater depths (see e.g., Figure 3 of Sass and others, 1976). Therefore, the series of 'T' holes about 18 m (60 feet) deep was planned to enhance and outline the known anomalies and those discovered during the course of the Q and QH drilling. This series (T-1 through T-31, Figure 2) was obtained very rapidly and cheaply with an average production of between 6 and 8 holes per shift.

Acknowledgments. Tom Moses designed and supervised the technical phases of the drilling program. Drilling operations were performed in an efficient and professional manner by Western Geophysical crew GT-3 under the supervision of John Clingan. Gene Smith set up the thermal conductivity laboratory in Winnemucca and performed most of the thermal conductivity measurements on core. Frank Olmsted and Mike Sorey offered valuable advice during the planning stages of the project. Fred Henderson assisted in collecting some of the samples and lithologic logging.

We are indebted to Dennis Simontacchi of the Bureau of Land Management for his conscientious and prompt action on applications for drilling permits, particularly for the T-series, when the drill was very close behind the planners.

Dave Magleby, Bureau of Reclamation, kindly advised us on coring operations and loaned us coring equipment.

TEMPERATURES

Temperature logs were run in all holes within a few days of completion and at least once a month or so after completion. The most recent temperature log for each Q and QH hole is reproduced in Appendix A. These logs were made between 1 1/2 and 4 months after completion of the holes and represent near-equilibrium temperatures. A contour map (Figure 7) of temperatures at 15 meters in all holes (H, Q, QH and T) outlines the three major anomalies. Groups of temperature profiles (Figures 8 through 12) illustrate the variation of temperature with depth within individual areas in the region. Temperature gradients in the upper 10-20 meters are systematically higher than those at greater depths, most probably because the water table is generally deeper than 20 m and the rocks above it are not completely saturated, resulting in a systematically lower conductivity. The greatest variation in temperature occurs near the springs (Figures 7 and 8); temperatures at 15 m range from about 14°C in T-23 to over 80°C in H-10 (Figures 2 and 8). Outside of the spring area (Figures 9 through 12), the variability in temperature, and the essentially conductive thermal regime in the upper 50-100 m of most holes is evident from the profiles.

The surface elevations of the holes range from about 1350 to 1600 meters. On the average, land surface temperature should decline with increasing elevation at the rate of about 5°C/km or 6°C/km (see Birch, 1950; Clark and Niblett, 1956; Sass and others, 1967). All of the holes

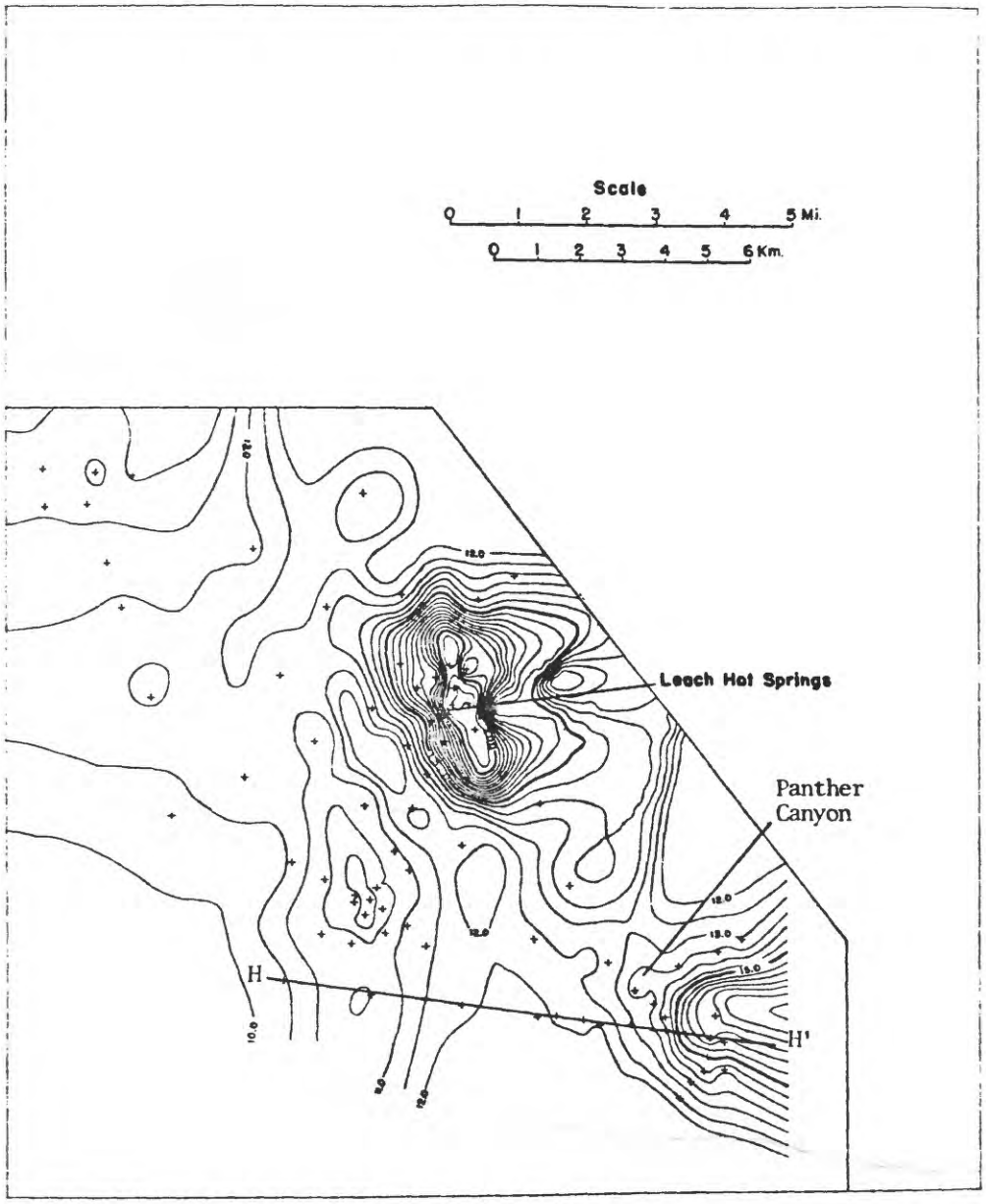

Figure 7. Temperatures at a depth of 15 m below ground surface in Grass Valley, contour interval, 0.5°C.

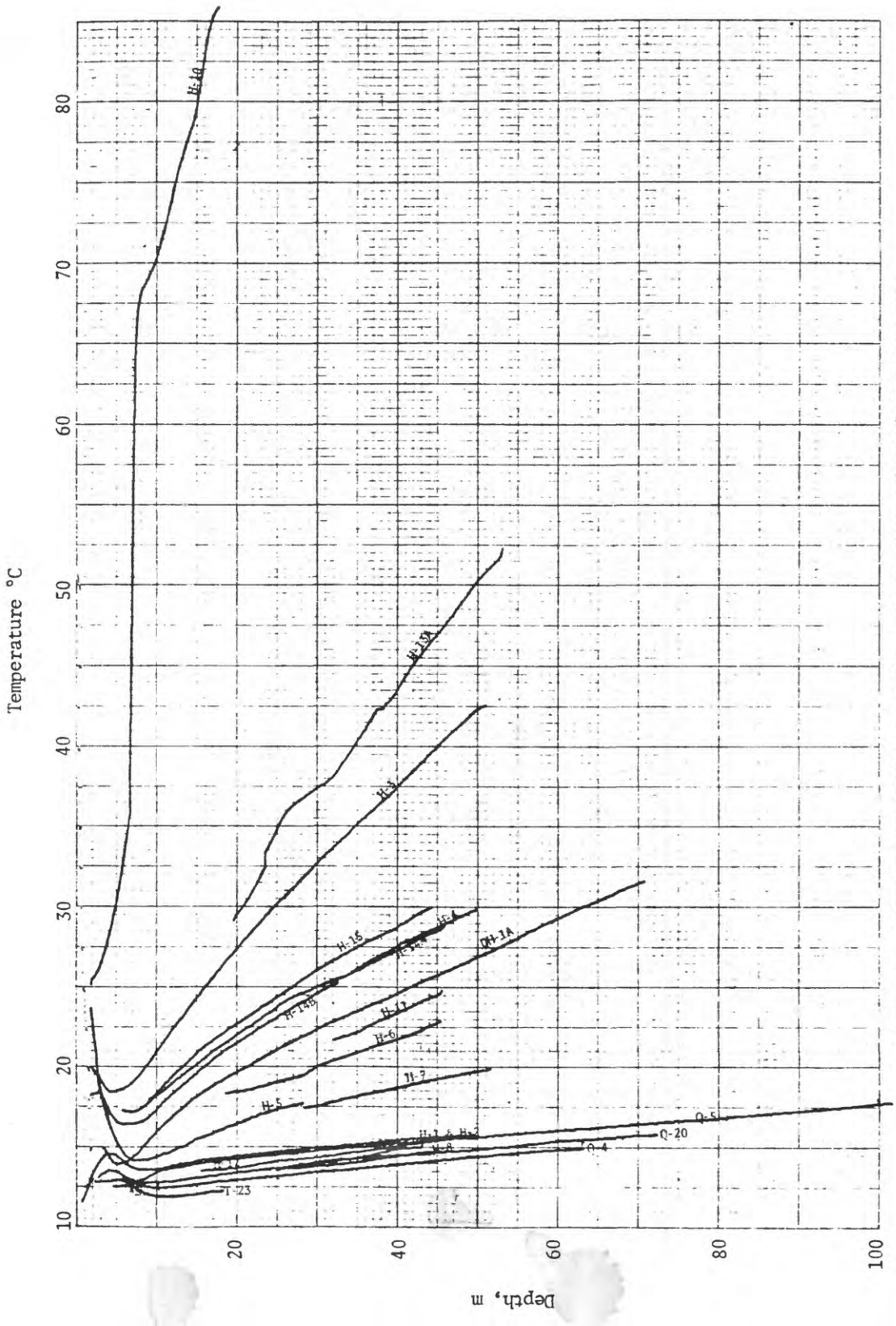

Figure 8. Temperature profiles within a 3-km radius of Leach Hot Springs.

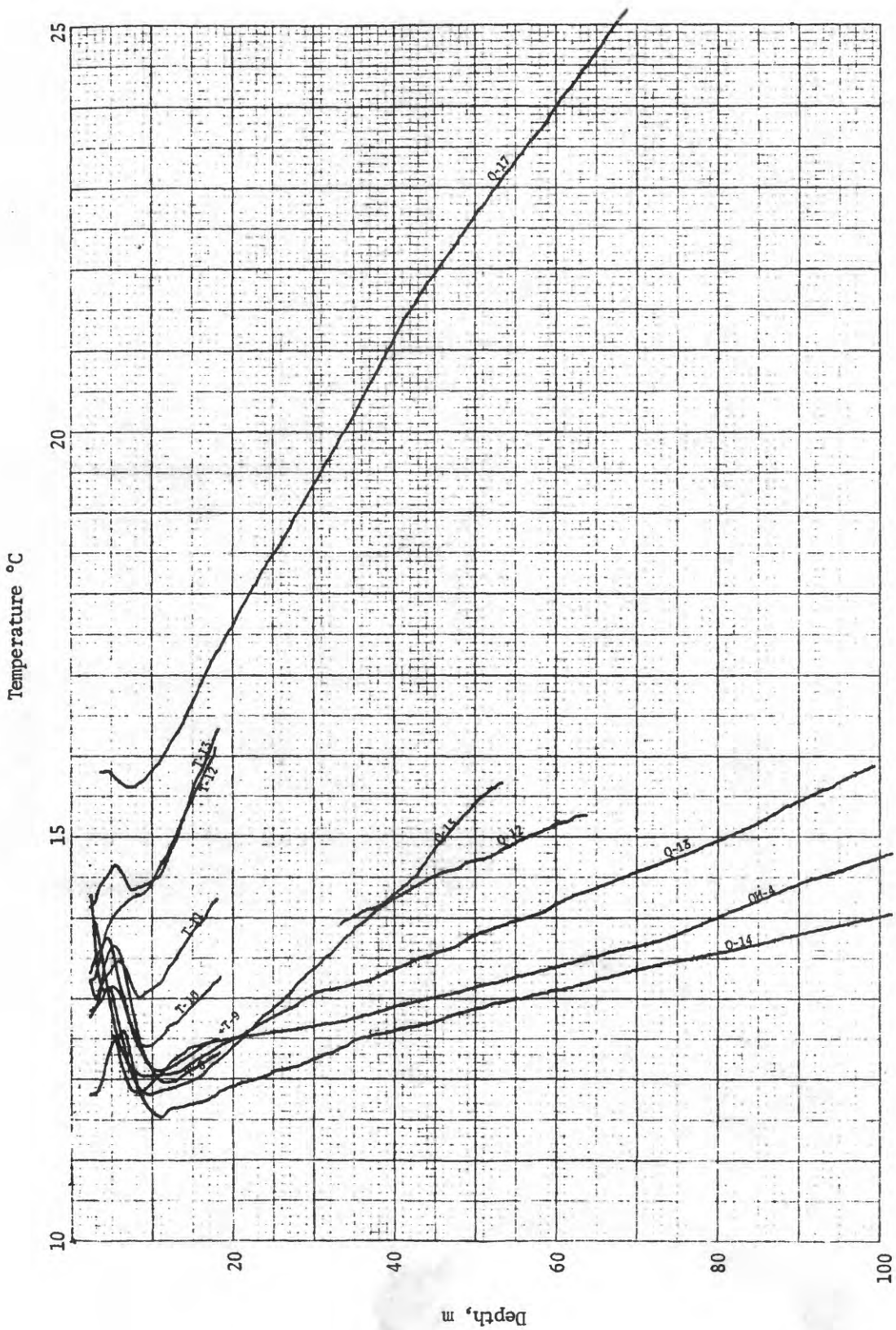

Figure 9. Temperature profiles along HH'.

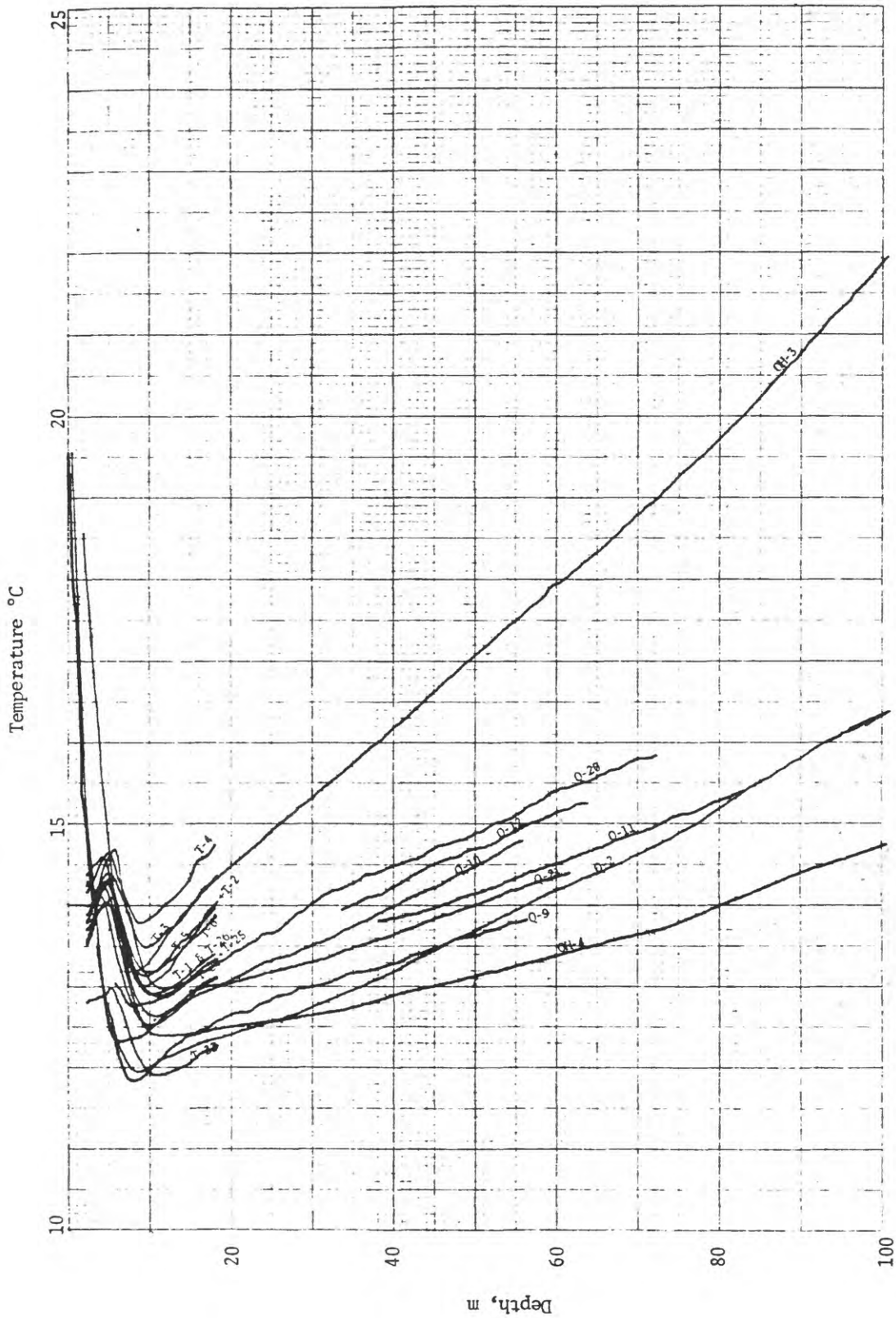

Figure 10. Temperature profiles within a 3-km radius of hole QH-3.

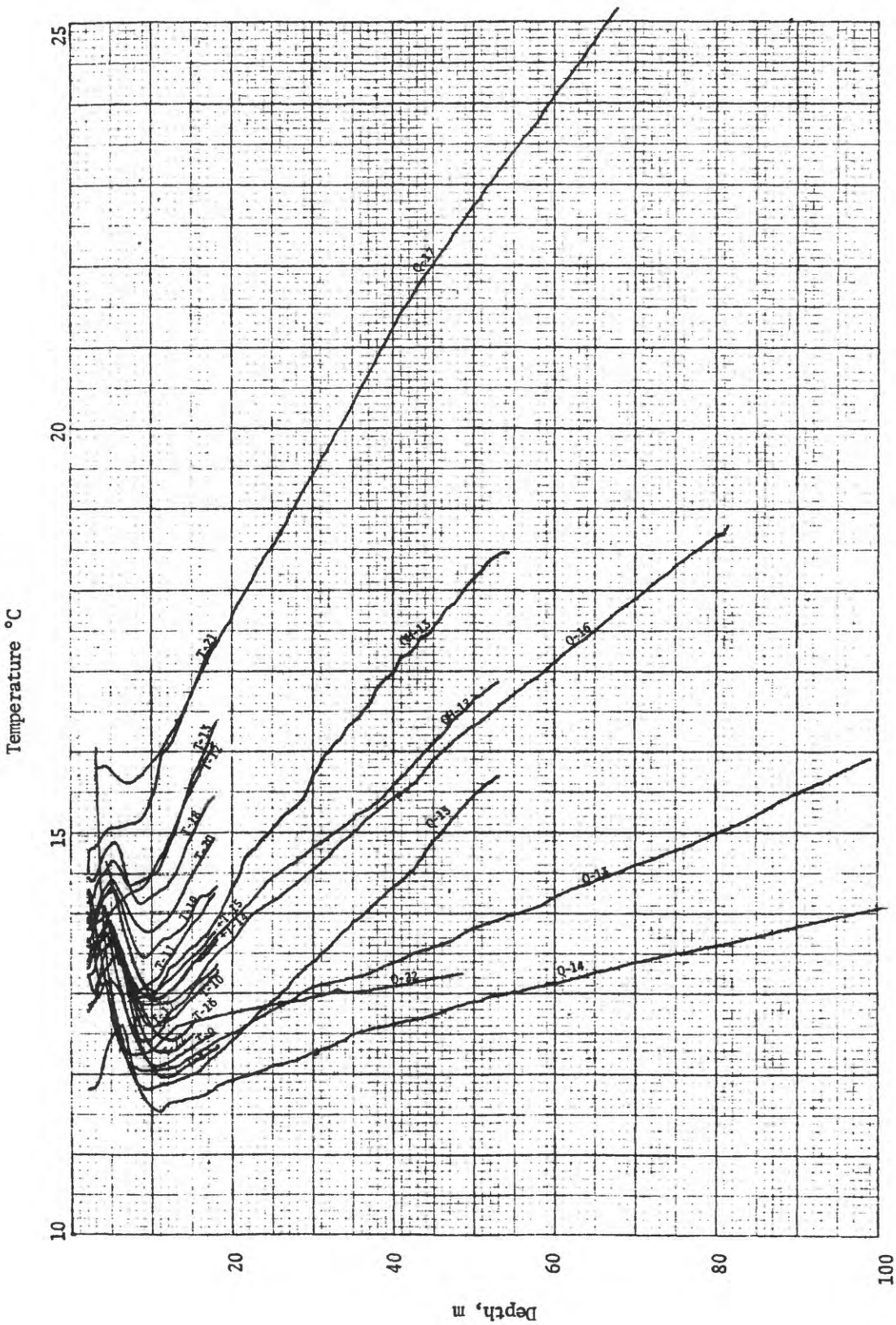

Figure 11. Temperature profiles in the Panther Canyon area.

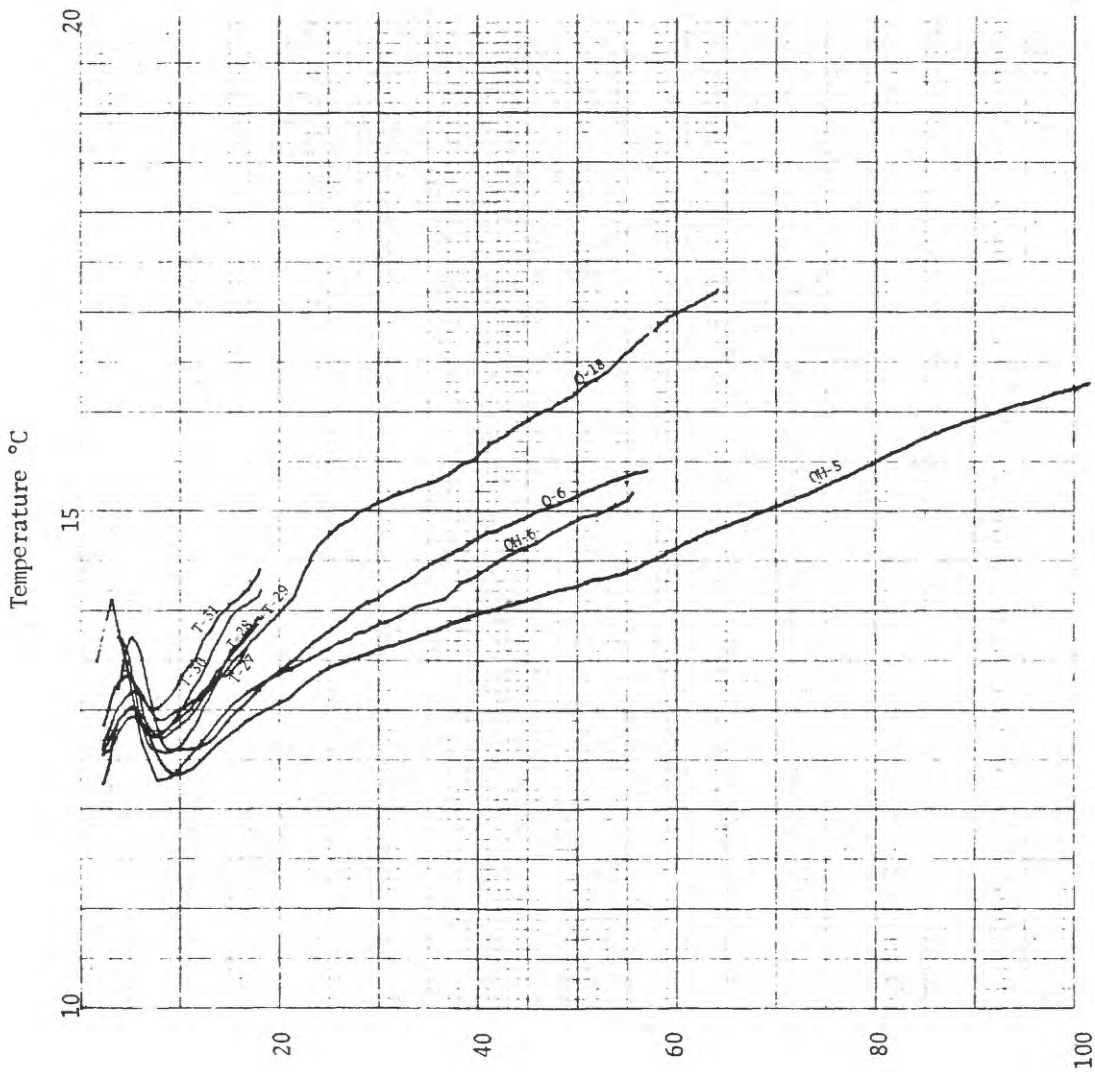

Figure 12. Temperature profiles from northern part of study area.

drilled in this work were on flat or gently undulating terrain with no great variation in vegetation except within the drainage of the hot springs themselves (Olmsted and others, 1975) nor is there appreciable variation in the appearance of the land surface. Because of this, we might expect that microclimatic effects (Blackwell, 1973; D. D. Blackwell, personal communication) would not have a large effect on surface temperature, and that the variation in near-surface temperatures not attributable to elevation would reflect variations in heat flow, and near-surface thermal conductivity (caused in turn by variations in composition, porosity, and depths to the zone of saturation). Temperatures at 15 meters (Figure 13) show a large scatter, some of which certainly is attributable to differences in heat flow, but there is no obvious correlation with elevation even when heat-flow variation is taken into account. We attempted to correlate temperatures at 15 meters for narrow ranges of heat flow with depth to water and lithology; but no clear-cut relations could be found.

It thus seems likely that subtle differences in vegetation distribution and other near-surface conditions contribute to the scatter in near-surface temperatures as has been observed elsewhere (D. D. Blackwell, personal communication).

Figure 13. **Temperature at 15m vs Elevation**
Leach Hot Springs, Nev.

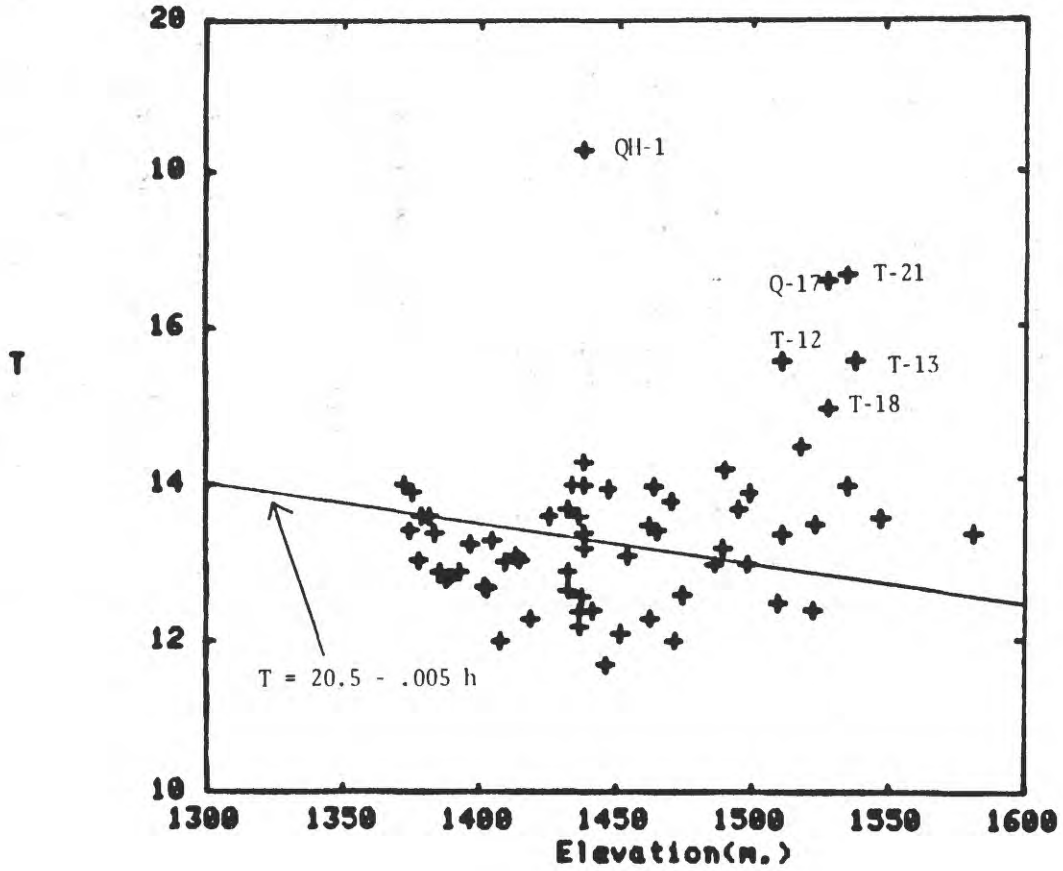

THERMAL CONDUCTIVITY AND POROSITY

Two distinct methods were used to determine thermal conductivity:

1) For each core, the needle-probe technique was used at spacings of between 5 and 15 cm along the core (Appendix B) to obtain thermal conductivity values (K_{np}) representative of the formation in the cored interval. Measurements were made at the drill site or in the Winnemucca field laboratory. Under the conditions encountered during this study, this method has a reproducibility of $\pm$2 to 3%.

2) The thermal conductivity of the solid component (K_s) of the porous sedimentary rocks encountered in all holes was determined from measurements on cuttings (see Sass and others, 1971a) obtained during drilling. K_s was determined at intervals of between 5 and 10 meters for all holes (Appendix A). The reproducibility of this type of measurement is about $\pm$10%.

Histograms for both types of conductivity measurement (Figure 14) show near-normal distributions with means of 3.75 and 7.90 tcu for K_{np}, and K_s, respectively.

The high cost of coring and the difficulty in coring much of the material encountered severely limited the number of cores and, hence, the number of high-quality conductivity data (K_{np}) that could be obtained. The "chip" conductivities (K_s) are much more widely distributed (compare conductivity columns, Appendix A), but a knowledge of the in situ porosity is necessary to calculate the thermal conductivity of the formation using K_s.

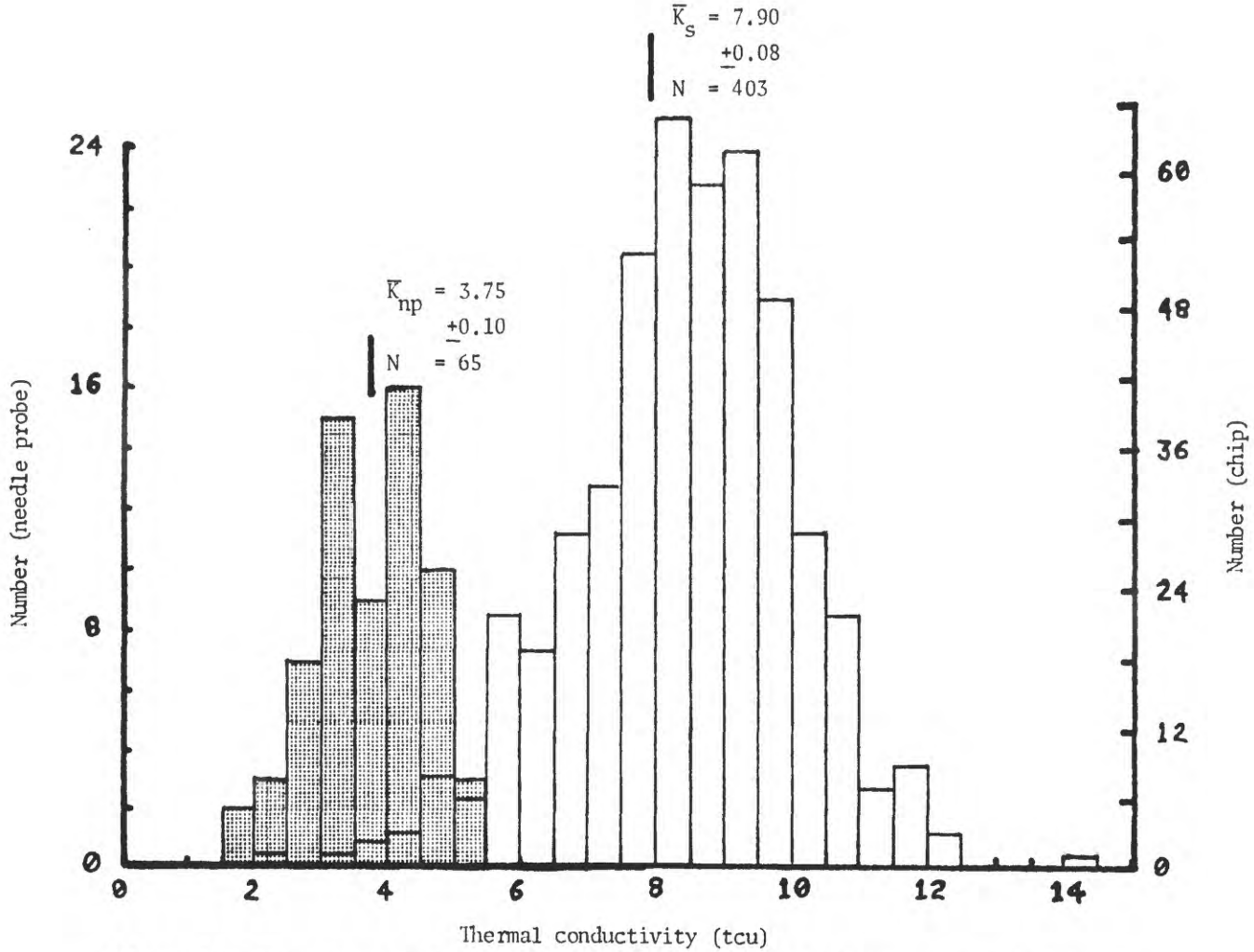

Figure 14. Histograms of thermal conductivities for Grass Valley. Unshaded histogram gives K_s, the solid component as measured on chips. Stippled histogram shows needle-probe measurements on core (K_{np}).

The average porosity for the entire study area was estimated from comparison of K_{np} and K_s at the same depths. In addition, porosity measurements were made on all suitable core samples. The average of these measurements compared favorably with our original estimate (compare Figures 16 and 19).

The needle-probe method is identical in principle to that first described by Von Herzen and Maxwell (1959) and summarized by Langseth (1965). The system is an updated version of the one described by Lachenbruch and Marshall (1966).

For the work at Grass Valley, two identical needle-probe systems were employed. One was mounted in the USGS logging vehicle, the other in the laboratory in Winnemucca, ∿50 km north of the field area. Most cores were taken into Winnemucca at the end of the shift and the measurements were made there the following day. Sufficient measurements were made in the logging truck at the drill sites, however, to establish that no loss of data quality resulted from the transportation and time lag between core recovery and measurement.

All core samples were doubly wrapped and sealed in plastic at the drill site and were transported in capped PVC tubes to which sufficient water had been added to maintain a 100% humidity environment. We are satisfied that no significant moisture loss occurred between retrieval and physical properties measurements (both conductivity and porosity).

Most conductivities were measured with the needle probe perpendicular to the core axis (K_{rad}); however, many were measured along the core axis

(K_{ax}; superscript a in Appendix B). To test for anisotropy, the average K_{rad} was plotted against $\bar{K}_{ax}$ for all cores in which 2 or more values of K_{ax} were measured (Figure 15). The correlation is good (R = 0.92) with an indication of slight anisotropy, on the order of 5% (Figure 15).

Thermal conductivities were measured on the 483 samples of drill cuttings (Figure 14) using the method described by Sass and others (1971a). The procedure involves packing the crushed drill cuttings (chips) into a cell, saturating them with water, measuring the conductivity of the aggregate (K_a) on a divided-bar apparatus, and finally calculating the solid component conductivity K_s (Appendix A) from the geometric mean model (see e.g., Woodside and Messmer, 1961),

$$K_a = K_s^{(1-\phi)} \cdot K_w^{\phi} \qquad (1)$$

where K_w is the conductivity of water ($\sim$1.4 tcu at 15°C) and ϕ is the fractional water content (by volume) of the aggregate in the cell.

It is customary in the geothermal exploration industry to measure K_s from chips and to combine it with independent estimates (or guesses) of the formation porosity (ϕ) to arrive at a value (K_f) characteristic of the formation. To achieve some redundancy in estimates of heat flow and to provide as complete a "case history" of geothermal techniques as possible, we measured K_s for most ditch samples obtained in this study and attempted to arrive at a reasonable average porosity.

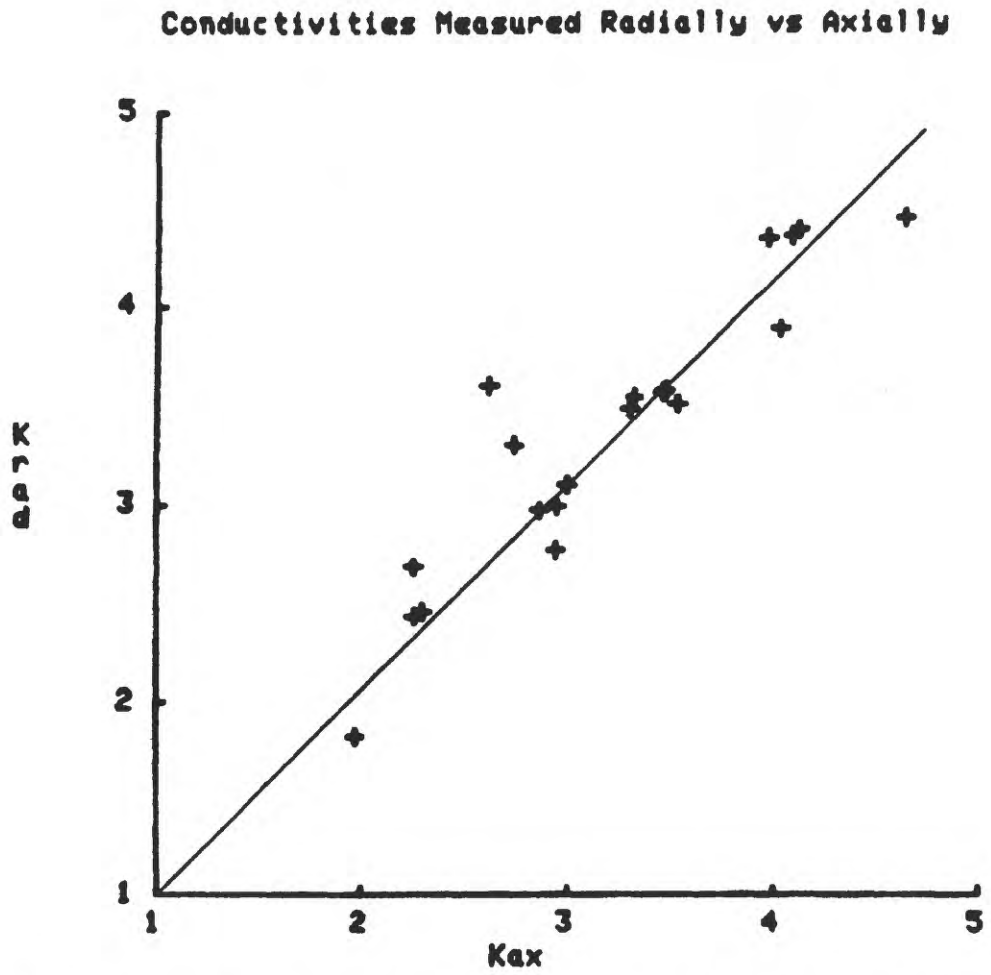

Figure 15. Needle-probe conductivities measured with probe perpendicular to the core axis (K_{rad}) versus parallel to the axis (K_{ax}), Grass Valley, Nevada.

When we know K_s and ϕ, a number of models can be used to calculate K_f. The simplest is the geometric mean already outlined for the chip method (equation 1).

In this case we may write

$$K_f = K_s^{(1-\phi)} \cdot K_w^{\phi} \qquad (2)$$

where ϕ is the formation porosity, and K_s and K_w are as defined in equation (1) K_f is, of course, the conductivity of the water-saturated part of the formation. It is probably futile to attempt an estimate of the formation conductivity above the zone of complete saturation from measurements on chips.

In Figure 16, the geometric mean model is used to compare needle-probe conductivities from core with the chip conductivities measured over the same depth interval. If we set $K_f \equiv K_{np}$, we may rewrite equation (2) as:

$$\ell n(K_s/K_{np}) = \phi \ \ell n(K_s/K_w) \qquad (3)$$

Thus, if there is a single porosity (ϕ) characteristic of the entire sedimentary section, then all of the data pairs defined by (3) should be on a straight line with slope ϕ.

Considerable scatter exists (Figure 16). However most ($\sim$2/3) of the points plot between lines with slopes (ϕ) of 0.3 and 0.5 (30% to 50%

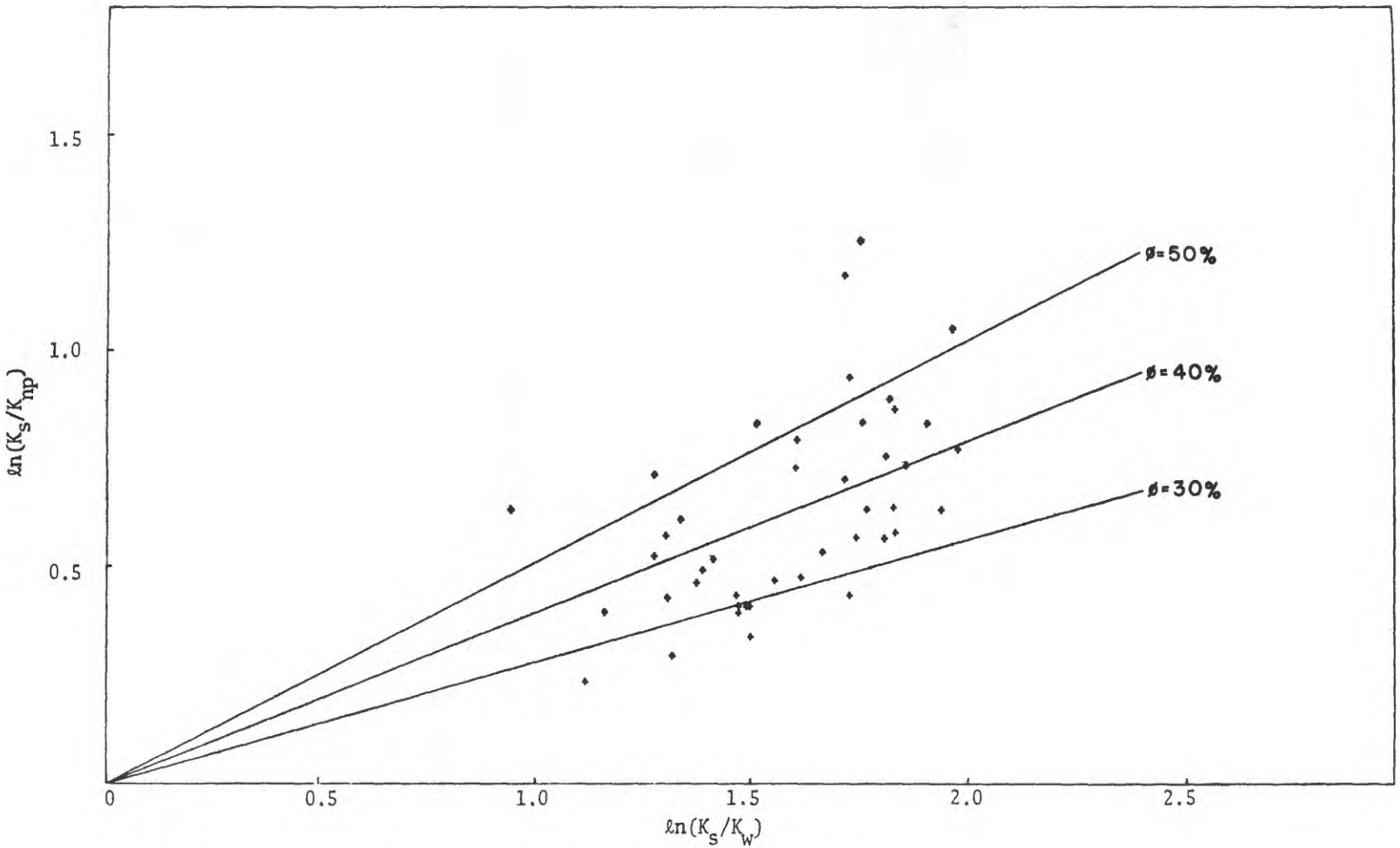

Figure 16. A comparison of chip conductivities (K_s) and needle-probe values (K_{np}) using the geometric mean model (equation 3).

porosity). The least-squares line calculated for the complete data set has a slope of 0.4 $\pm$ 0.06 (40% $\pm$ 6% porosity). This average seems high for the poorly sorted, gravelly material characteristic of Grass Valley (F. H. Olmsted, written communication; Manger, 1963) and the question arises as to whether a sampling bias was introduced because the clay-rich samples were easier to core.

Porosity was also measured on different sections of all suitable cores (cores that had not dried out or disintegrated) in our own laboratory and at the USGS Hydro Lab in Lakewood, Colorado (Table 1). There are considerable differences between the two labs for independent measurements on separate sections of the same core (Table 1) but taken as a whole, there is no systematic difference between the two data sets (Figure 17). This leads us to conclude that the differences are real and are the result of differences in porosity between two sections of the same core, rather than of experimental errors. Some support for this conclusion may be found by examining individual conductivity values in Table B-1. For example, conductivities in the lower part of the core from Q-19 are much higher than those in the upper part (Table B-1). There is a corresponding difference in the porosity measurements on the two sections of core (Table 1). Generally, the average of the two calculated conductivities (Kg, a and b) in Table 1 agrees well with the average needle-probe value K_{np} for the entire core.

There appears to be no correlation between porosity and depth (Figure 18), which is reasonable in view of the extreme heterogeneity and generally poor sorting of these materials (F. H. Olmsted, written communication).

Table 1. Porosity from cores and thermal conductivity from cores and cuttings, Grass Valley, Nevada

Hole No.	Depth interval (m)	Porosity (%)† ϕ		Thermal conductivity (mcal/cm sec °C)†† K_s	K_g		K_{np}
		a	b		a	b	
Q-4	51.8 - 53.3	36.0	41.8	5.56	3.38	3.12	3.49
Q-5	76.2 - 77.1		14.6	7.0		5.53	3.69
Q-6	57.0 - 58.5		23.7	6.22		4.37	4.12
Q-7	32.3 - 34.1	33.8		8.15	4.49		3.37
	57.9 - 59.4	24.5	28	6.3	4.36	4.13	4.17
Q-8	29.0 - 30.5	69.7		3.6	1.86		1.91
	64.6 - 66.1	57.4	48.1	4.46	2.29	2.55	3.01
	64.6 - 66.1	58.8	48.1	4.46	2.26	2.55	3.01
Q-9	48.8 - 50.3	42.0		10.05	4.39		3.49
Q-10	33.5 - 35.1	39.1	43.8	8.3	4.14	3.81	2.90
Q-12	46.3 - 47.9		26.0	8.3		5.23	4.39
	57.9 - 59.4	24.0		5.16	3.77		3.35
Q-13	85.3 - 86.9	29.5	36.8	7.1	4.40	3.91	4.38
Q-14	29.3 - 30.8	32.2		8.8	4.87		4.93
Q-15	29.0 - 30.5	67.3		5.03	2.13		2.45
	42.7 - 44.2	35.9	60.4	5.03	3.18	2.32	2.97
Q-16	48.8 - 50.3	27.9		7.01	4.47		3.16
	75.3 - 76.8		26.9	7.4		4.73	4.63
Q-17	33.5 - 35.1	29.9		8.6	5.00		4.06
Q-18	27.4 - 29.0	18.9	20.6	5.23	4.08	3.99	3.89
Q-19	24.4 - 25.9	46.8	21.4	6.09	3.06	4.45	4.03
Q-22	24.4 - 25.9	39.0	17.2	8.1	4.08	5.99	3.41
QH-6	27.4 - 29.0	20.4	32.7	6.66	4.85	4.00	4.16
QH-7	34.4 - 36.0	36.0		5.6	3.40		3.43
	61.0 - 62.5	54.5	54.9	7.9	3.08	3.06	3.07
QH-8	34.4 - 36.0	54.9	46.8	7.0	2.89	3.3	3.35
	44.2 - 45.7	30.3		5.33	3.55		2.90

Table 1. Porosity from cores and thermal conductivity from cores and cuttings, Grass Valley, Nevada (continued)

Hole No.	Depth interval (m)	Porosity (%)† ϕ		Thermal conductivity (mcal/cm sec °C)†† K_s	Kg		K_{np}
		a	b		a	b	
QH-11	39.6 - 41.1	59.6		4.14	2.17		2.31
	49.7 - 51.2	63.0	47.4	4.0	2.06	2.43	2.41
QH-12	39.6 - 41.1	54.1	54.9	6.4	2.81	2.78	2.77
QH-13	35.1 - 36.6	25.2		7.4	4.86		4.46

†Porosity (ϕ) a) Lakewood; b) Menlo Park.

††Thermal conductivity: K_s, conductivity of solid component over the depth specified.
K_{np}, harmonic mean of needle-probe determinations (see Table B-1).
Kg, $\equiv K_s^{(1-\phi)} \cdot K_w^{\phi}$, where ϕ is fractional porosity.
K_w, conductivity of liquid water at ∿15°C (∿1.4 mcal/cm sec °C).

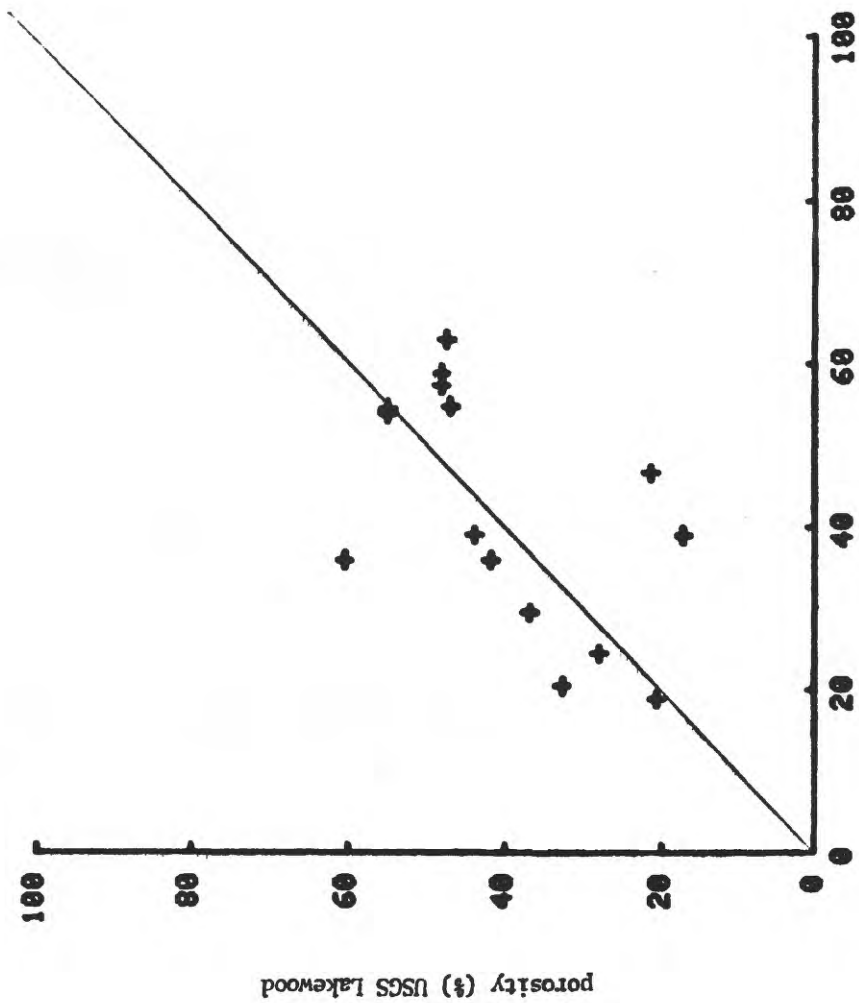

Figure 17. Lakewood porosity versus Menlo Park porosity

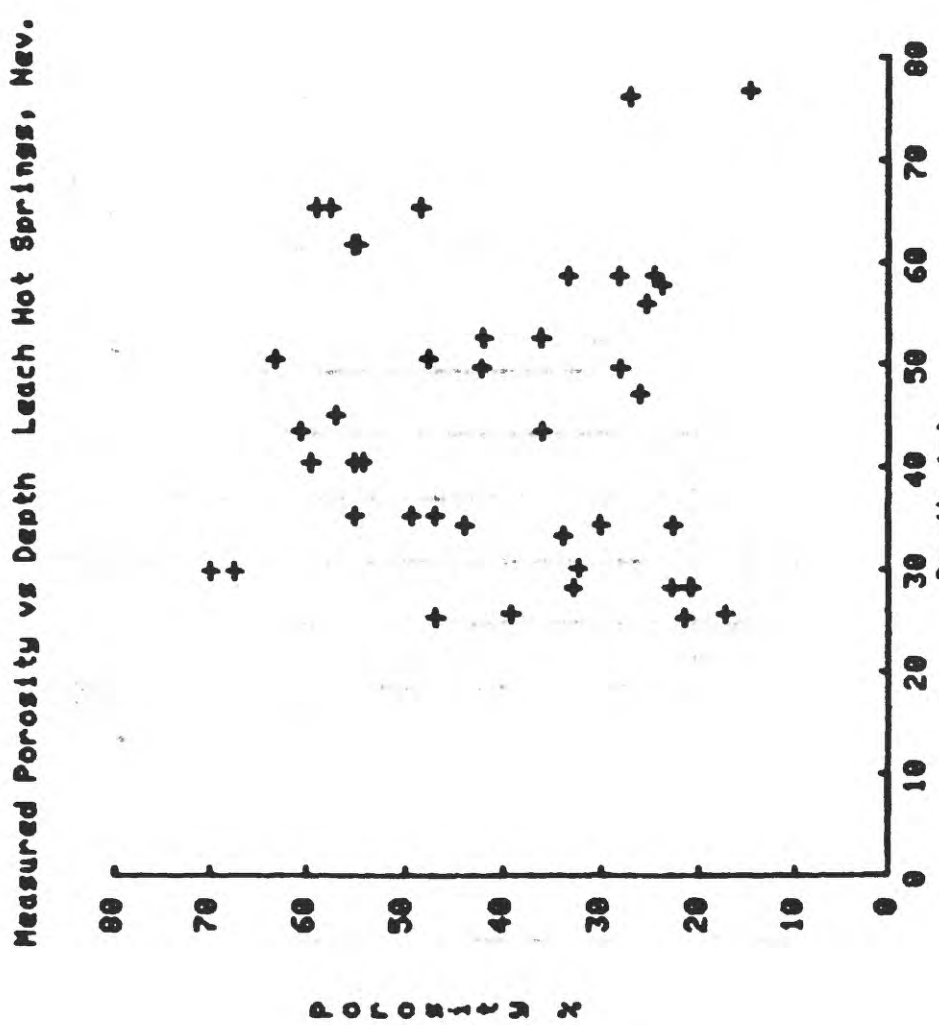

Figure 18. Porosity versus depth for cores from Grass Valley.

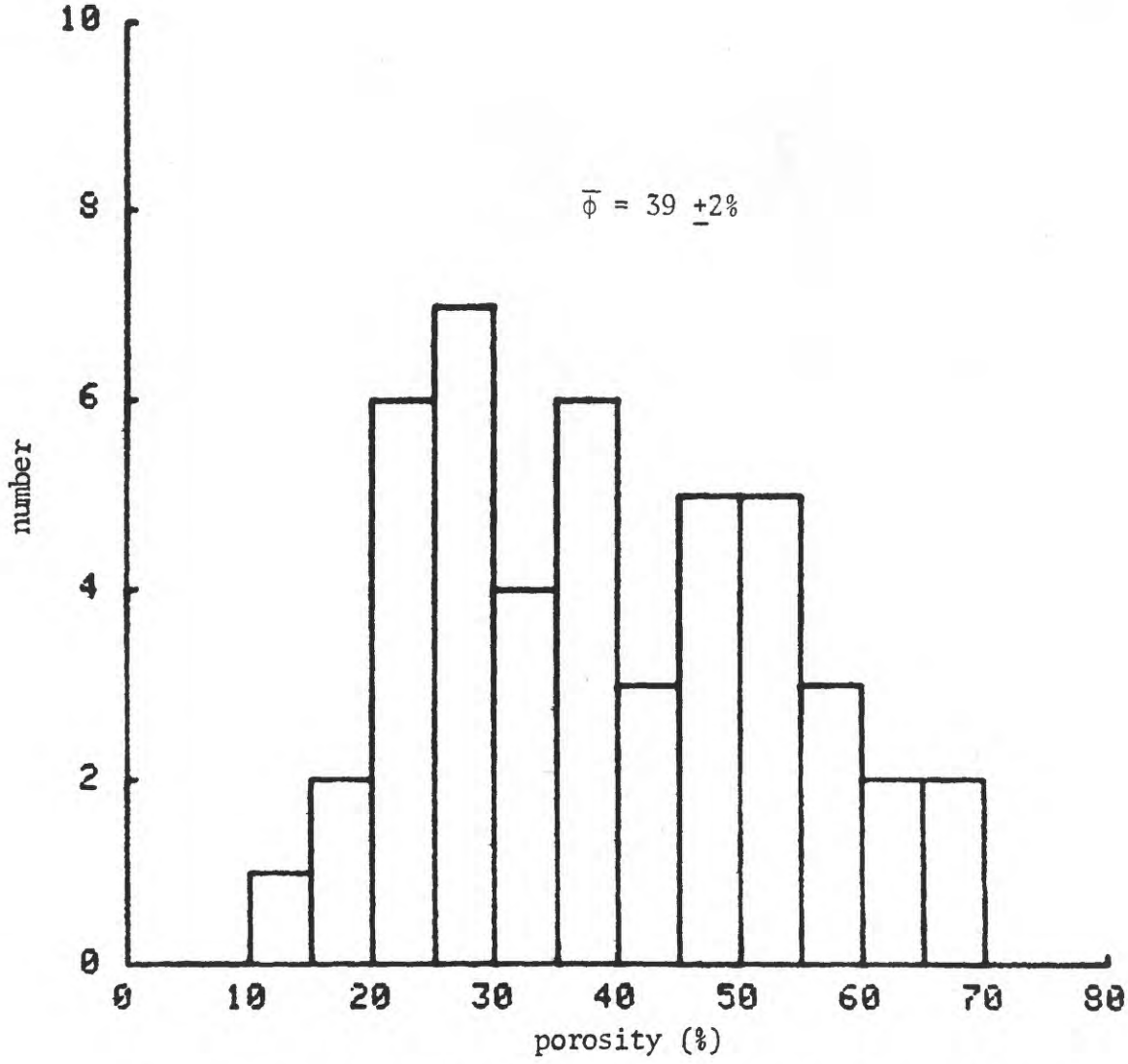

Figure 19. Histograms of measured porosities, Grass Valley, Nevada

The distribution of porosity (Figure 19) is bimodal, with peaks between 20% and 30% and between 45% and 55%. This is consistent with the distribution of points obtained in the comparison of $\ell n(K_s/K_{np})$ versus $\ell n(K_s/K_w)$ (Figure 16). An attempt to correlate porosity with lithology was inconclusive, mainly because most cores contained a combination of the predominant lithologic units (clay sand $\pm$ some gravel), and it was difficult to quantify "lithology." There was a tendency, however, for clay-rich material to have a lower porosity than sandier sections, and the bimodality of the distribution (Figure 19) may be largely the result of this difference. This tendency is, however, counter to that usually observed (Olmsted and others, 1975; F. H. Olmsted, written communication), and leads us to suspect that the cores are not an adequate sample of the valley sediments. Most of the holes penetrated predominantly gravelly material (see lithologic summaries, Appendix A) which was difficult to core, and thus is under-represented in cores, porosity determinations, and needle-probe conductivities. The few gravelly sections successfully cored had porosities spanning most of the range measured on the other lithologies with an average of about 40%. The material with highest porosity ($\sim$70%) was tuffaceous and had very low measured conductivity (e.g., Q-8, 30 m, Table 1).

From the foregoing discussion and from the results summarized in Figures 16 and 19, we adopt the following scheme for calculating K_f from K_s and ϕ (equation 2):

1) An average porosity of 40% is assumed. From Figure 19, we note that the porosity is just as likely to be 30% or 50% as the assumed

value, but we have insufficient correlation with lithology to choose between them in individual cases.

2) Assuming complete saturation, the "formation conductivity" K_f is then calculated from the K_s for a given depth interval using equation 2 and the value of 1.4 tcu for K_w.

Some indication of the adequacy of this scheme may be obtained by calculating a mean K_f from $\overline{K}_s$ (Figure 14) (which represents a complete sample of all drill cuttings) using the mean porosity of 40% $\pm$ 6% determined from cores. The resulting value, 3.95 $\pm$ 0.4 is in good agreement with the average $\overline{K}_{np}$ of 3.75 $\pm$ 0.1. This indicates that the range of solid components found in the cores is an adequate sample, but it leaves unanswered the question of whether or not the porosities measured on core adequately represent the more gravelly material characteristic of most of the valley.

We are confident that the thermal conductivities obtained from K_s in this manner are sufficiently accurate to make comparisons among heat-flow values in this valley for the purposes of delineating thermal anomalies, characterizing the average heat flow of the study area, and making heat budget calculations. On the other hand, these conductivities are not sufficiently well determined to be useful in calculating regional heat-flow values of the quality normally attained by more traditional methods.

HEAT FLOW

Estimates of heat flow were made in all holes including those discussed previously by Olmsted and others (1975). Because of the limited conductivity information from the latter series, the mean of all needle-probe values (3.7 tcu) was used to estimate the heat flow (Table 2) in the "H" series holes. This conductivity value is about 10% lower than the mean for QH-1 in the same area. It should provide reasonable estimates of heat flow from all holes except H-2 and H-5 in which all temperatures were measured above the water table (Sass and others, 1976, Table 2). In these two holes, we have probably overestimated heat flow by 20% or so (see Olmsted and others, 1975).

In Tables 3 and 4, our best estimates of heat flow from the Q and QH holes are summarized along with the locations, elevations and temperature at 15 meters (see Appendix C for details of the calculations). The uncertainty of an individual heat-flow determination within this data set (Tables 3 and 4) is on the order of $\pm$0.3 to 0.5 hfu, mainly because of the difficulty in characterizing the thermal conductivity at individual sites.

Heat flows within 2 km of Leach Hot Springs (shaded area, Figure 2) are irregularly distributed with a mean of 13.6 hfu (Figure 20). Away from the springs (Figure 21) heat flow ranges from 1.0 to 6.5 hfu with an average of 2.4, less than the characteristic value for the Battle Mountain High. The modal value of heat flow in this region (Figure 21) is about 1.7 hfu.

Table 2. Estimates of heat flow from USGS hydrologic test wells near Leach Hot Springs

Hole	Depth interval (m)	Γ °C/km	$q^{\dagger}$ μcal/cm²sec
H-1	23 - 43	66	2.5
H-2	34 - 42	44	1.6
H-3	20 - 50	485	18.0
H-4	34 - 50	260	9.6
H-5	10 - 27	194	7.2
H-6	30 - 45	175	6.5
H-7	30 - 50	111	4.1
H-8	30 - 44	70	2.6
H-9	36 - 42	630	23.3
H-10	10 - 16	2,000	74
H-11	32 - 45	240	8.9
H-12	30 - 43	80	3.0
H-13	40 - 52	700	26
H-14	33 - 39	300	11.1
H-15	28 - 44	270	10.0

†Calculated using K ≡ 3.7 mcal/cm sec °C (which is the average of the harmonic mean <K> needle-probe values for all holes)

Table 3. Heat flows from Q holes, Grass Valley, Nevada

Hole	Location Number	Lat.	Long.	Elev. (m)	Temp., 15 m Obs.	Temp., 15 m Corr.†	Heat flow HFU
Q-1	32/38-26bba	40° 38'	117° 41'	1386	12.9	12.98	2.2
Q-2	31/39-12daa	40° 34'	117° 39'	1419	12.3	12.53	2.0
Q-3	31/39-28aad	40° 32'	117° 35'	1491	14.2	14.84	4.9
Q-4	32/38-24ccd	40° 38'	117° 40'	1403	12.68	12.84	2.0
Q-5	32/39-30bba	40° 38'	117° 38'	1448	13.95	14.33	1.6
Q-6	32/38-29bba	40° 37'	117° 44'	1393	12.90	13.01	3.0
Q-7	31/38-4dab	40° 35'	117° 42'	1402	12.71	12.86	1.5
Q-8	31/38-8aac	40° 35'	117° 43'	1437	12.38	12.72	3.0
Q-9	31/38-10dcc	40° 34'	117° 41'	1438	12.58	12.94	1.5
Q-10	31/38-12cdc	40° 34'	117° 39'	1415	13.05	13.21	1.7
Q-11	31/38-14ccc	40° 34'	117° 41'	1466	13.42	13.89	1.6
Q-12	31/38-23dca	40° 33'	117° 40'	1463	13.49	13.95	1.7
Q-13	31/39-24ddd	40° 32'	117° 39'	1437	12.19	12.51	1.8
Q-14	31/39-29bbb	40° 32'	117° 37'	1447	11.69	12.07	1.5
Q-15	31/39-28bcb	40° 32'	117° 36'	1472	12.01	12.53	3.0
Q-16	31/39-21dcb	40° 33'	117° 36'	1496	13.7	14.32	3.0
Q-17	31/39-27acc	40° 32'	117° 34'	1529	16.63	17.42	6.5
Q-18	32/38-18aba	40° 39'	117° 45'	1375	13.42	13.44	2.7
Q-19	32/38-34bbd	40° 37'	117° 42'	1389	12.82	12.91	2.3
Q-20	31/38-2dcc	40° 35'	117° 40'	1405	13.30	13.3	2.5
Q-21	31/38-13cdd	40° 33'	117° 39'	1433	12.66	13.0	1.7
Q-22	31/39-20bbc	40° 33'	117° 37'	1442	12.40	12.77	1.0

†Temperature at 15 meters reduced to a common elevation of 1372 meters (4500 feet) assuming a decrease in surface temperature of 5°C/km.

Table 4. Heat flows from QH holes, Grass Valley, Nevada

Hole	Location Number	Lat.	Long.	Elev. (m)	Temp., 15 m		Heat flow
					Obs.	Corr.†	HFU
QH-1	32/39-31bbb	40° 36.6'	117° 38.4'	1446	18.3	18.66	9.0
QH-2	32/39-19dba	40° 37.9'	117° 37.8'	1490	13.2	13.76	1.5
QH-3	31/38-14abc	40° 33.7'	117° 40.1'	1435	14.0	14.54	5.1
QH-4	31/38-22caa	40° 32.6'	117° 42.7'	1519	12.4	13.16	1.4
QH-5	32/38-14acc	40° 38.9'	117° 40.2'	1391	12.79	12.88	1.6
QH-6	32/38-21ada	40° 38.2'	117° 42.2'	1378	13.04	13.06	2.1
QH-7	31/38-3aac	40° 35.7'	117° 41.1'	1397	13.25	13.37	1.6
QH-8	31/39-5ccc	40° 34.9'	117° 37.4'	1465	13.99	14.51	2.0
QH-9	31/39-17abc	40° 33.9'	117° 36.7'	1471	13.80	14.32	2.2
QH-11	31/38-16abd	40° 33.8'	117° 42.5'	1484			1.3
QH-12	31/39-34bba	40° 31.4'	117° 34.8'	1512	13.38	14.08	3.5
QH-13	31/39-22abc	40° 33.0'	117° 34.4'	1548	13.58	14.47	5.5
QH-14	32/38-32acc	40° 36.3'	117° 43.6'	1407	13.03	13.2	1.2

†Temperature at 15 meters reduced to a common elevation of 1372 meters (4500 feet) assuming a decrease in surface temperature of 5°C/km.

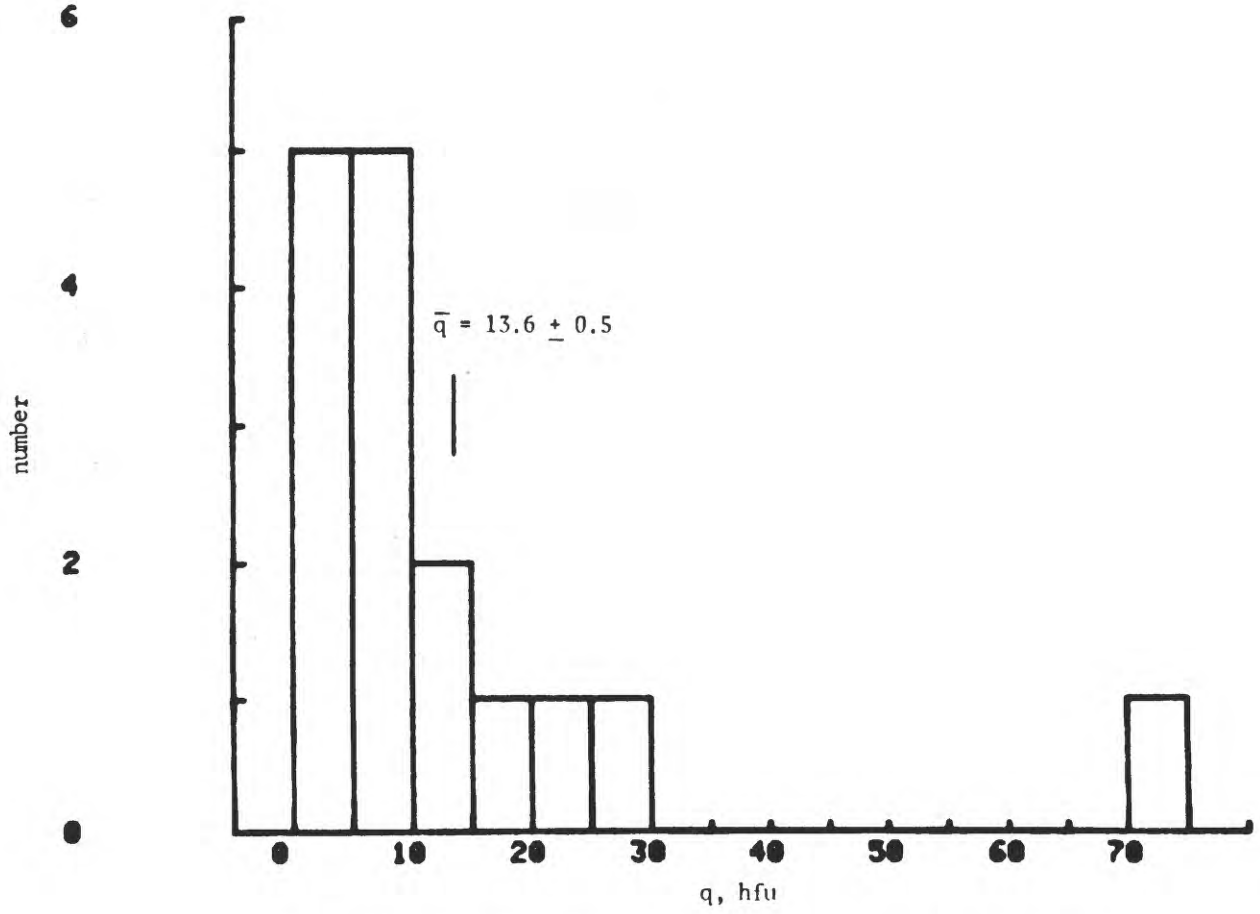

Figure 20. Heat flow within a 2-km radius of Leach Hot Springs.

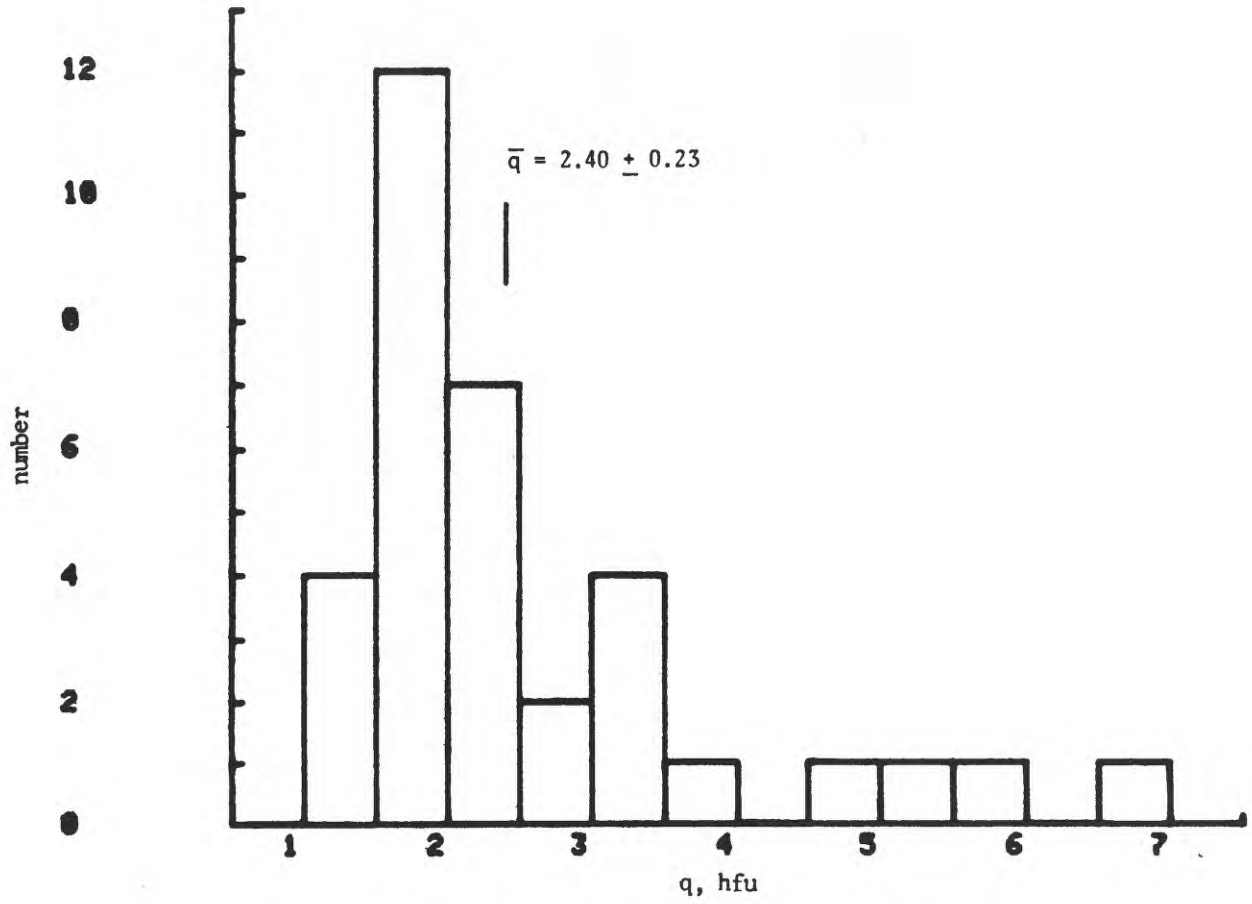

Figure 21. Heat flows at distances greater than 2 km from Leach Hot Springs.

The heat-flow contours (Figure 22) outline in detail, the thermal anomalies reported by Sass and others (1976). The anomaly around the springs is not very different from the interpretation of Olmsted and others (1975, Figure 34). The anomaly centered on QH-3 seems to be elongated in roughly a north-south direction. The strike of the Panther Canyon anomaly coincides with the major structural trends in the area (see discussion below).

Inspection of Figure 3 of Sass and others (1976) revealed that the temperature at 12 to 15 meters correlated reasonably well with temperature gradient and heat flow at depth for the holes drilled in 1975. Part of our strategy in the present work was to investigate whether the cost-effectiveness of heat-flow estimates in the geothermal exploration mode might be increased relative to the research-type drilling done previously. To do this, we drilled a series of T holes (60 feet deep) to interpolate between more widely spaced, deeper holes and to improve the resolution of the boundaries of known anomalies. These holes were drilled very rapidly and cheaply (6 to 8 per day) and, as evidenced by the contours of temperature at 15 meters (Figure 7), they were sufficiently deep to outline the major thermal anomalies in this valley.

We have attempted to extend the information derived from temperatures alone by: 1) obtaining a quantitative relation between the temperature at 15 meters (T_{15_m}) and heat flow in the Q and QH holes; and 2) estimating heat flows from the T holes based on this relation. Before this was done, T_{15_m} was reduced to a common datum of 1372 meters (4500 feet)

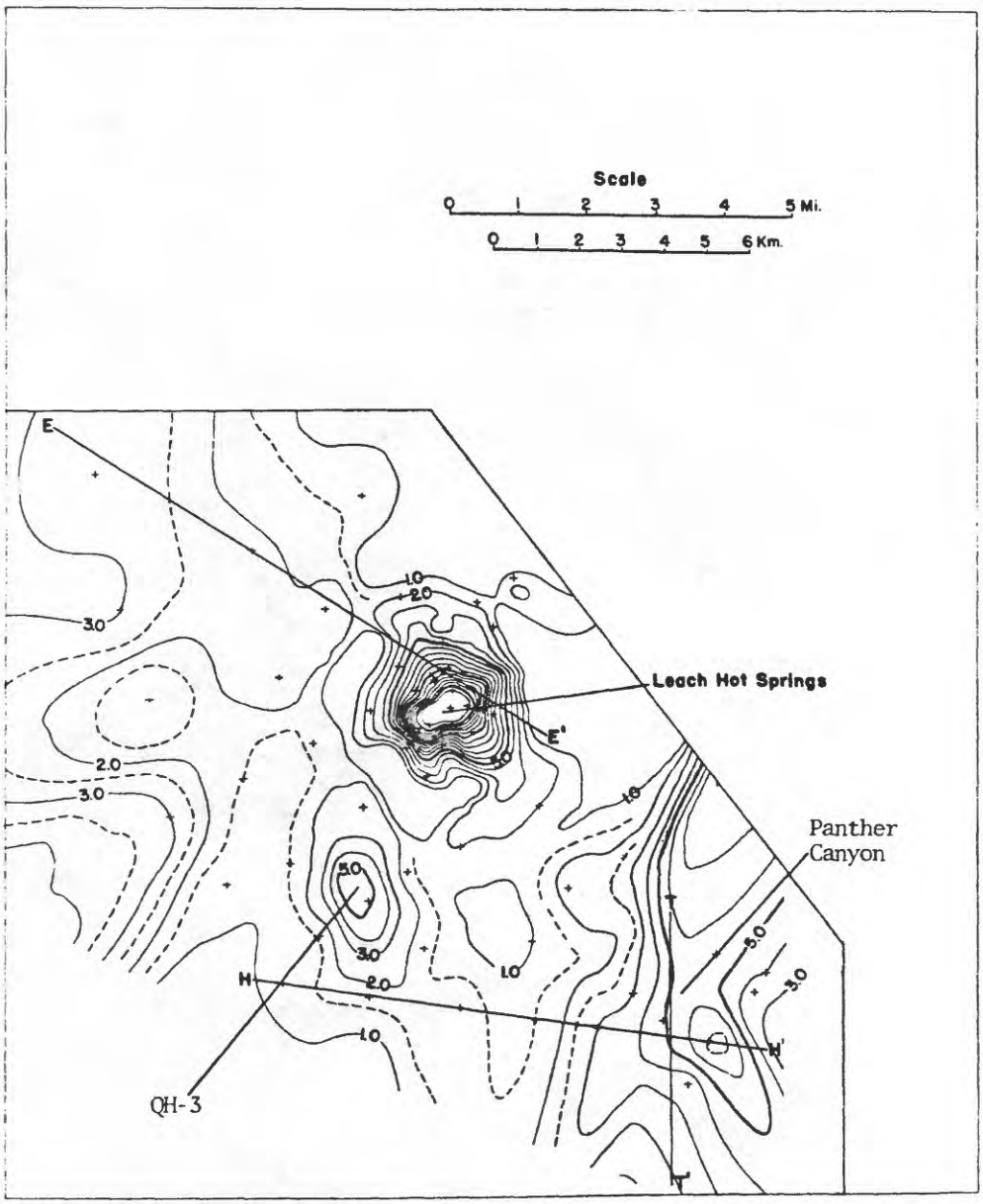

Figure 22. Heat-flow contours for H, Q, and QH holes. Contour interval, 1 hfu with dashed contours at 0.5 hfu. Control is indicated by +. Lettered lines are geophysical traverses conducted in the LBL studies.

assuming a temperature lapse rate of 5°C/km (Tables 3 and 4). The plot of q versus T_{15_m} shows considerable scatter (Figure 23) but there is a positive correlation (R = 0.83) between the two quantities. The determination of slope is most strongly influenced by data from the two holes with highest heat flow (QH1 and Q-17).

A further refinement of this process involved subdividing the study area into three regions (Table 5, Appendix D). The resulting least-squares lines (Figure 24) were then used to estimate heat flow from the T holes.

The heat-flow estimates (Table 6) cover the same range as the Q and QH holes and are significant in the context of outlining areas of potential economic importance. The uncertainty of a given estimate is on the order of 0.5 to 1 hfu. Thus, estimates from the T holes are not adequate for outlining details of areas of lower heat flow (1-3 hfu), but they may be useful in refining the interpretation of the anomalous zones (3-10 hfu). A comparison of Figures 22 and 25 reveals that the T holes provide some additional detail (much of it probably spurious) in the lower heat-flow areas. The hot springs and QH-3 anomalies are essentially unchanged, but the closure of the Panther Canyon anomaly represents an important difference in interpretation between the two maps.

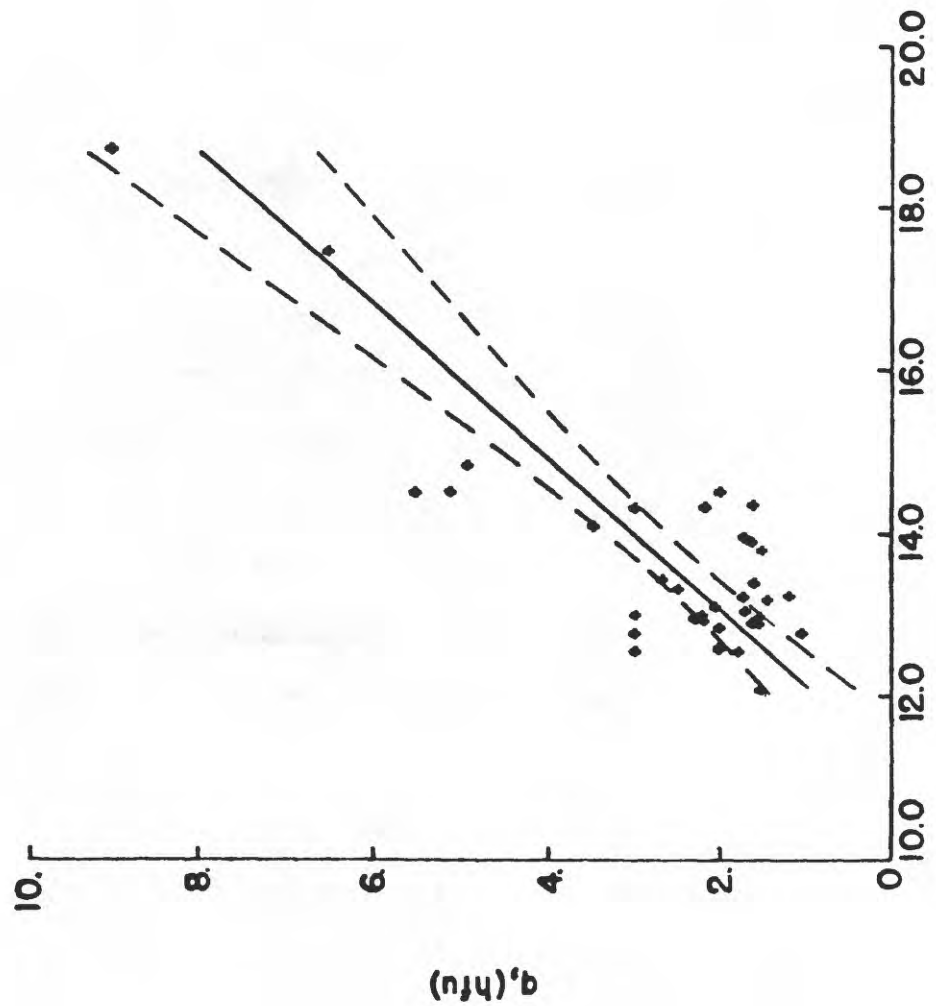

Figure 23. Heat flow versus temperature at 15 meters for Q and QH holes. Solid line is least-squares fit, dashed curves enclose zone of 95% confidence.

Table 5. Intercept (T_o), slope (dq/dT), and coefficient of correlation (R) for the heat flow versus T_{15_m} relation, Grass Valley, Nevada

Regions	Holes used for correlation	T_o	dq/dT	R
Northwest (Q-18)	QH-5, QH-6, Q-18	-22.9	1.9	0.99
Mid-valley (QH-3)	QH-3, Q-9, Q-20, Q-2, Q-10, Q-21	-21.7	1.8	0.91
Southeast (Panther Canyon)	Q-14, Q-15, Q-3, Q-16, QH-12, Q-17, QH-13	- 8.3	0.9	0.89
Entire region	All Q and QH holes	-12.1	1.1	0.83

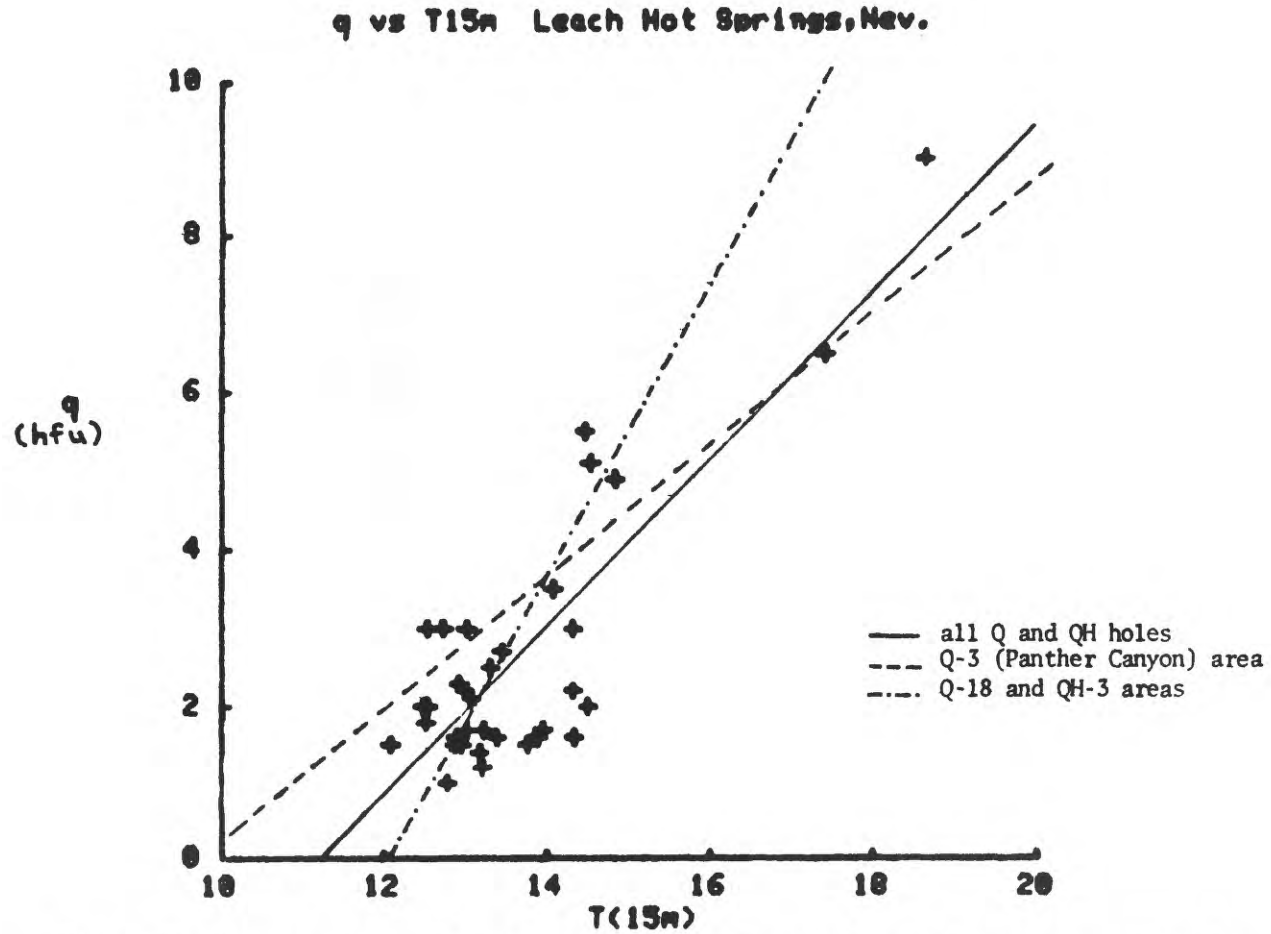

Figure 24. Heat flow versus T_{15_m} for all Q and QH holes showing the least-squares lines for different regions (see Table 5 and Appendix D).

Table 6. Heat flow (derived from the relations in Table 5) for T holes

Hole	Location number	Lat.	Long.	Elev. (m)	Temp., 15 m		Heat flow††
					Obs.	Corr.†	HFU
T-1	31/38-14bbb	40° 34.0'	117° 40.9'	1439	13.4	13.7	3.1
T-2	31/38-14bda	40° 33.8'	117° 40.3'	1437	13.6	13.9	3.5
T-3	31/38-14bdd	40° 33.7'	117° 40.3'	1439	14.0	14.3	4.2
T-4	31/38-14dbb	40° 33.6'	117° 40.2'	1439	14.3	14.6	4.8
T-5	31/38-14dab	40° 33.6'	117° 39.9'	1433	13.7	14.0	3.7
T-6	31/38-14aac	40° 33.9'	117° 40.0'	1426	13.6	13.9	3.5
T-7	31/38-13cbd	40° 33.4'	117° 39.5'	1433	12.9	13.2	2.2
T-8	31/39-29bad	40° 32.2'	117° 37.0'	1452	12.1	12.5	2.4
T-9	31/39-29abd	40° 32.2'	117° 36.6'	1463	12.3	12.8	2.7
T-10	31/39-28bda	40° 32.1'	117° 35.8'	1487	13.0	13.6	3.3
T-11	31/39-28ada	40° 32.0'	117° 35.3'	1500	13.9	14.5	4.1
T-12	31/39-27bcd	40° 32.0'	117° 34.9'	1512	15.6	16.3	5.7
T-13	31/39-27dab	40° 31.9'	117° 34.1'	1539	15.6	16.4	5.8
T-14	31/39-19ddd	40° 33.3'	117° 34.0'	1582	13.4	14.4	4.0
T-15	31/39-22bcb	40° 32.8'	117° 35.0'	1524	13.5	14.3	3.9
T-16	31/39-21bcb	40° 32.9'	117° 36.2'	1475	12.6	13.1	2.9
T-17	31/39-21ddc	40° 32.4'	117° 35.5'	1499	13.0	13.6	3.3
T-18	31/39-27cad	40° 31.7'	117° 34.5'	1529	15.0	15.8	5.2
T-19	31/39-27dca	40° 31.5'	117° 34.3'	1536	14.0	14.8	4.4
T-20	31/39-27cdd	40° 31.5'	117° 34.6'	1519	14.5	15.2	4.7
T-21	31/39-27abc	40° 32.2'	117° 34.4'	1536	16.7	17.5	6.7
T-22	31/39-34bca	40° 31.1'	117° 35.1'	1510	12.5	13.2	3.0

Table 6. Heat flow (derived from the relations in Table 5) for T holes (continued)

Hole	Location number	Lat.	Long.	Elev. (m)	Temp., 15 m		Heat flow††
					Obs.	Corr.†	HFU
T-23	31/38-12bba	40° 34.9'	117° 39.4'	1408	12.0	12.2	0.4
T-24	31/38-12cbc	40° 34.4'	117° 39.7'	1414	13.1	13.3	2.4
T-25	31/38-14cdc	40° 33.2'	117° 40.5'	1455	13.1	13.5	2.8
T-26	31/38-14dda	40° 33.3'	117° 39.9'	1439	13.2	13.5	2.8
T-27	32/38-19daa	40° 38.0'	117° 44.5'	1384	13.4	13.5	2.8
T-28	32/38-18dba	40° 38.7'	117° 44.8'	1379	13.6	13.6	3.0
T-29	32/38-18cbc	40° 38.7'	117° 45.5'	1382	13.6	13.6	3.0
T-30	32/38-18bbb	40° 39.2'	117° 45.5'	1376	13.9	13.9	3.3
T-31	32/38-17bca	40° 39.1'	117° 44.0'	1373	14.0	14.0	3.7

†Temperature at 15 meters reduced to a common elevation of 1372 meters (4500 feet) assuming a decrease in surface temperature of 5°C/km.

††Heat flow calculated from heat flow versus $T_{15\ m}$ relations for Q and QH holes (see Table 5).

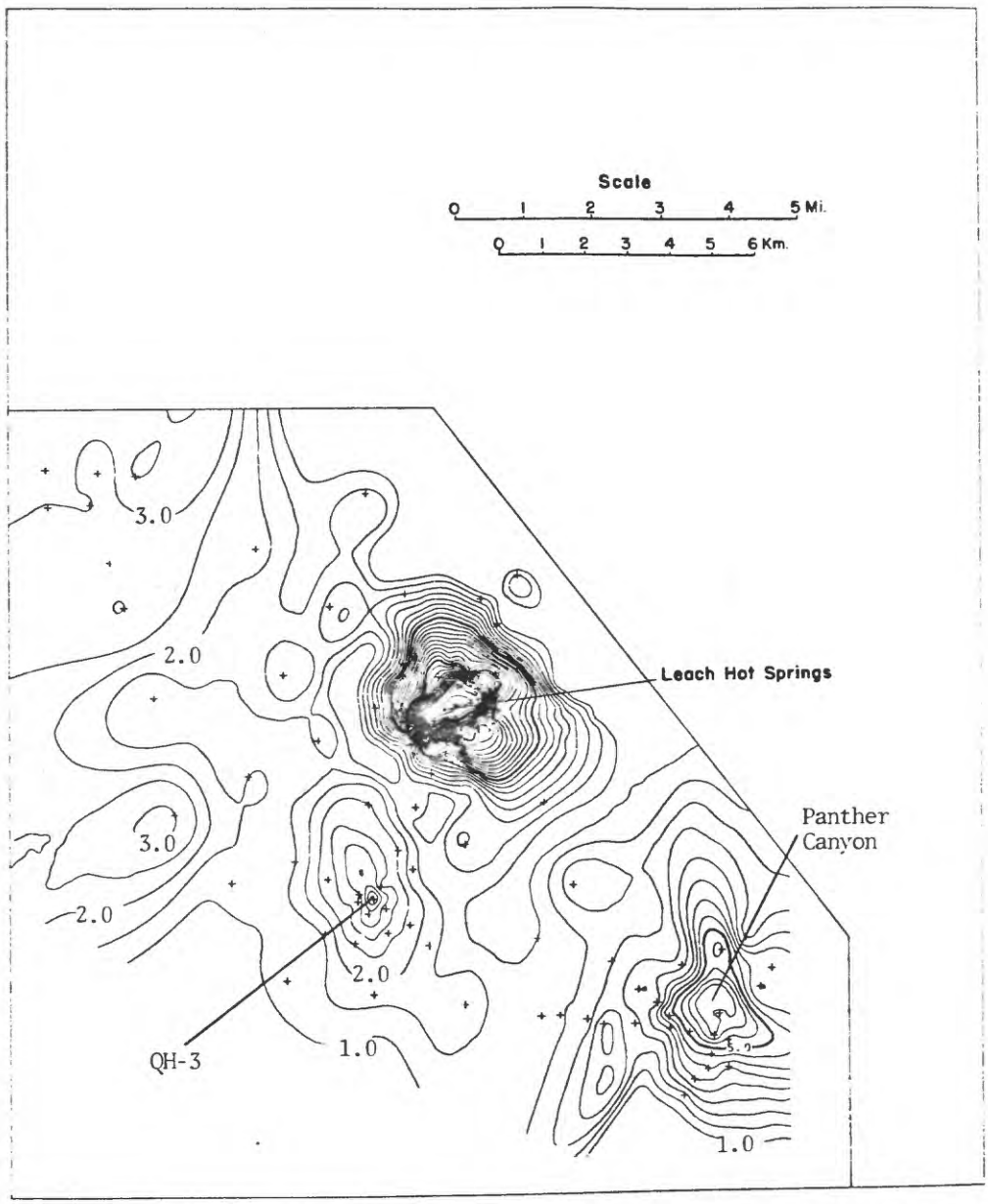

Figure 25. Contour map of heat flows from all holes (Q, QH, H, and T); contour interval 0.5 hfu.

DISCUSSION

The heat-flow distribution found in this study may be viewed within the topographic setting of the area and compared with the various geological and geophysical parameters summarized by Beyer and others (1976). The hot springs and Panther Canyon anomalies (Figure 26) appear to be related physiographically to the western boundaries of the Sonoma and Tobin Ranges, but there is no apparent surface expression of the mid-valley anomaly centered on QH-3. The QH-3 anomaly does, however, appear to be related to a buried bedrock structure (a horst) inferred from gravity studies (Grannell, 1977). This inference seems to have been confirmed from recent deep drilling by the Water Resources Division of the USGS at the QH-3 site (M. L. Sorey, personal communication, 1977). The new hole (QH3-D) intersected pre-Tertiary(?) bedrock at about 1230 feet (~375 m). At this depth, there is a reversal in the temperature profile (Figure 27) indicating that the high heat flow measured to a depth of 175 meters in QH-3 has a hydrologic origin. (The increasing temperature gradient with depth below 150 m is matched by decreasing thermal conductivity in clay-rich impermeable sediments.) The depth to the static water level in the casing (which was grouted in place and then perforated at 1342 feet (409 m)) is only about 6 meters as compared with 61-62 m in QH-3B and QH-3C, indicating a substantial positive hydraulic gradient between 175 and 375 meters (F. H. Olmsted and M. L. Sorey, oral communication, 1977).

The hot springs and Panther Canyon anomalies correspond with major structural trends in bedrock geology (Figure 28), and they are contained

within the band of NNW trending faults mapped by Noble (1975) (Figure 29). By contrast, the QH-3 anomaly is an area almost totally devoid of surface faults (Figure 29). The hot springs anomaly is associated with the zone of intersection of NW-striking range-front faults and NE-striking cross faults. The Panther Canyon anomaly strikes parallel to the range-front faults, and coincides roughly with resistivity, seismic, and gravity anomalies (Beyer and others, 1976).

Heat budget calculation. As pointed out by Lachenbruch and Sass (1977) the mean heat flow within a hydrothermal convection system supported by regional heat flow may be greater than, equal to, or less than the regional heat flow, depending on the age, and geometry of the system and on flux conditions at the boundaries of the system. To gain some insight into the state of the Leach system we have performed a simple calculation to determine the mean flux. For the purposes of this calculation, we rather arbitrarily define the "system" to be somewhere between the outer boundaries of drilling and the outer boundary of our contour plots (see e.g., Figure 29). There is some justification for this as heat flows on all sides of the study area (Figure 1 and preliminary USGS data) are in the range (2.5 to 3.5 hfu) normally associated with the Battle Mountain High. Our definition results in an area for the system of between 200 and 300 km^2. At distances greater than 2 km from Leach Hot Springs (Figure 2), the mean heat flow is 2.4 hfu (Figure 21). Within 2 km of the springs, it is 13.6 hfu (Figure 20). From the latter

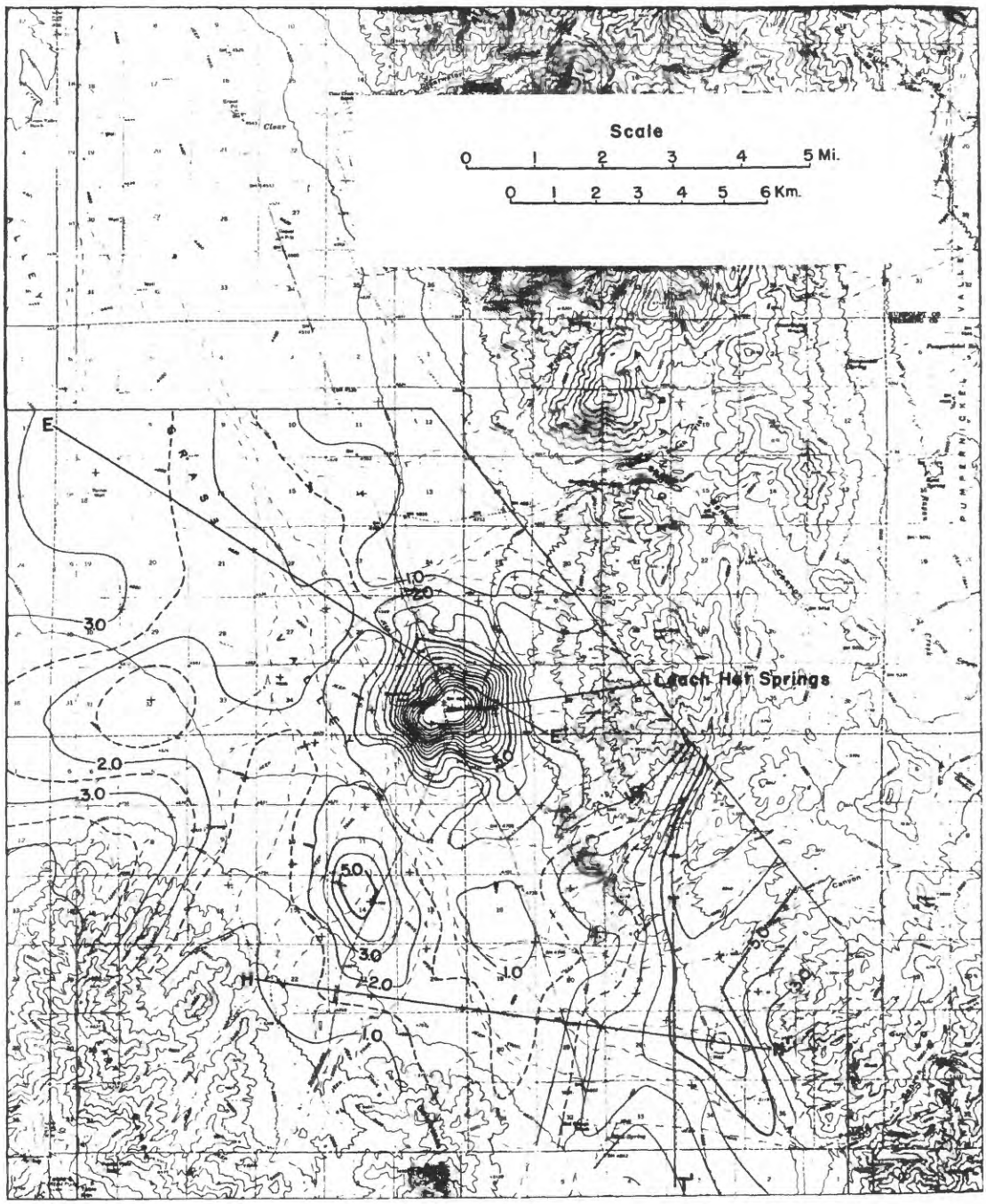

Figure 26. Heat-flow contours superimposed on topography, Leach Hot Springs, Nevada. Contour interval 1 hfu with supplementary (dashed) contours at intervals of 0.5 hfu.

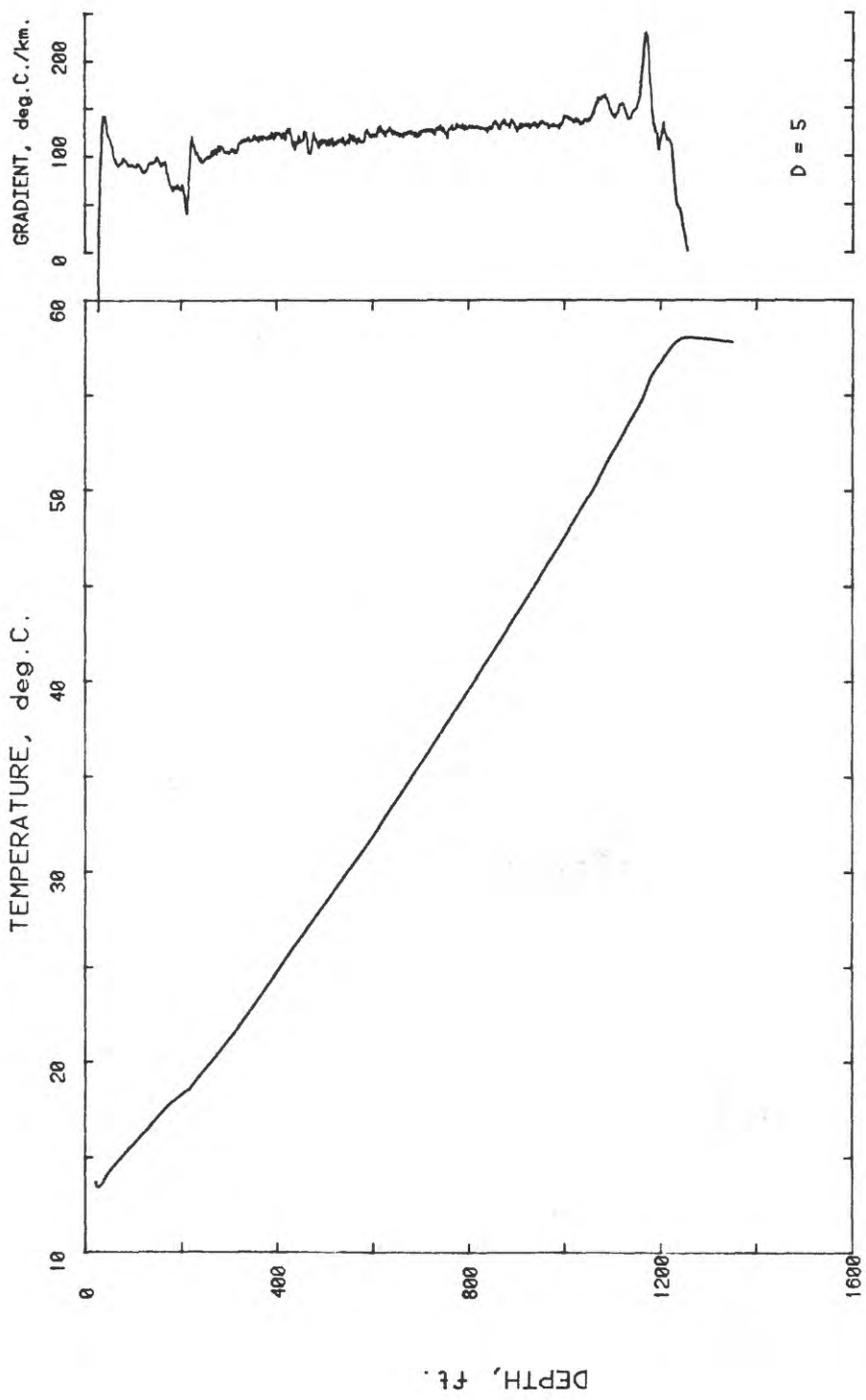

Figure 27. Temperatures and temperature gradients (sliding average over 3 meters) in hole QH-3D.

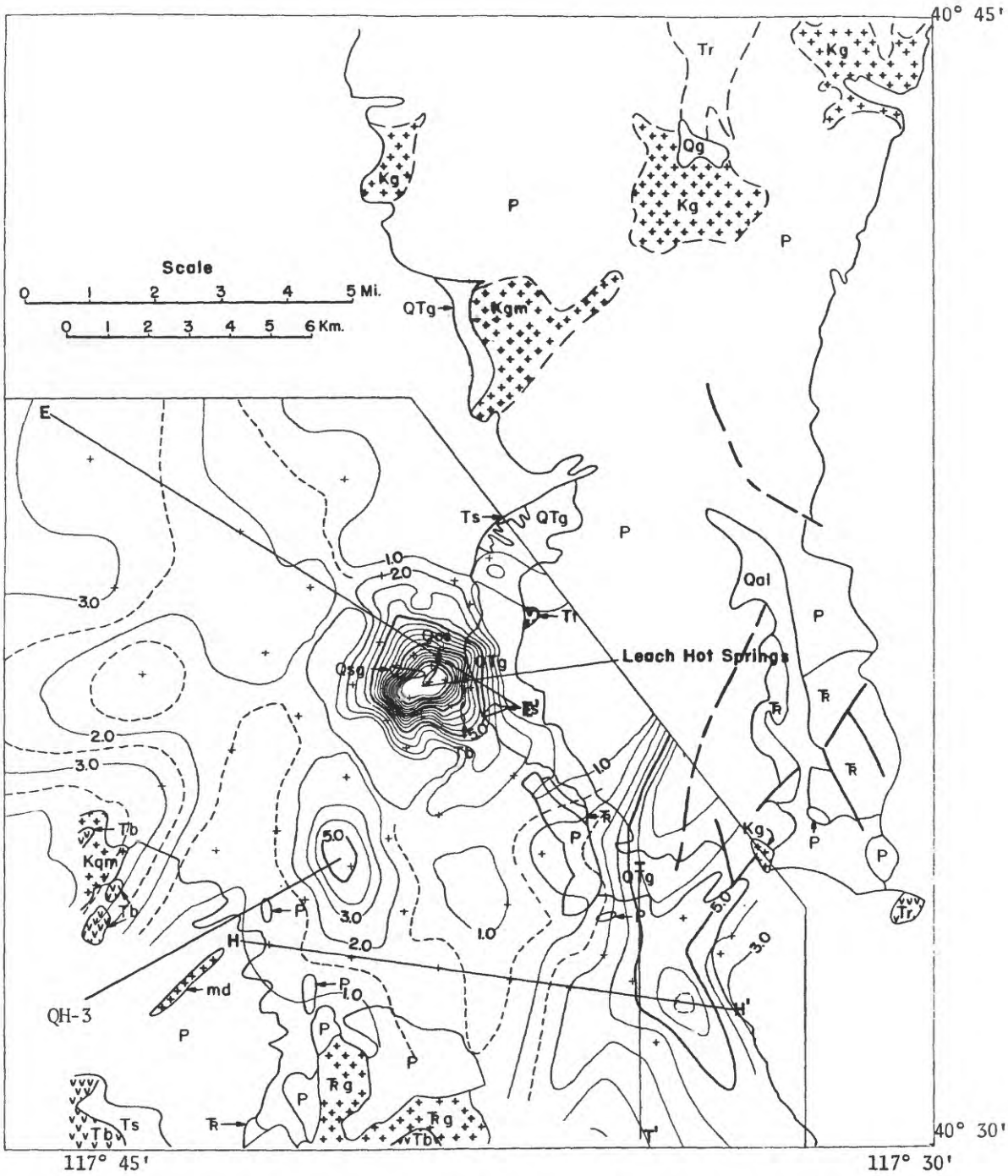

Figure 28. Heat-flow contours superimposed on a generalized bedrock map (contour interval, 1 hfu).

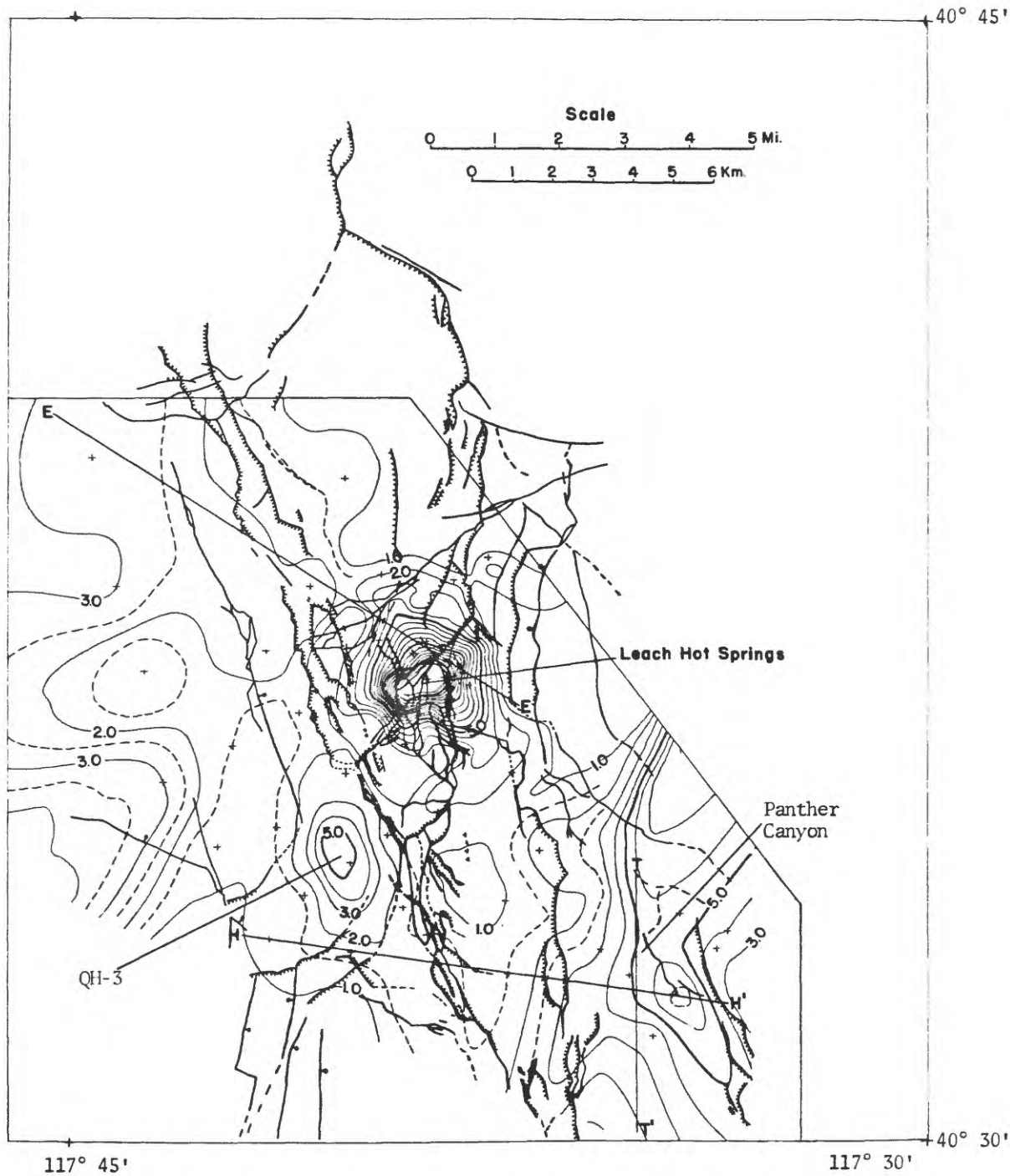

Figure 29. Heat-flow contours superimposed on a fault map of the Leach Hot Springs area (Noble, 1975). Contour interval, 1 hfu. Hachured lines indicate down-faulted sides of scarplets; ball symbol indicates downthrown side of other faults.

figure, we estimate a conductive flux of 1.7 x 10^6 cal/sec from the spring area. Combined with the convective discharge of $\sim$0.9 x 10^6 cal/sec (see Olmsted and others, 1975, p. 196-200), the net heat discharge from the spring system is thus 2.6 x 10^6 cal/sec.

If we assume that the heat discharge near the springs is balanced by recharge in other parts of our system, we may take the mean (weighted by area) of the heat fluxes as representing the heat flow from the entire "system." For the upper estimate of total area (300 km^2), this value is 3.3 hfu and for the smaller "system," the mean heat flow is 3.7 hfu. If we compare these values with the surrounding regional heat flows (Figure 1) we may conclude that the Leach system is in a "stationary stable" phase as defined by Lachenbruch and Sass (1977).

A suggested exploration strategy. Based on the extensive measurements of heat flow described above, we enumerate a few "rules of thumb" which might be useful in planning heat flow measurements for evaluation of similar systems:

1) Drill 5 to 10 deep (150 to 200 meters) holes spaced a few kilometers apart to obtain background heat flow and hydrologic data. Drill cuttings should be collected from all holes and as much coring as possible should be done to evaluate the range of conductivity and porosity within the region of interest. If possible, calibrated radiation logs (i.e., neutron and gamma-gamma) and sonic logs should be obtained in all holes so that empirical relations between the log parameters and thermal

conductivity can be established (e.g., Goss and Combs, 1976) and used for heat-flow calculations.

2) Drill 5 to 10 holes to depths below the water table (and below the zone of annual temperature variation) in the immediate discharge area to obtain data bearing on the heat flow and local "plumbing" (see e.g., Olmsted and others, 1975).

3) If no clear-cut relation is found between heat flow and shallow temperatures in phase 1, drill 10 to 20 intermediate depth holes (50-100 m) to delineate anomalous zones and possibly to extend coverage. If a reasonable average porosity value has been established in phase 1), coring can be kept to a minimum, and reasonable values of conductivity can be estimated from measurements on drill cuttings and calibrated geophysical logs.

4) If heat flow is found to be strongly related to shallow temperatures (15 - 20 m) in phase 1, as many shallow holes as considered necessary can be drilled within the area covered by phase 1 to provide the detail required to characterize the heat flow within the area.

No two areas are the same, of course, and for a given problem, various combinations of phases 1 through 4 and some novel approaches suited to the locality under study might have to be employed.

References

Beyer, H., Dey, A., Liaw, A., Majer, E., McEvilly, T. V., Morrison, H. F., and Wollenberg, H., 1976, Preliminary open file report, Geological and geophysical studies in Grass Valley, Nevada: LBL-5262.

Birch, F., 1950, Flow of heat in the Front Range, Colorado: Geol. Soc. America Bull., v. 61, 567-630.

Blackwell, D. D., 1973, Surface ground temperature variations in mountainous regions and a new topographic correction technique for heat flow measurements (abstract): EOS (Am. Geophys. Union Trans.), v. 54, p. 1207.

Clark, S. P., and Niblett, E. R., 1956, Terrestrial heat flow in the Swiss Alps: Royal Astron. Soc. Monthly Notices, Geophys. Suppl., v. 7, p. 176-195.

Ferguson, H. G., Muller, S. W., and Roberts, R. J., 1951, Geology of the Winnemucca Quadrangle, Nevada: U.S. Geol. Survey Geol. Quad. Map 11.

Fournier, R. O., White, D. E., and Truesdell, A. H., 1974, Geochemical indicators of subsurface temperature, Part I, Basic assumptions: U.S. Geol. Survey Jour. Research, v. 2, no. 3, p. 259-262.

Goss, R., and Combs, J., 1976, Thermal conductivity measurement and prediction from geophysical well log parameters with borehole application, in Second U. N. Symposium on the Development and Use of Geothermal Resources, Proceedings (San Francisco, Calif., May 20-29, 1975): U.S. Government Printing Office, v. 2, p. 1019-1027.

Grannell, R. B., 1977, A detailed analysis of Basin and Range faulting, Grass Valley area, north-central Nevada (abstract): Geol. Soc. America, Cordilleran Sec. Ann. Mtg., 73rd, Sacramento, California, 1977, Abstracts with Programs, v. 9, no. 4, p. 424.

Lachenbruch, A. H., and Marshall, B. V., 1966, Heat flow through the Arctic Ocean floor: The Canada Basin - Alpha Rise boundary: Jour. Geophys. Research, v. 71, no. 4, p. 1223-1248.

Lachenbruch, A. H., and Sass, J. H., 1977, Heat flow in the United States and the thermal regime of the crust, in Am. Geophys. Union Geophys. Monogr., 20, edited by J. G. Heacock: AGU, Washington, D. C., in press.

Langseth, M. G., 1965, Techniques of measuring heat flow through the ocean floor, in Terrestrial Heat Flow, Geophys. Monogr. Ser., vol. 8, edited by W. H. K. Lee: AGU, Washington, D. C., p. 58-77.

Manger, G. E., 1963, Porosity and bulk density of sedimentary rocks: U.S. Geol. Survey Bull. 1144-E.

Mariner, R. H., Rapp, J. B., Willey, L. M., and Presser, T. S., 1974, The chemical composition and estimated minimum thermal reservoir temperatures of the principal hot springs of northern and central Nevada: U.S. Geol. Survey Open-File Report, 32 p.

Nichols, K. M., 1972, Triassic depositional history of China Mountain and vicinity, north-central Nevada: Ph.D. Thesis, Stanford University.

Noble, D. C., 1975, Geologic history and geothermal potential of the Leach Hot Springs area, Pershing County, Nevada: Preliminary Report to the Lawrence Berkeley Laboratory.

Olmsted, F. H., Glancy, P. A., Harrill, J. R., Rush, F. E., and VanDenburgh, A. S., 1975, Preliminary hydrogeologic appraisal of selected hydrothermal systems in northern and central Nevada: U.S. Geol. Survey Open-File Report 75-56, 267 pp.

Roberts, R. J., Hotz, P. E., Gilluly, J., and Ferguson, H. G., 1958, Paleozoic rocks of north-central Nevada: Am. Assoc. Petroleum Geologists Bull., v. 42, no. 12, p. 2813-2857.

Sass, J. H., Clark, S. P., Jr., and Jaeger, J. C., 1967, Heat flow in the Snowy Mountains of Australia: Jour. Geophys. Research, v. 72, no. 10, p. 2635-2647.

Sass, J. H., Lachenbruch, A. H., and Munroe, R. J., 1971a, Thermal conductivity of rocks from measurements on fragments and its application to heat-flow determinations: Jour. Geophys. Research, v. 76, no. 14, p. 3391-3401.

Sass, J. H., Lachenbruch, A. H., Munroe, R. J., Greene, G. W., and Moses, T. H., Jr., 1971, Heat flow in the western United States: Jour. Geophys. Research, v. 76, p. 6376-6413.

Sass, J. H., Olmsted, F. H., Sorey, M. L., Wollenberg, H. A., Lachenbruch, A. H., Munroe, R. J., and Galanis, S. P., Jr., 1976, Geothermal data from test wells drilled in Grass Valley and Buffalo Valley, Nevada: U.S. Geol. Survey Open-File Report 76-85.

Silberling, N. J., 1975, Age relationships of the Golconda thrust fault, Sonoma Range, north-central Nevada: Geol. Soc. America Special Paper 163.

Silberman, M. L., and McKee, E. H., 1971, K-Ar ages of granite plutons in north-central Nevada: Isochron/West, No. 71-1, p. 15-32.

Von Herzen, R. P., and Maxwell, A. E., 1959, The measurement of thermal conductivity of deep-sea sediments by a needle-probe method: Jour. Geophys. Research, v. 64, no. 10, p. 1557-1563.

Wollenberg, H. A., Asaro, F., Bowman, H., McEvilly, T., Morrison, H. F., and Witherspoon, P., 1975, Geothermal energy resource assessment: Lawrence Berkeley Laboratory, Report UCID-3762.

Woodside, W., and Messmer, J. H., 1961, Thermal conductivity of porous media: Jour. Appl. Physics, v. 32, p. 1688.

APPENDIX A

Lithologic summaries, thermal conductivities, and temperature profiles for Q and QH holes.

Figure A-0 explains the abbreviations and symbols used in the remainder of the figures (A-1 through A-28). All of the temperature profiles shown were obtained between October 29 and November 3, 1976, at least six weeks and up to four months after completion of the holes. Spot checks in the spring of 1977 confirmed that the holes were in thermal equilibrium below the zone of annual variation (10-15 m).

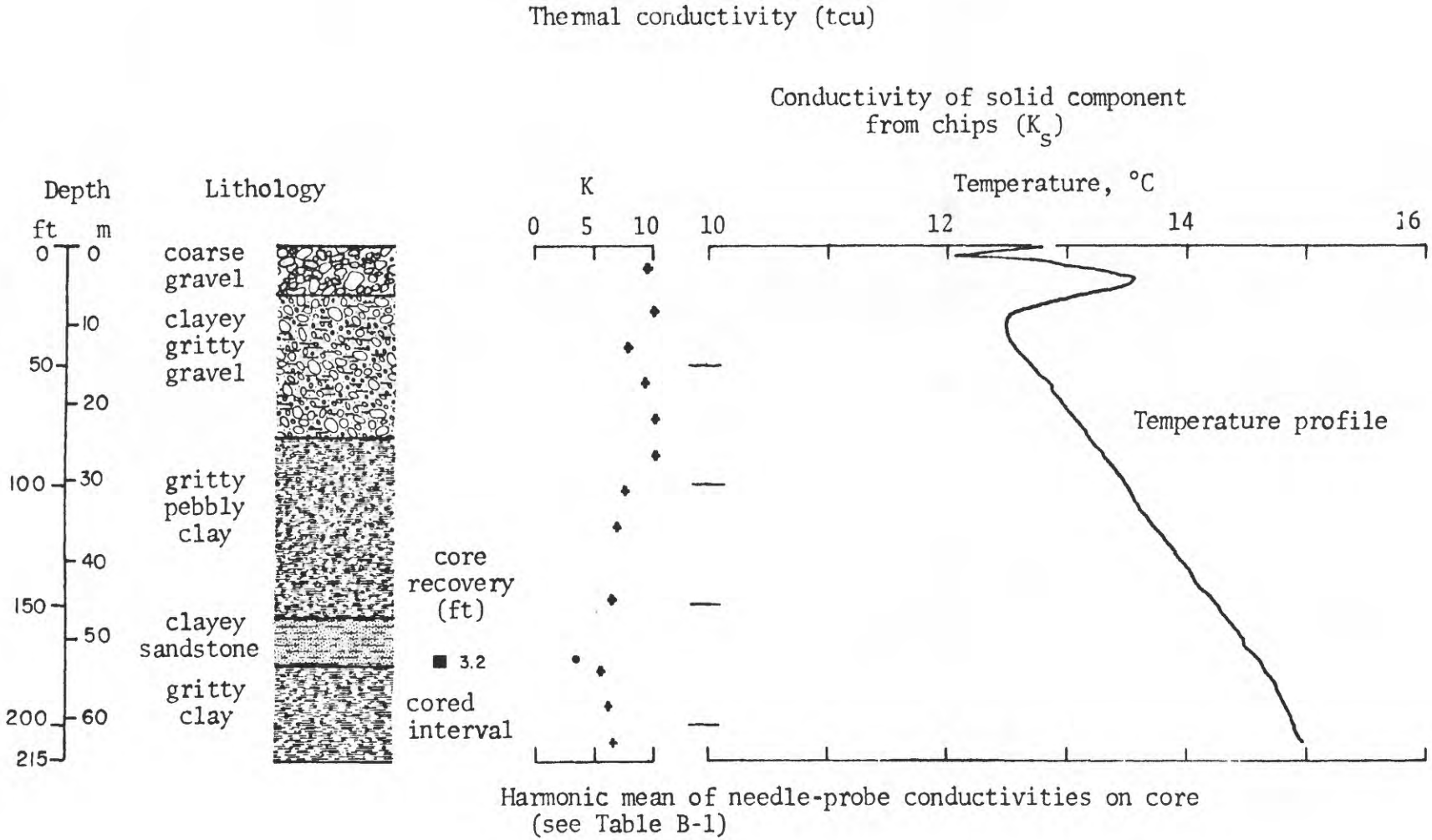

Figure A-0. Example of format used in presentation of basic data (Figures A-1 - A-28).

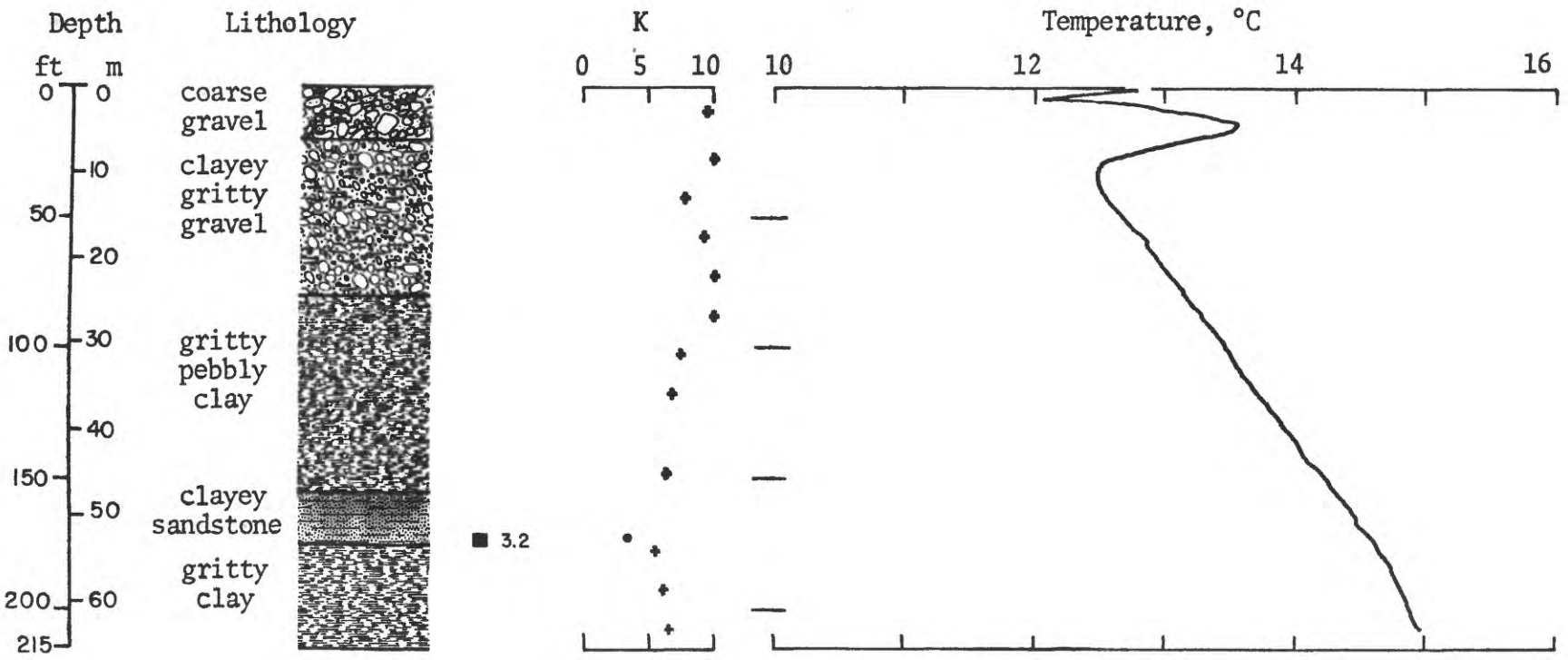

Figure A-1. Lithology, thermal conductivity, and temperature profile for hole Q-4.

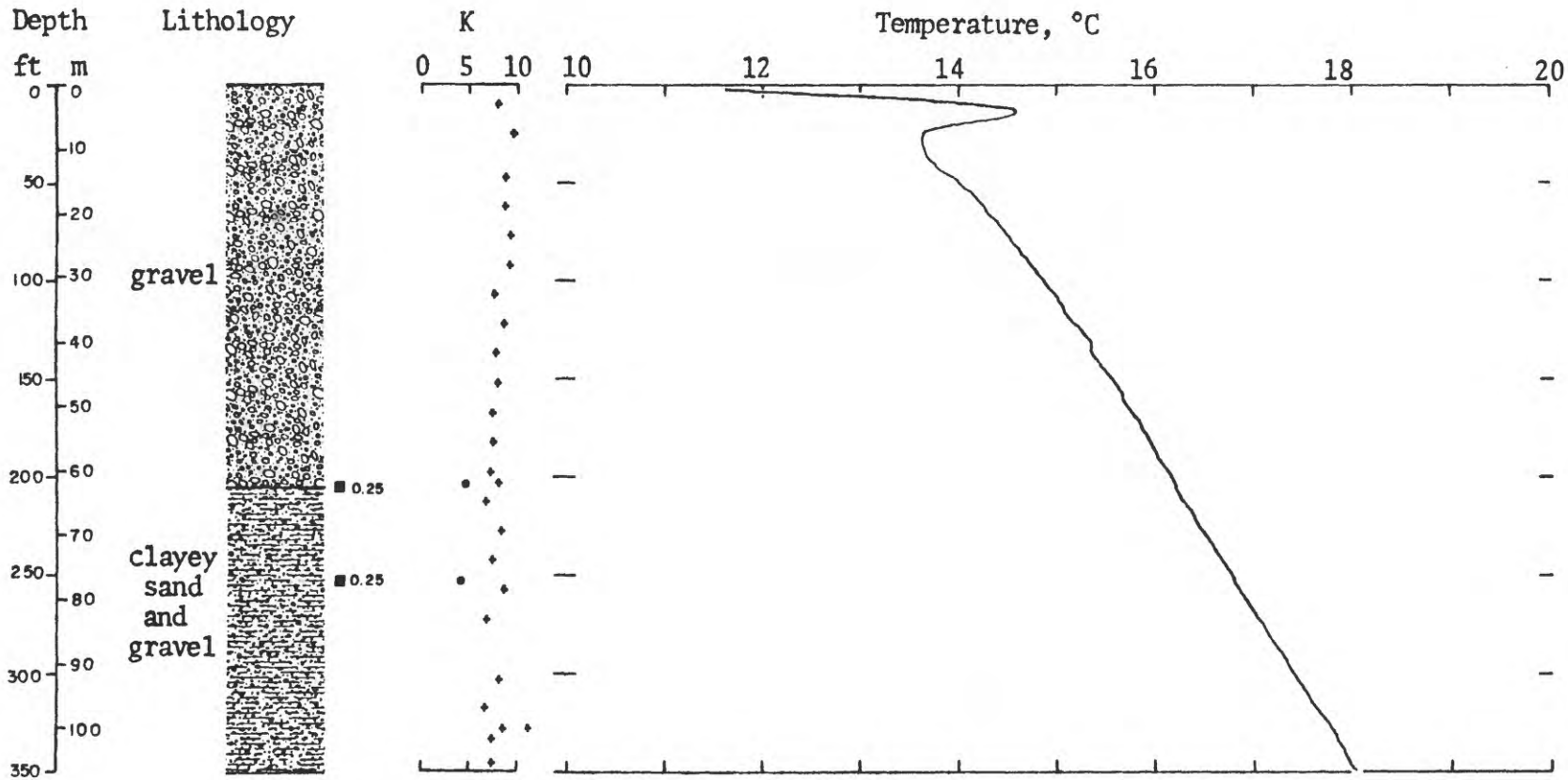

Figure A-2. Lithology, thermal conductivity, and temperature profile for hole Q-5.

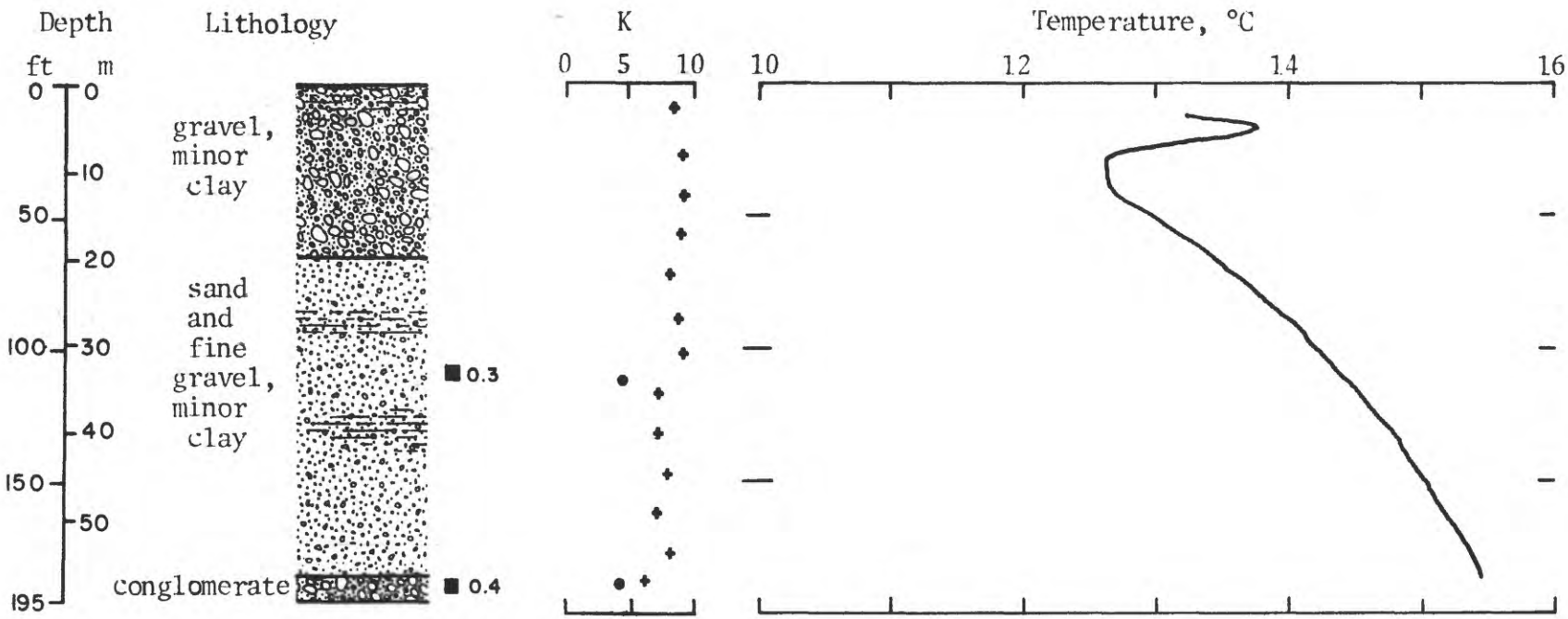

Figure A-3. Lithology, thermal conductivity, and temperature profile for hole Q-6.

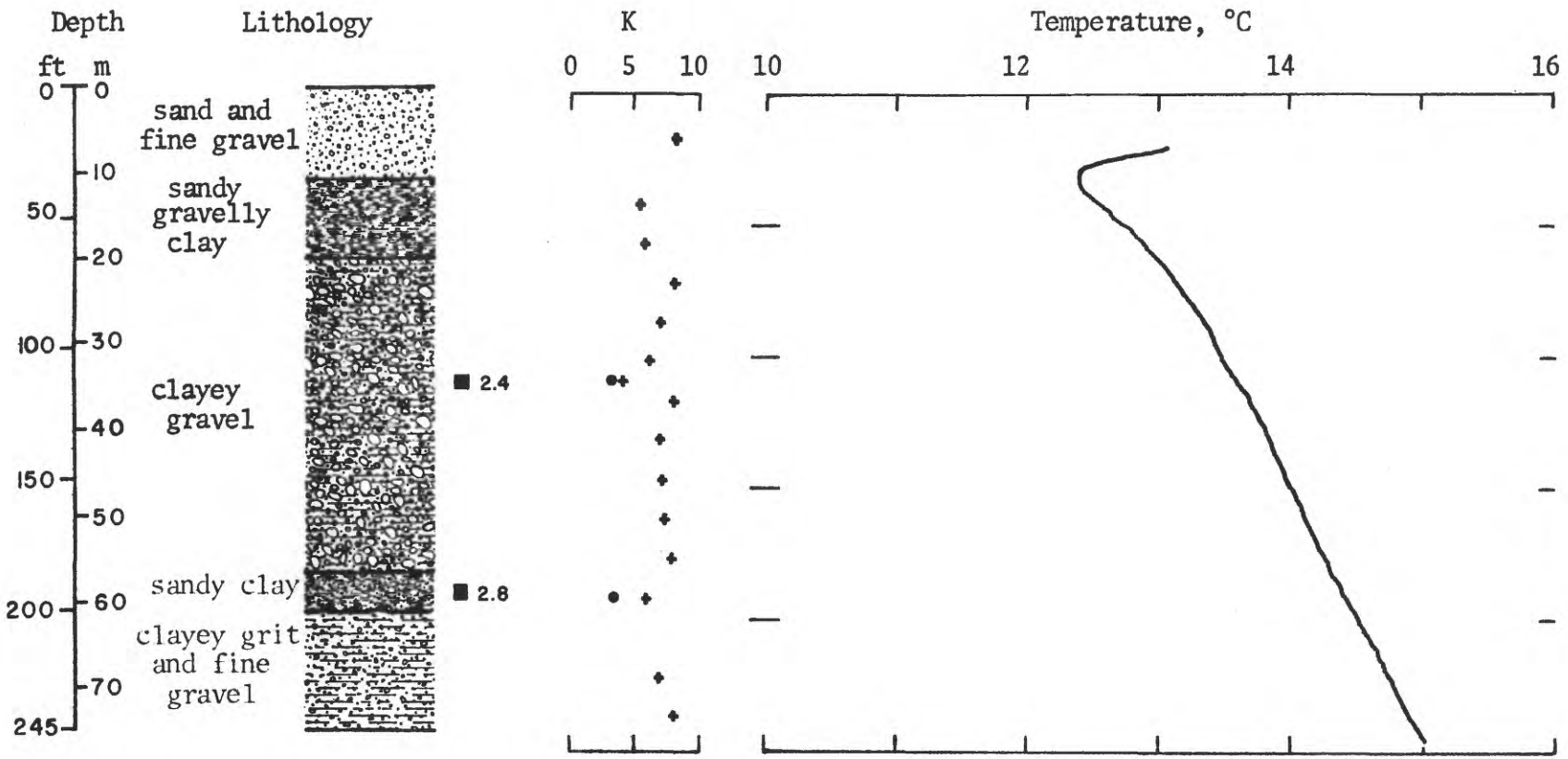

Figure A-4. Lithology, thermal conductivity, and temperature profile for hole Q-7.

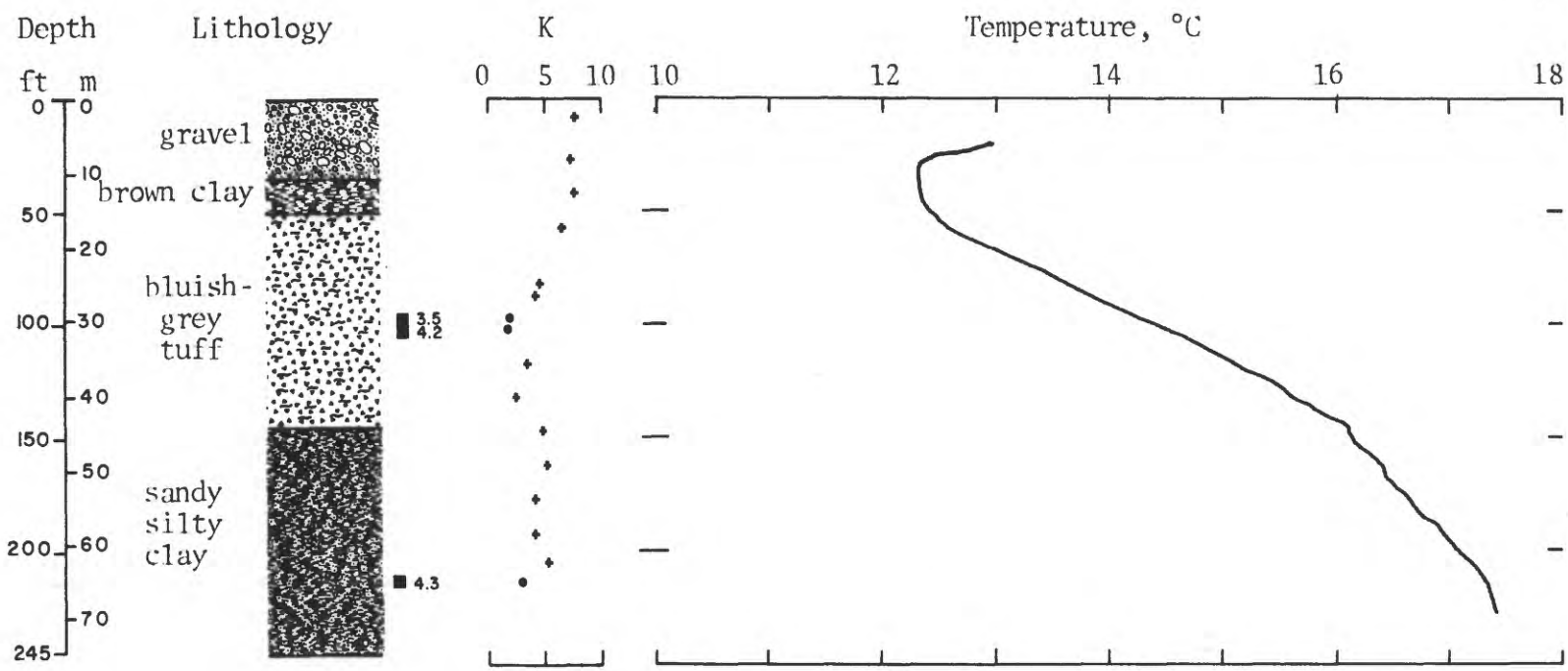

Figure A-5. Lithology, thermal conductivity, and temperature profile for hole Q-8.

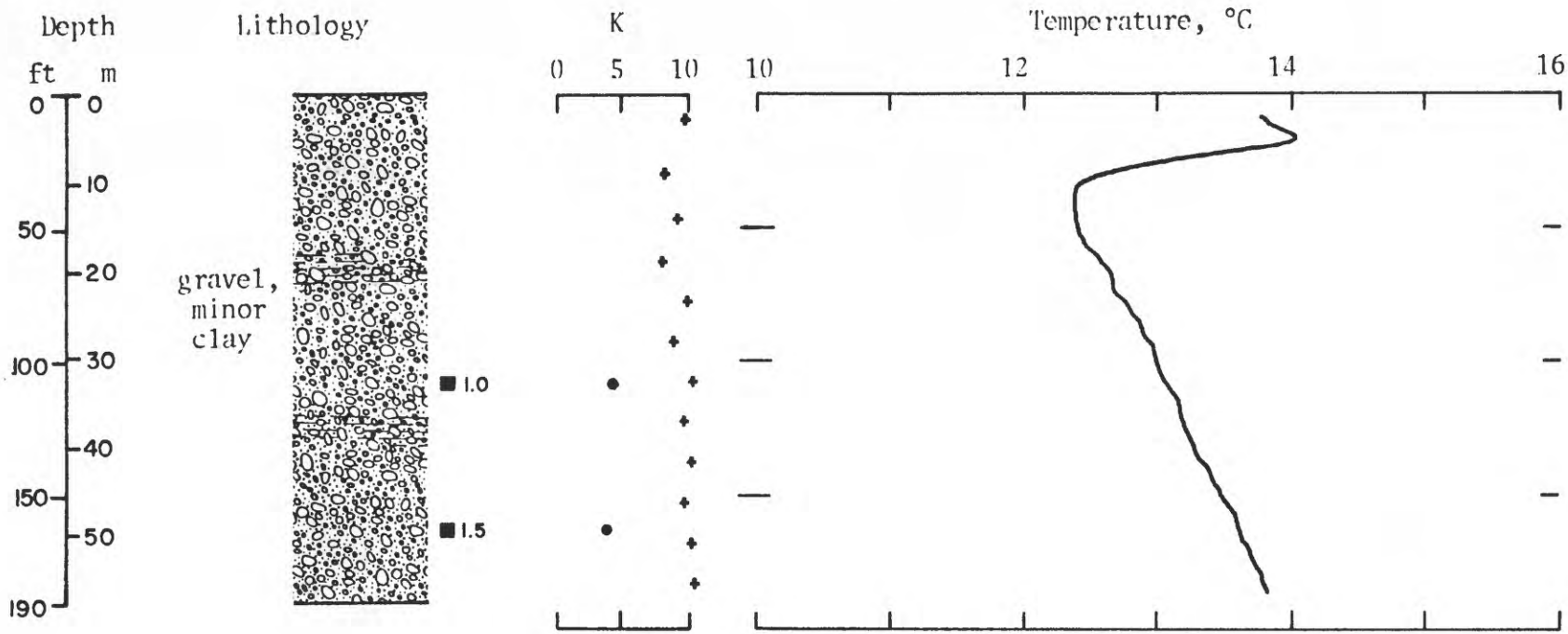

Figure A-6. Lithology, thermal conductivity, and temperature profile for hole Q-9.

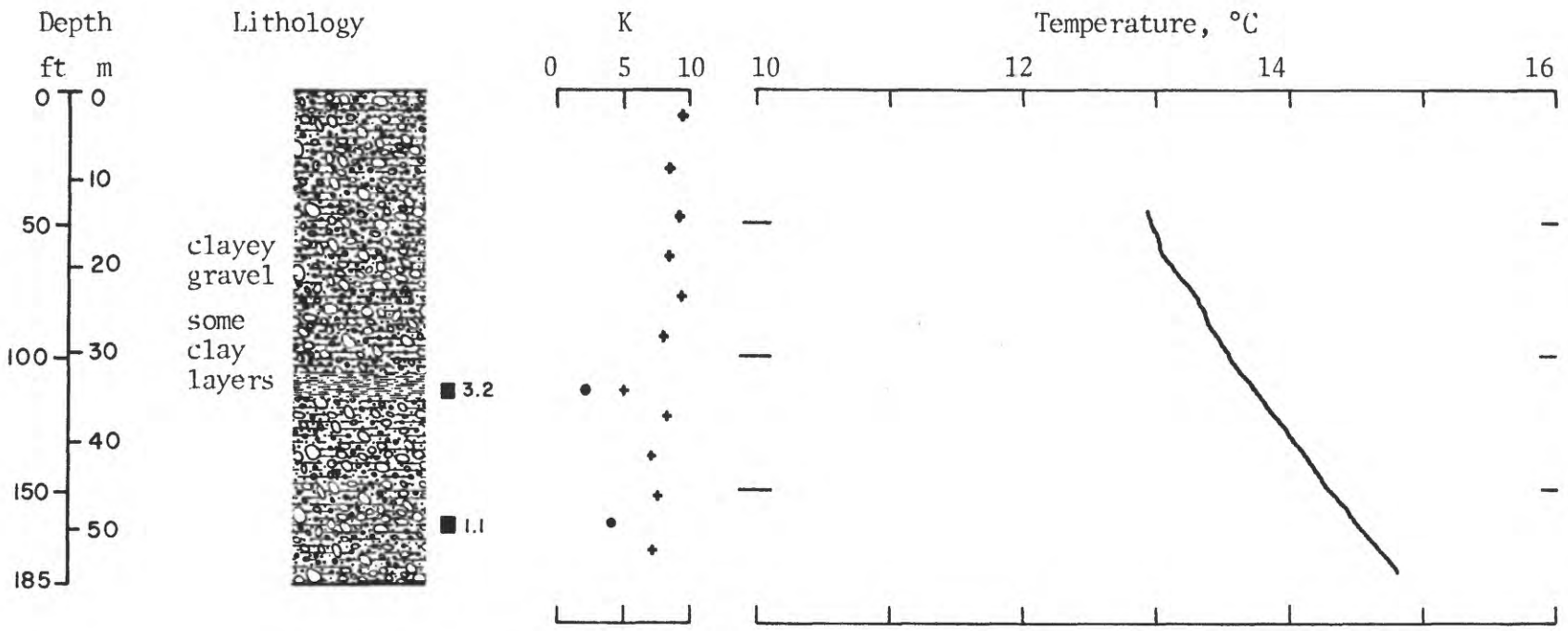

Figure A-7. Lithology, thermal conductivity, and temperature profile for hole Q-10.

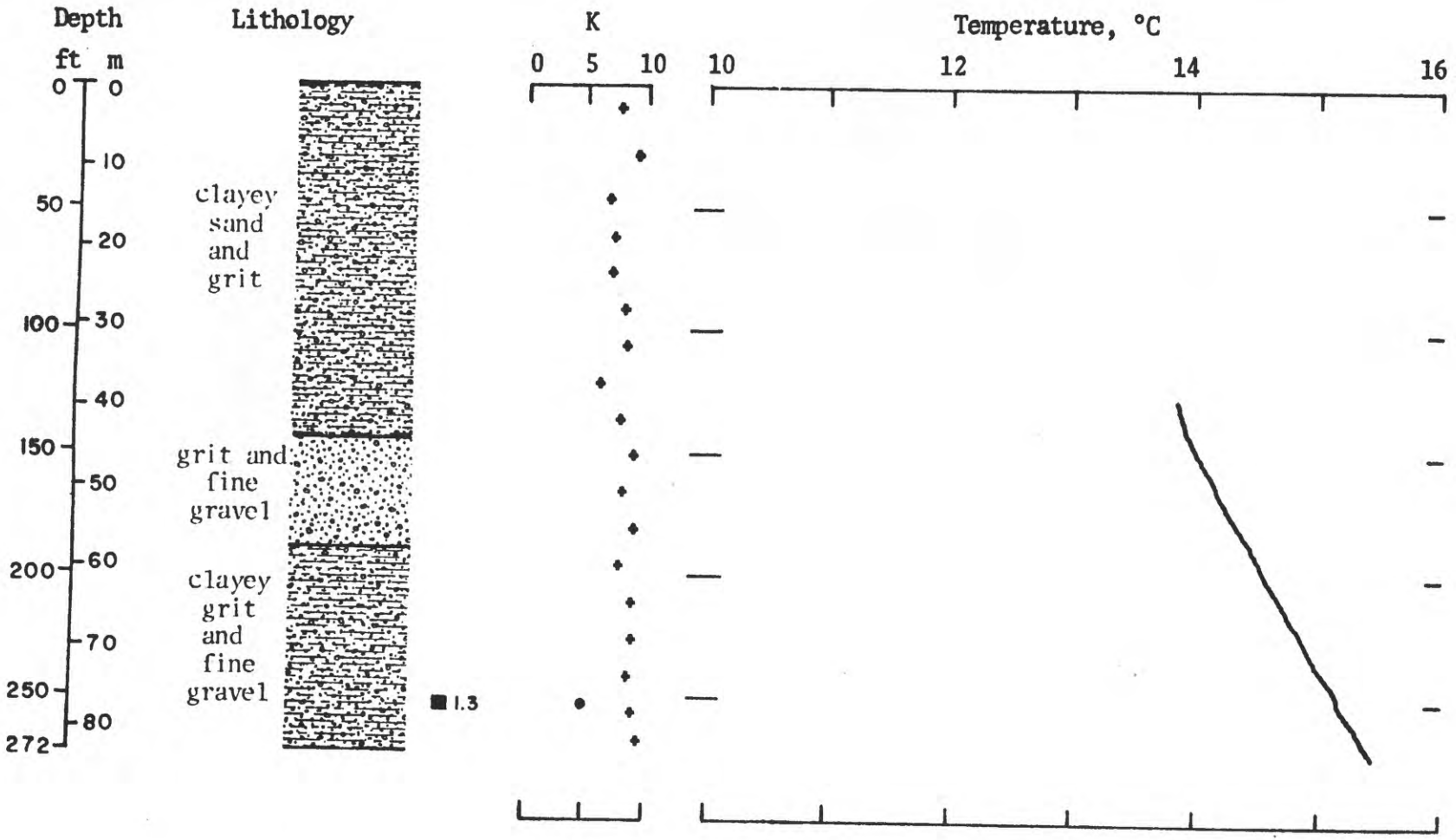

Figure A-8. Lithology, thermal conductivity, and temperature profile for hole Q-11.

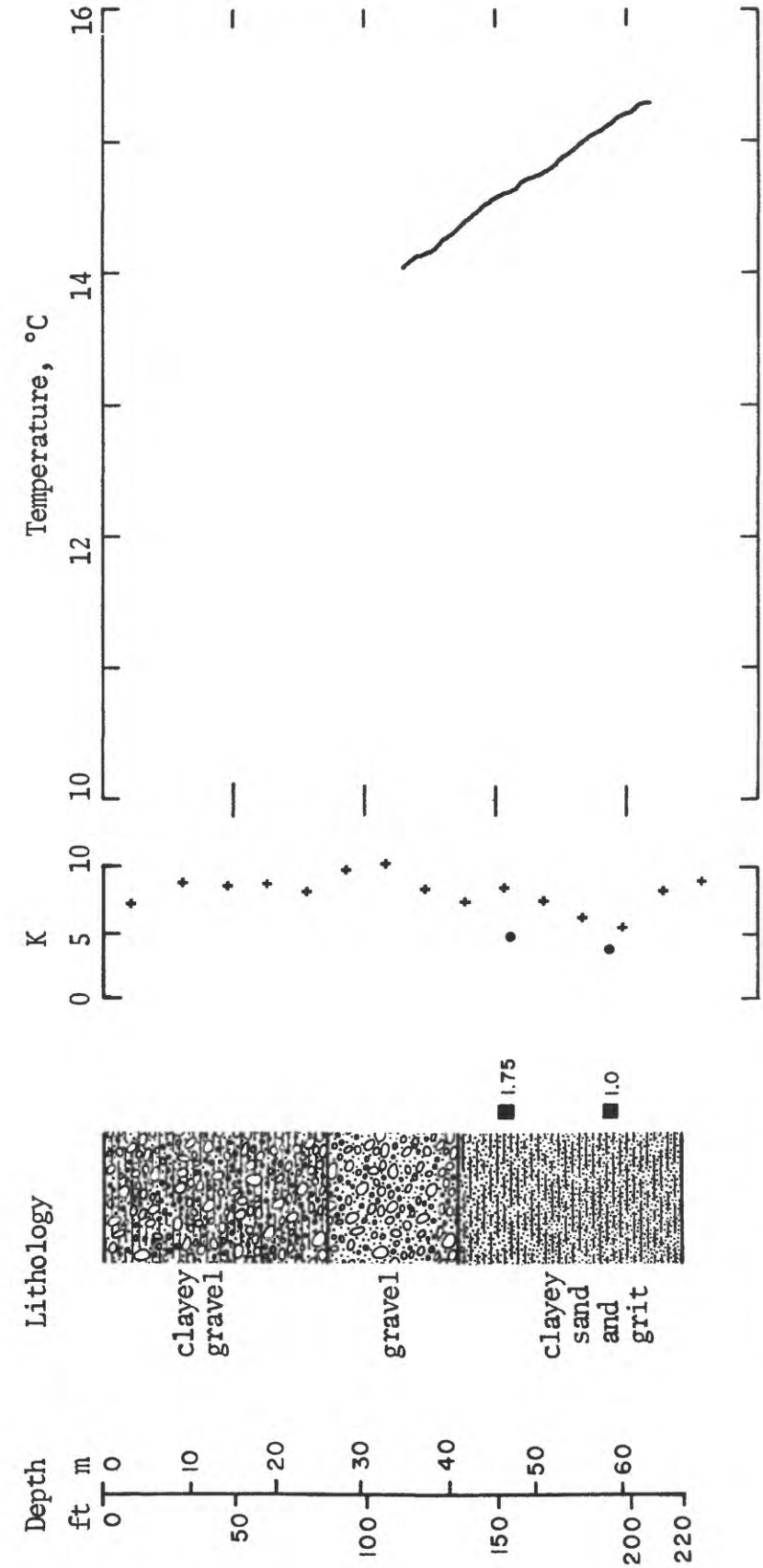

Figure A-9. Lithology, thermal conductivity, and temperature profile for hole Q-12.

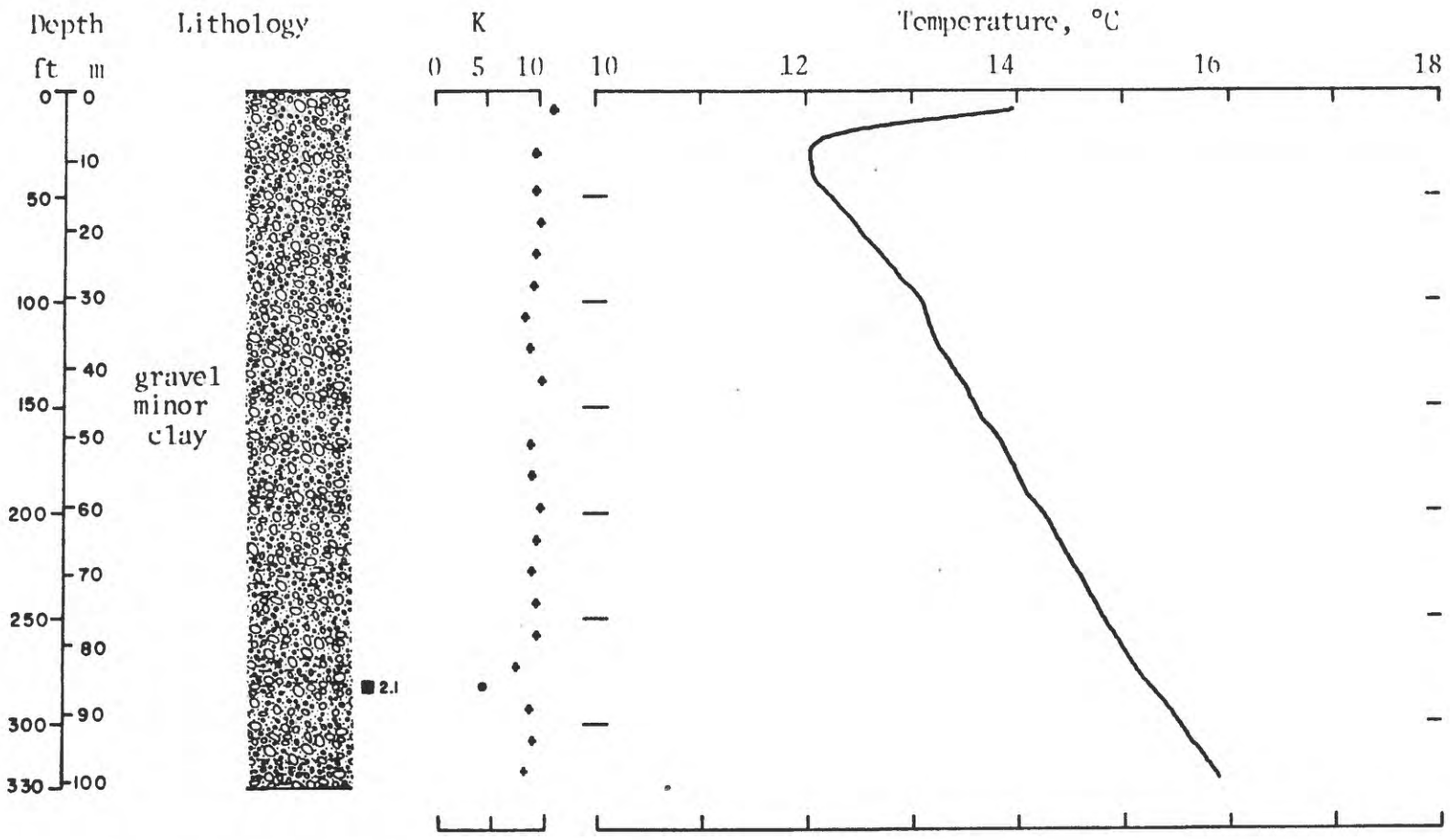

Figure A-10. Lithology, thermal conductivity, and temperature profile for hole Q-13.

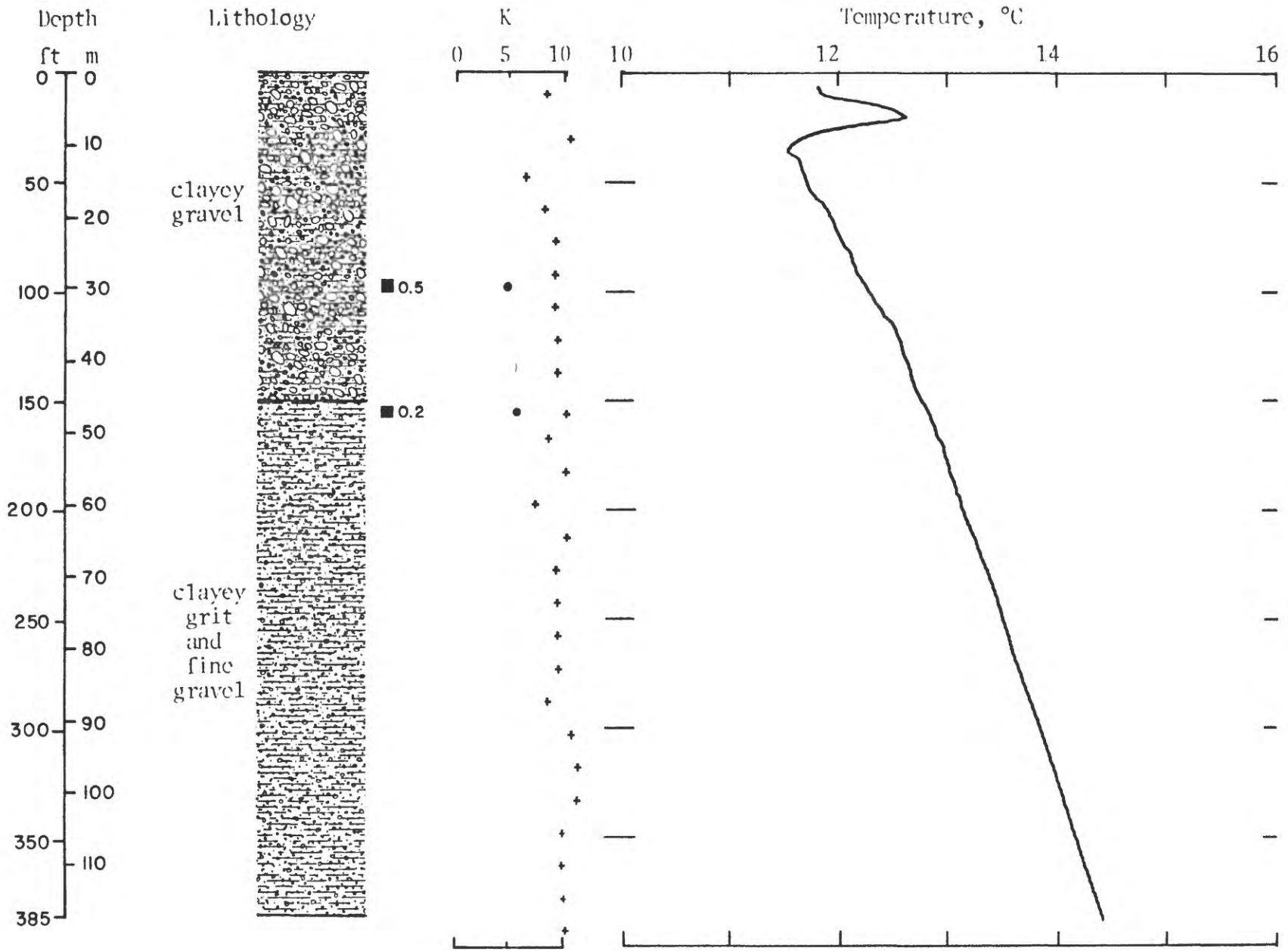

Figure A-11. Lithology, thermal conductivity, and temperature profile for hole Q-13.

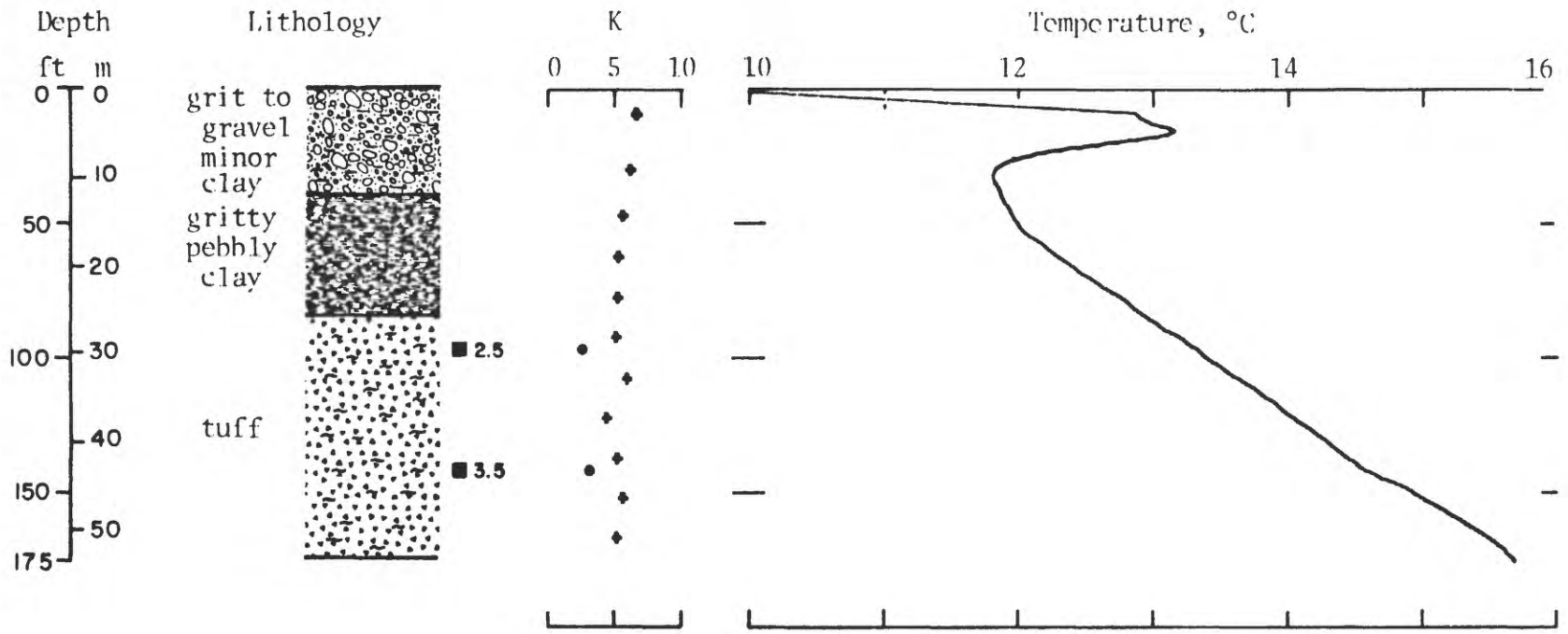

Figure A-12. Lithology, thermal conductivity, and temperature profile for hole Q-15.

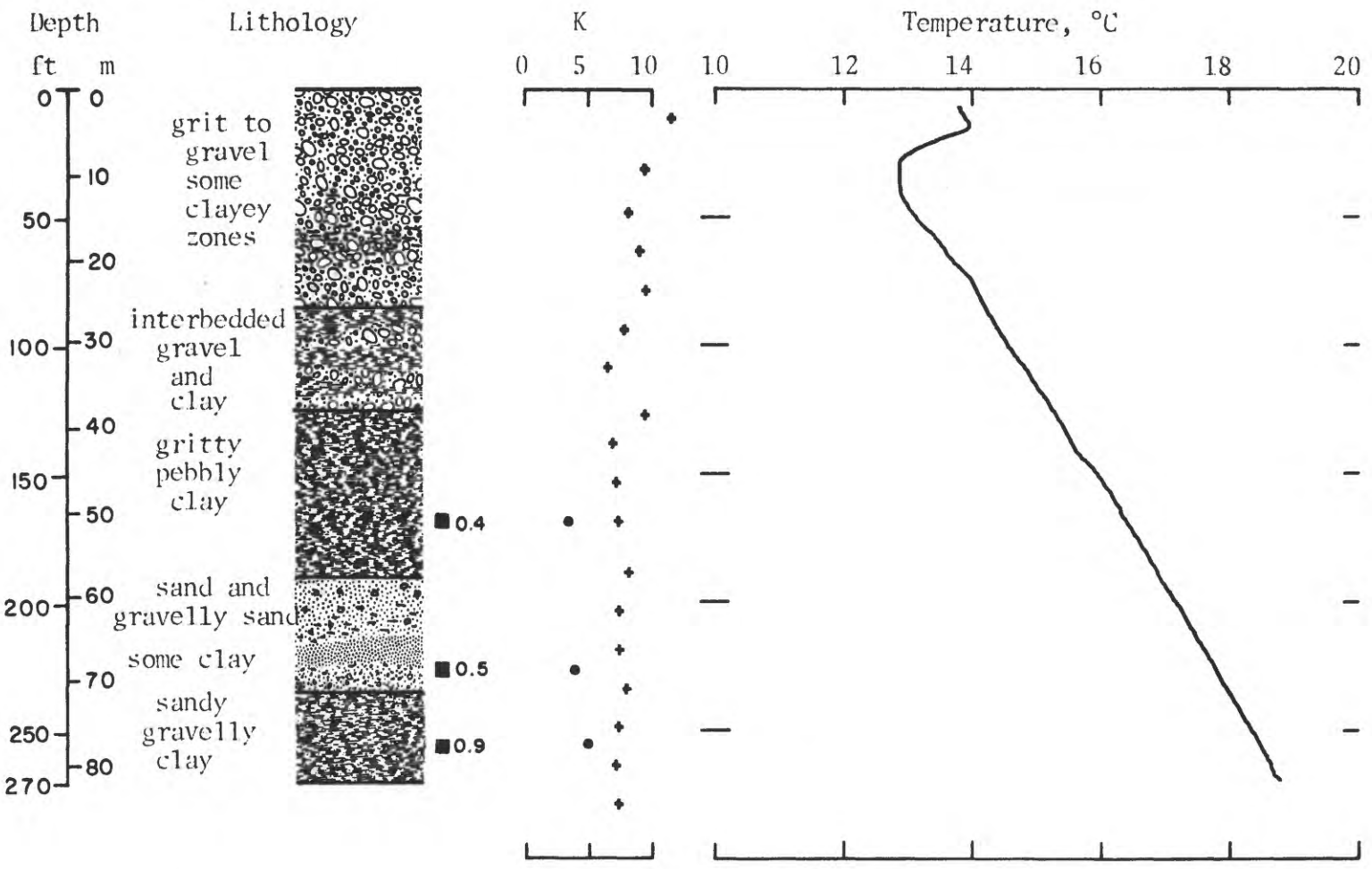

Figure A-13. Lithology, thermal conductivity, and temperature profile for hole Q-16.

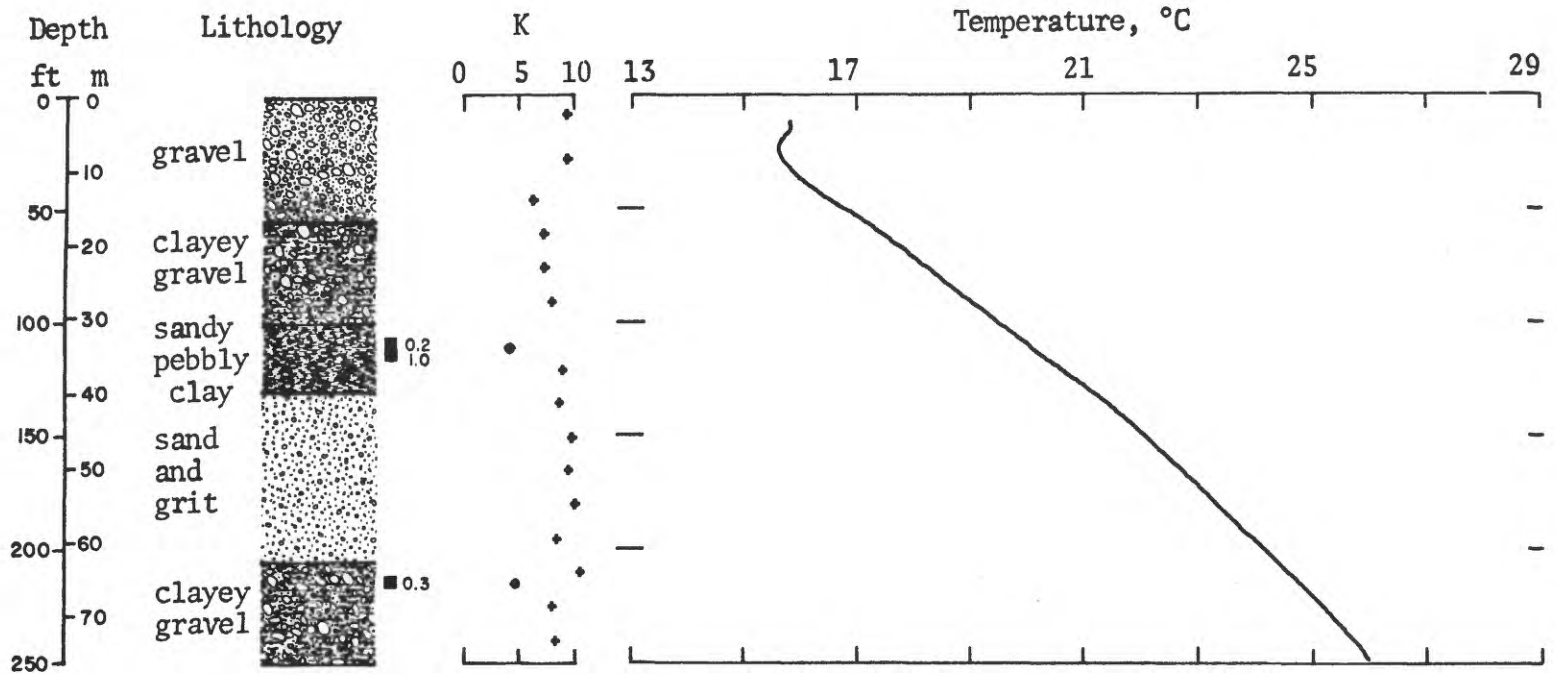

Figure A-14. Lithology, thermal conductivity, and temperature profile for hole Q-17.

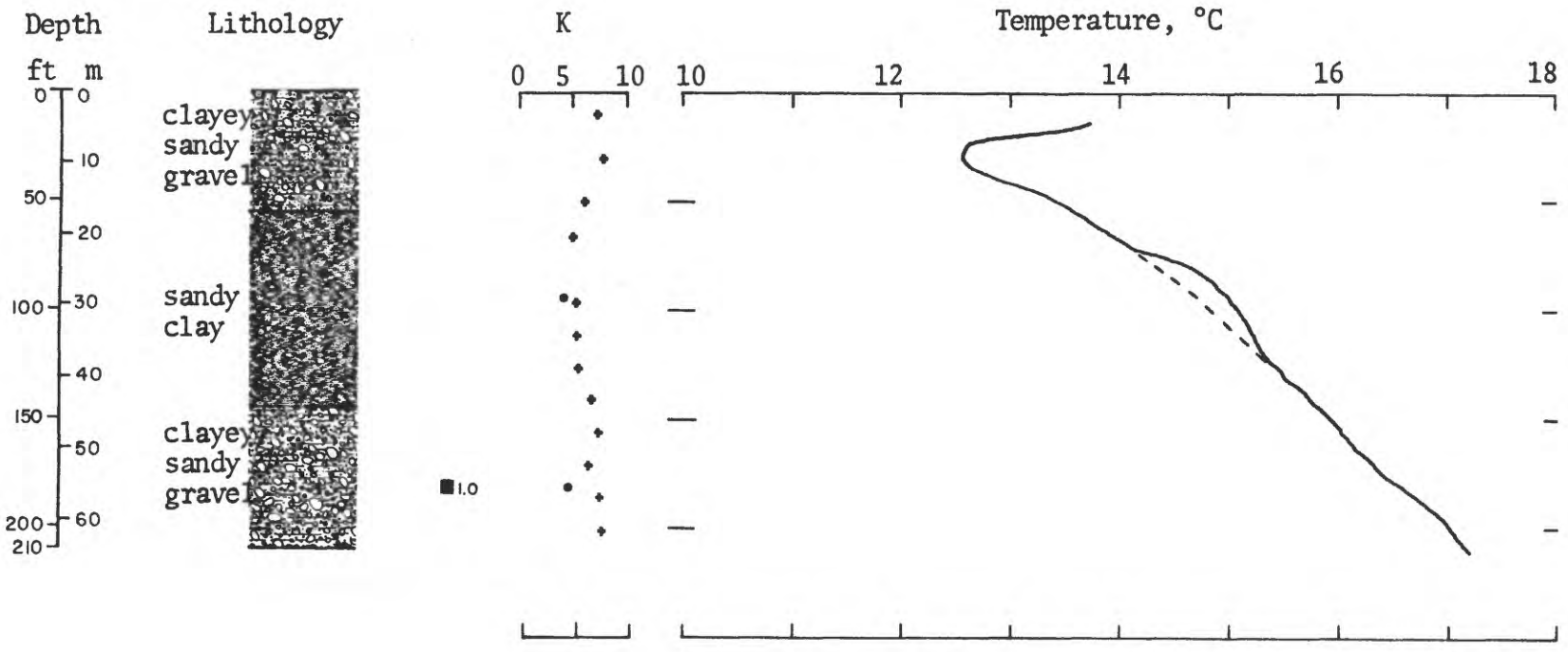

Figure A-15. Lithology, thermal conductivity, and temperature profile for hole Q-18.

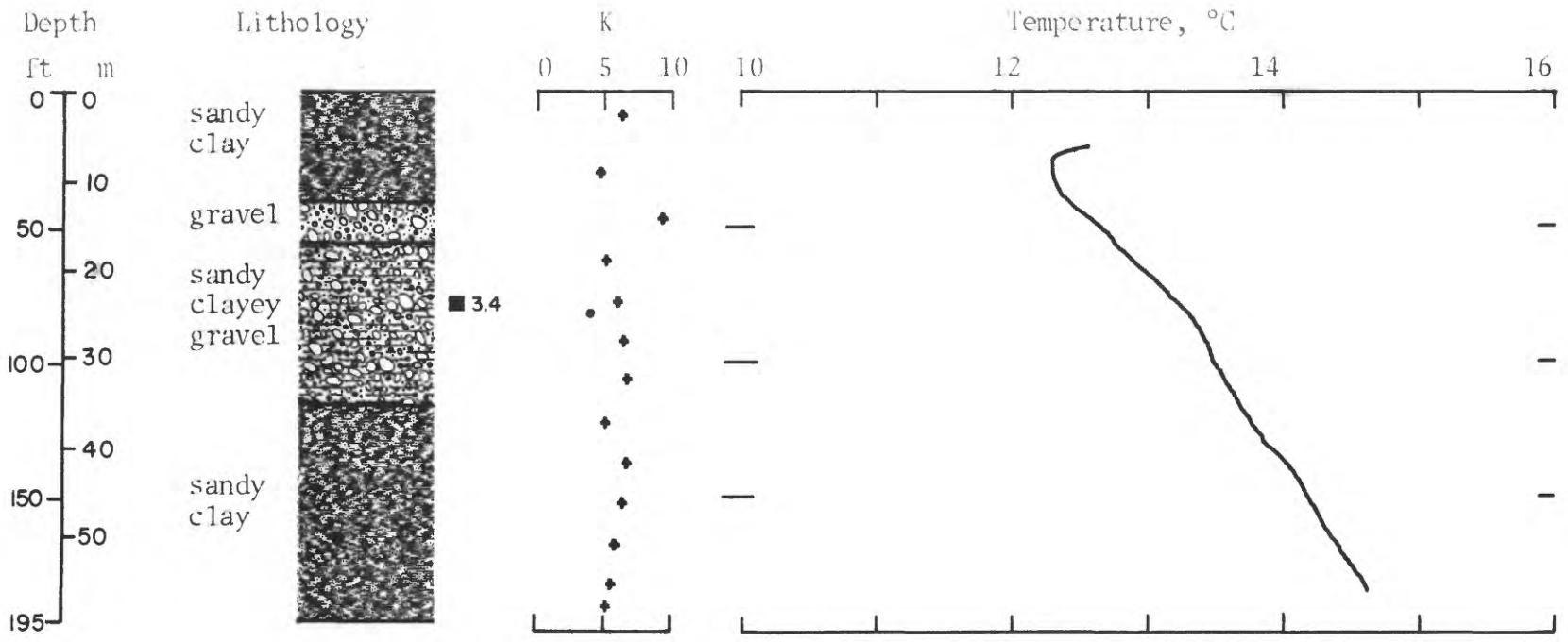

Figure A-16. Lithology, thermal conductivity, and temperature profile for hole Q-19.

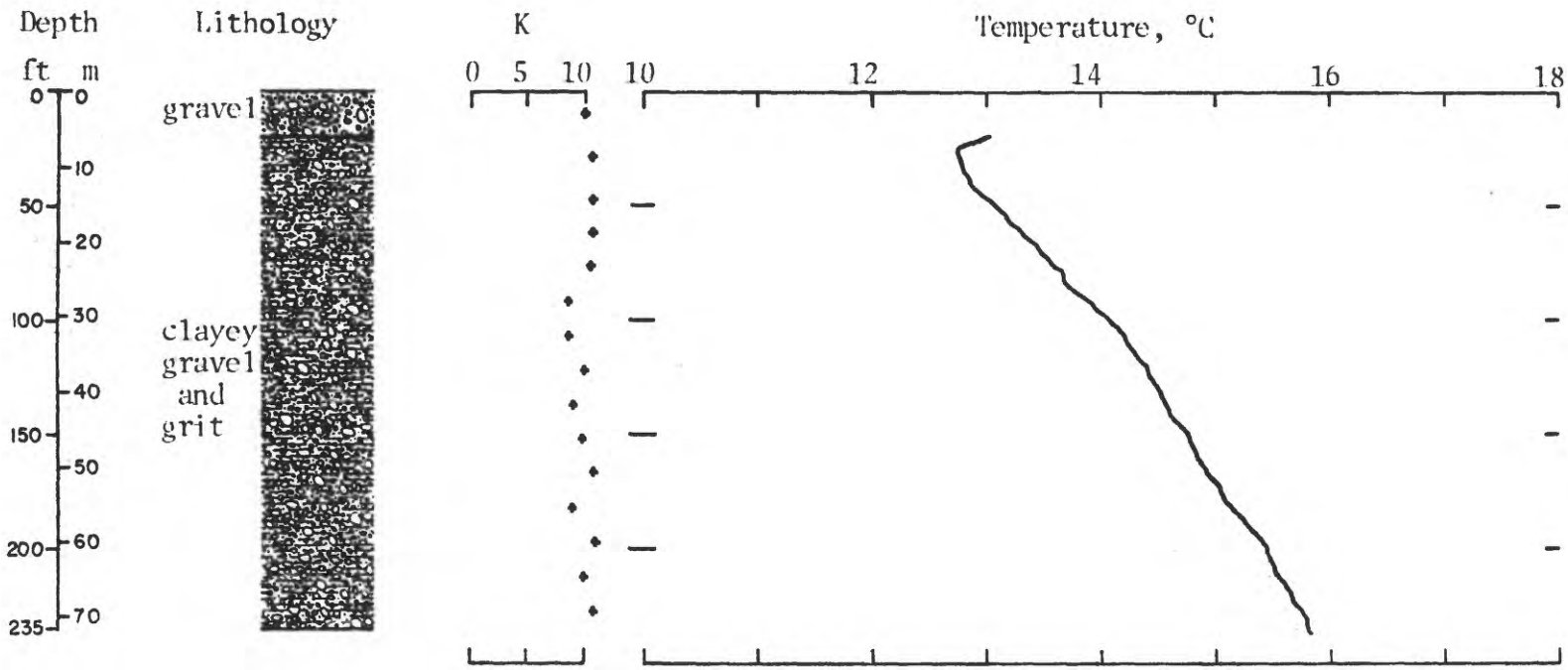

Figure A-17. Lithology, thermal conductivity, and temperature profile for hole Q-20.

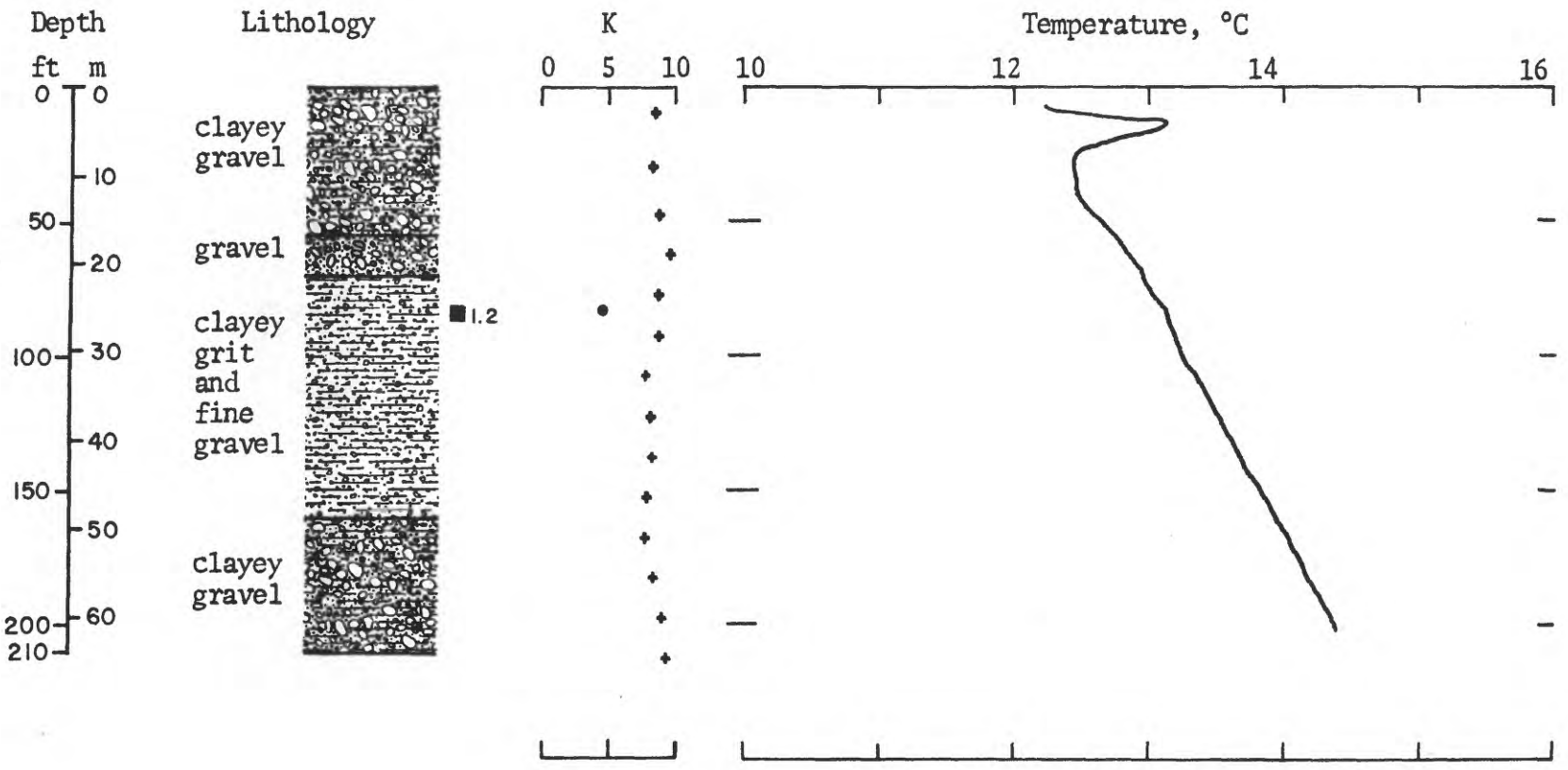

Figure A-18. Lithology, thermal conductivity, and temperature profile for hole Q-21.

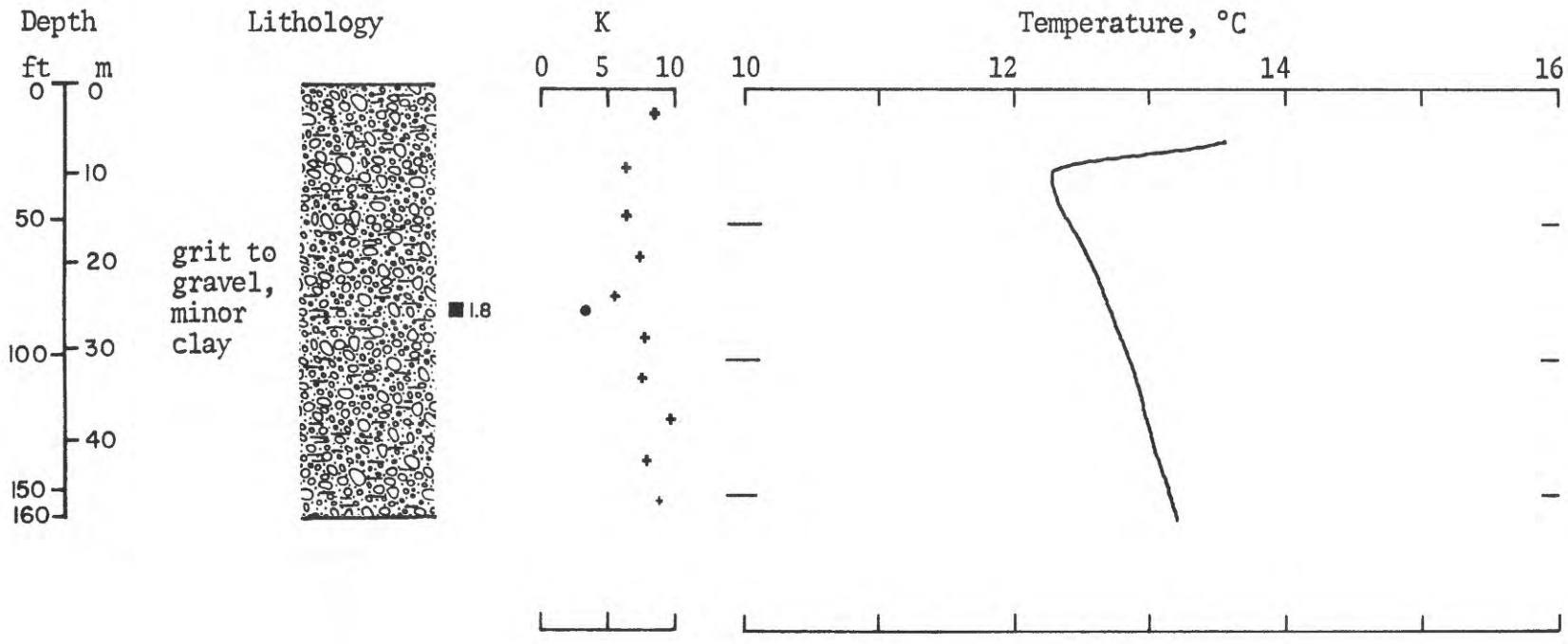

Figure A-19. Lithology, thermal conductivity, and temperature profile for hole Q-22.

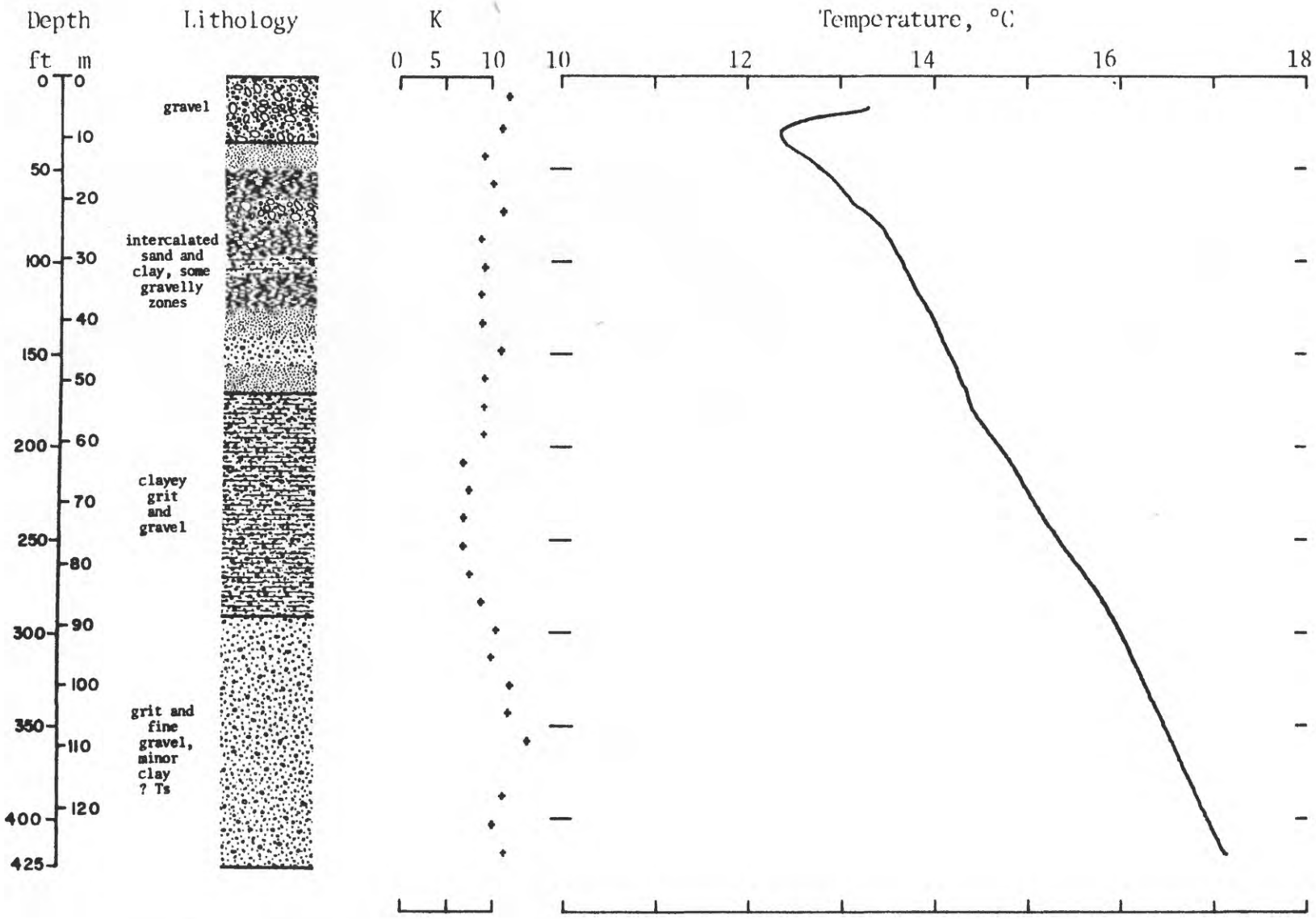

Figure A-20. Lithology, thermal conductivity, and temperature profile for hole QH-5.

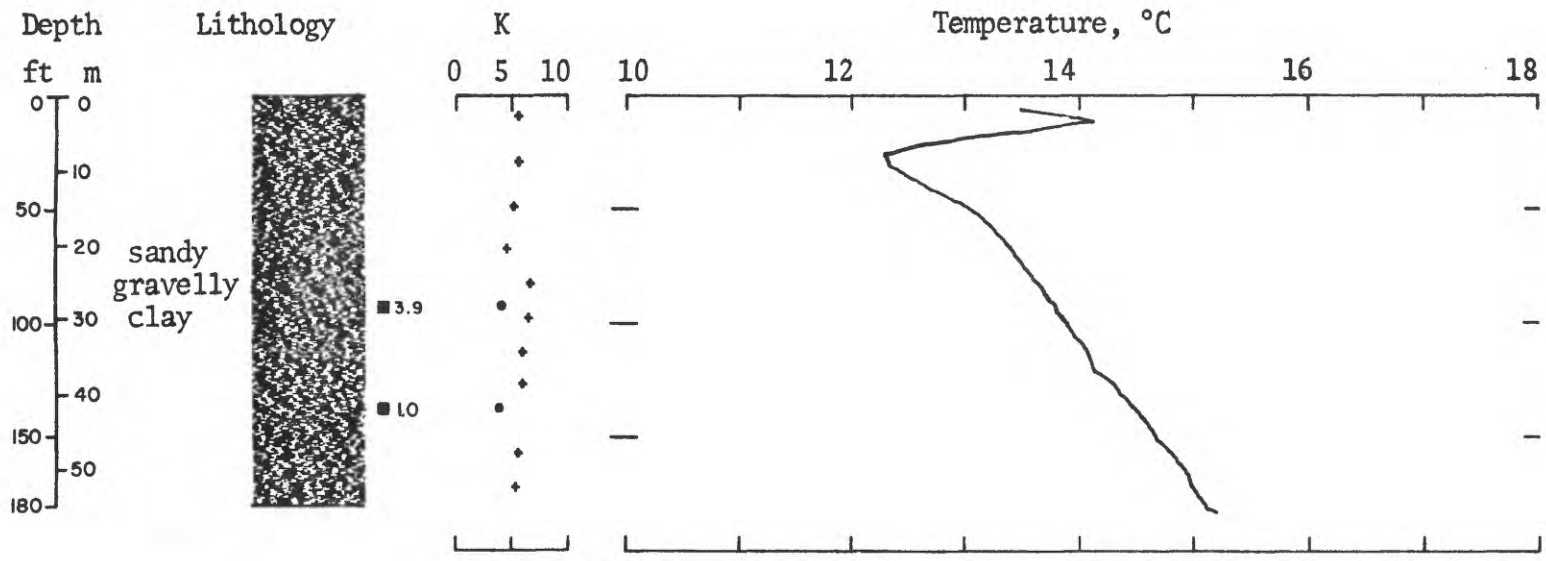

Figure A-21. Lithology, thermal conductivity, and temperature profile for hole QH-6.

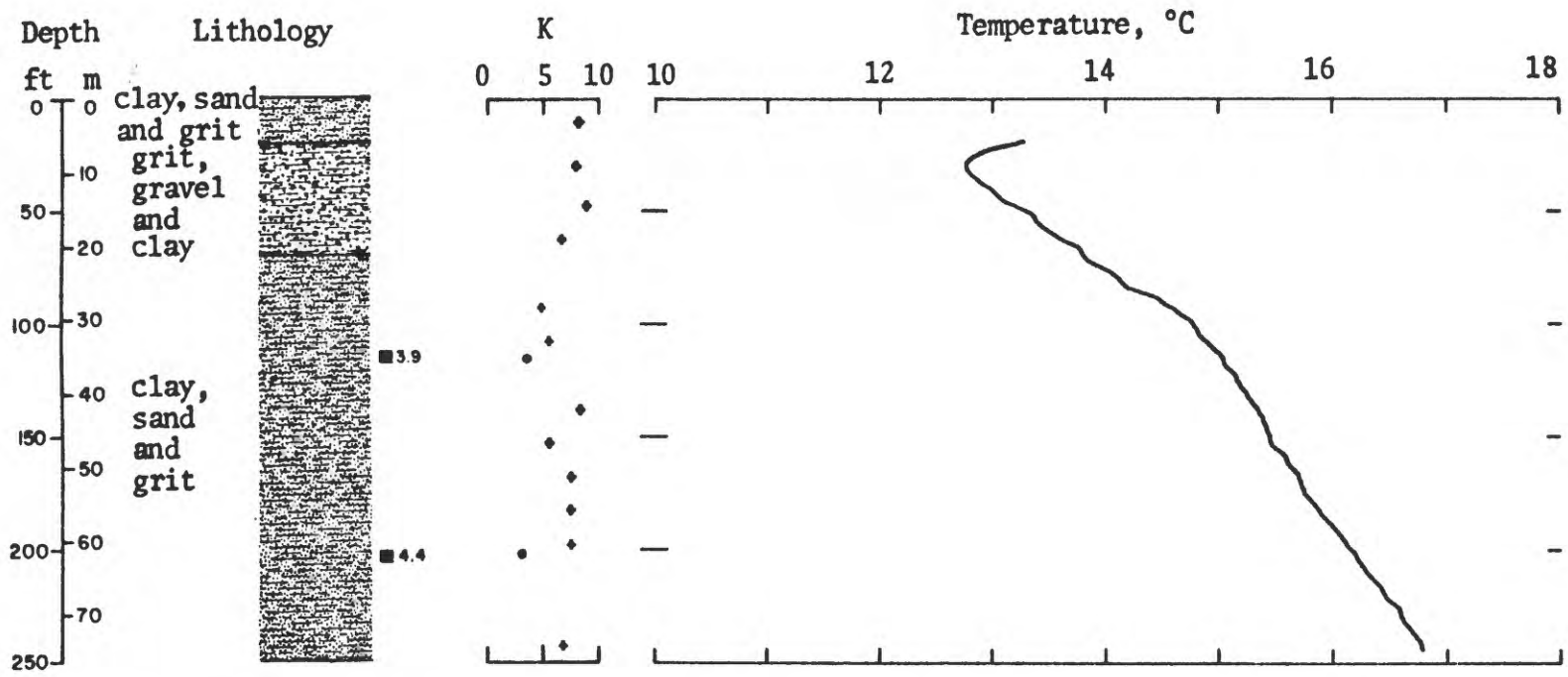

Figure A-22. Lithology, thermal conductivity, and temperature profile for hole QH-7.

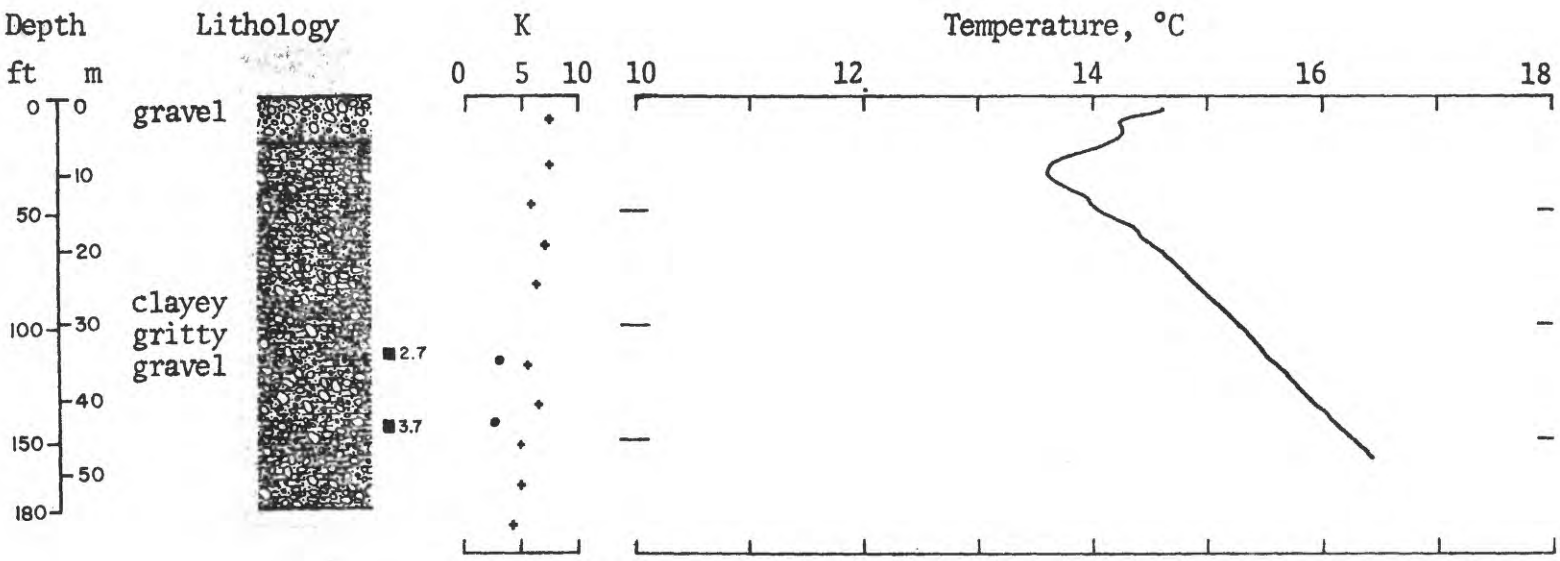

Figure A-23. Lithology, thermal conductivity, and temperature profile for hole QH-8.

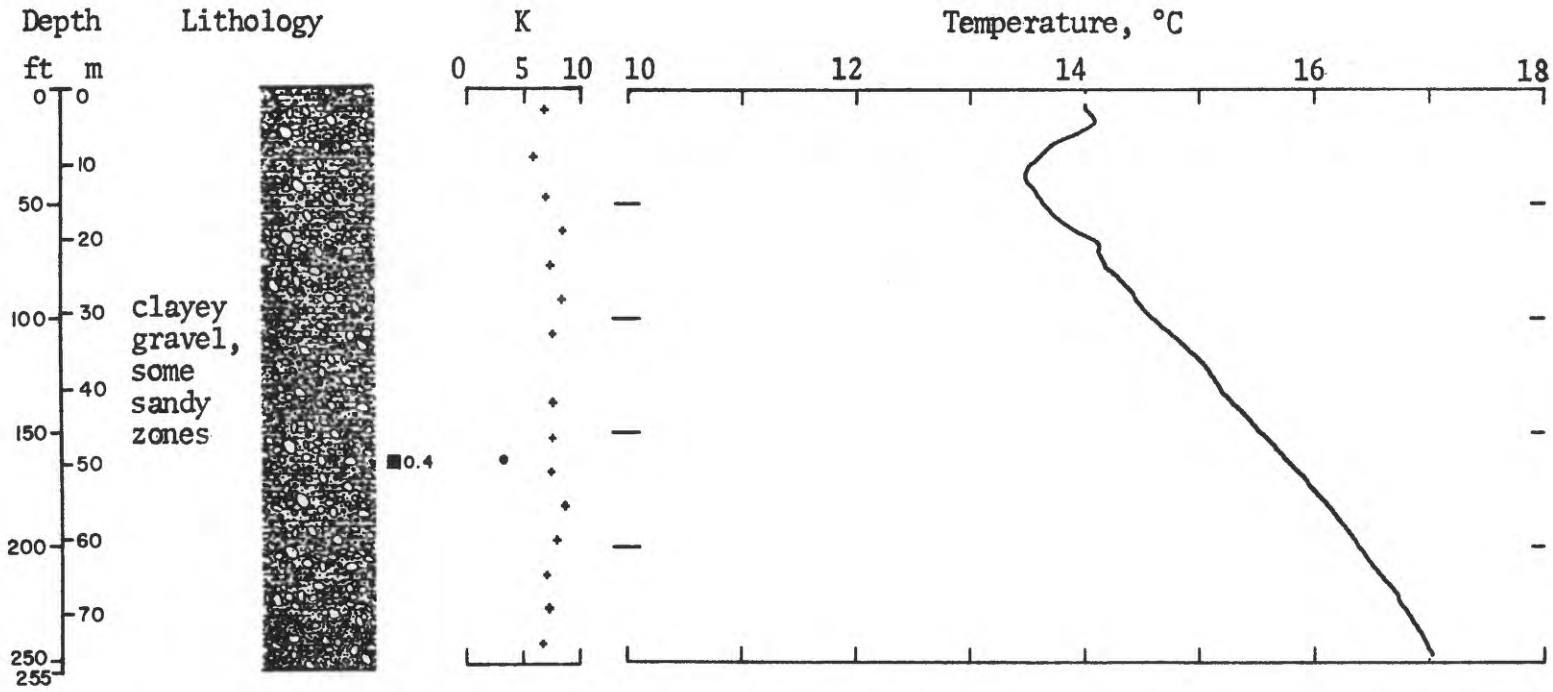

Figure A-24. Lithology, thermal conductivity, and temperature profile for hole QH-9.

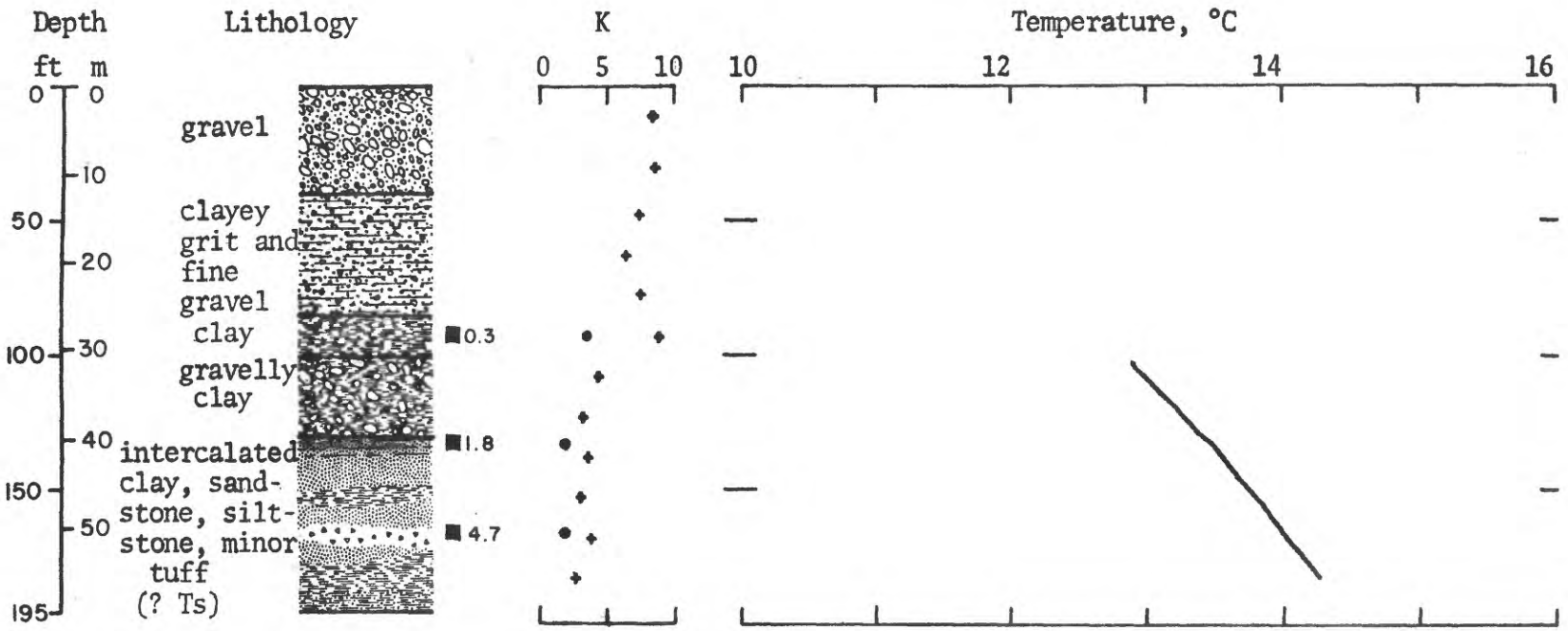

Figure A-25. Lithology, thermal conductivity, and temperature profile for hole QH-11.

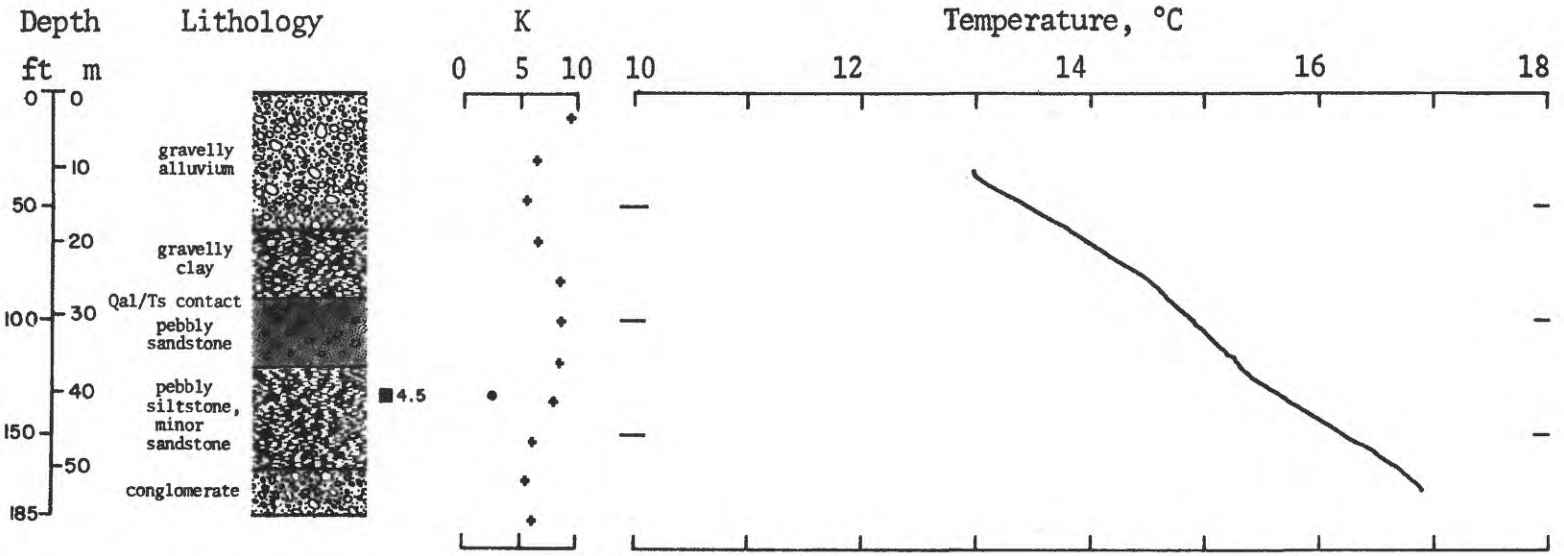

Figure A-26. Lithology, thermal conductivity, and temperature profile for hole QH-12.

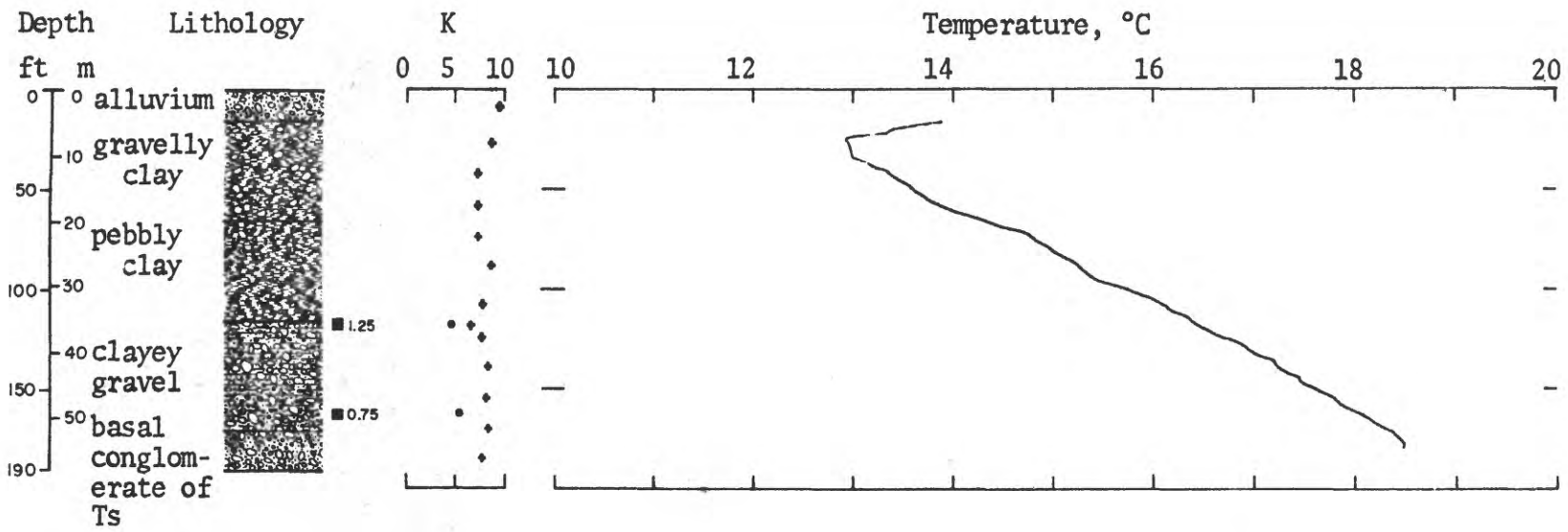

Figure A-27. Lithology, thermal conductivity, and temperature profile for hole QH-13.

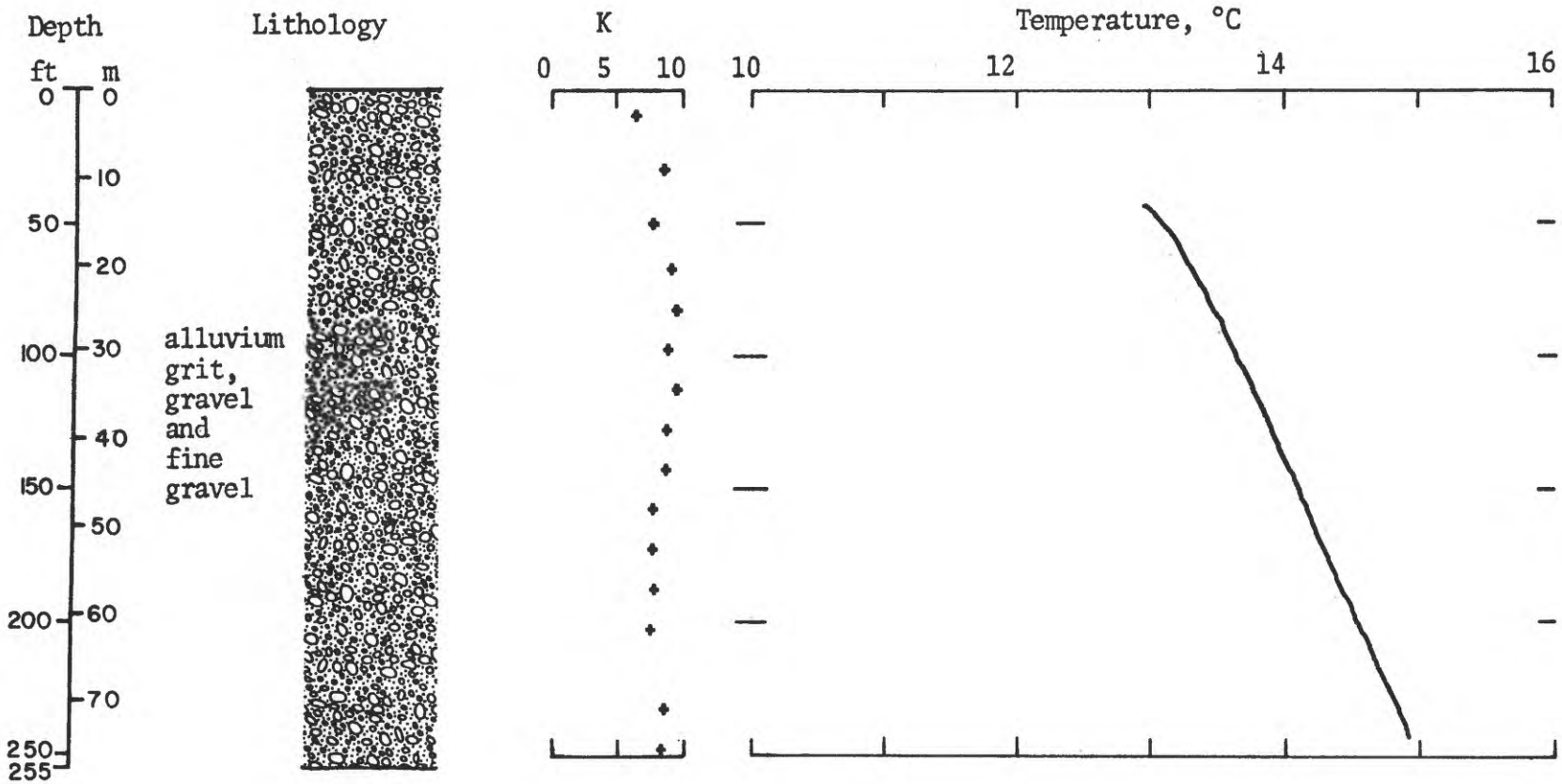

Figure A-28. Lithology, thermal conductivity, and temperature profile for hole QH-14.

APPENDIX B

Values of thermal conductivity of core obtained using the needle probe.

Individual determinations of thermal conductivity are listed (Table B-1) together with the harmonic mean for each core and a summary of the lithologic composition. Values with superscript "a" denote that the needle probe was emplaced along the axis of the core; all other values were obtained with the needle emplaced perpendicular to the axis.

Table B-1. Thermal conductivity and lithologic descriptions of cores, Leach Hot Springs area, Grass Valley, Nevada

Hole No.	Cored interval (m)	Sample depth (m)	Thermal conductivity mcal/cm sec °C		Lithology
			K	<K>	
Q-4	51.82 - 52.34	51.90	3.84		Yellowish-brown, poorly sorted clayey sandstone.
		51.99	3.78		
		52.06	3.87		
		52.12	3.93[a]		
		52.21	4.13		
		52.28	3.51[a]		
		52.28	3.28[a]		
		52.38	3.58		
		52.46	2.96		
		52.53	2.95[a]		
		52.65	2.87		
		52.79	3.74[a]		
				3.49	
				± .13	
Q-5	61.87 - 62.48	61.92	4.52		Coarse gravel and pebbles (sub-angular) in silty clayey matrix, poorly sorted.

	76.20 - 76.50	76.28	5.18		Poorly sorted gravelly, silty, buff-brown clay.
		76.30	2.87		
				3.69	
				±1.06	

Table B-1. Thermal conductivity and lithologic descriptions of cores, Leach Hot Springs area, Grass Valley, Nevada (continued)

Hole No.	Cored interval (m)	Sample depth (m)	Thermal conductivity mcal/cm sec °C		Lithology
			K	<K>	
Q-6	33.53 - 35.05	33.56	2.99		Large pebbles and cobbles (chert) with some gritty pebbly silty clay.
		33.59	7.87		
				4.33	
				±1.95	
	57.00 - 58.52	57.06	3.34		Very tight conglomerate.
		57.08	4.56		
		57.11	4.78[a]		
				4.12	
				± .49	
Q-7	32.92 - 34.14	33.02	2.93		Sandy clay and fine gravel.
		33.20	2.83		
		33.33	2.68[a]		
		33.43	4.41		
		33.52	3.87		
		33.69	4.40[a]		
				3.37	
				± .31	
	57.91 - 59.44	57.97	3.63		Sandy silty clay.
		58.02	3.81[a]		
		58.11	4.27		
		58.20	3.83[a]		
		58.35	5.06		

Table B-1. Thermal conductivity and lithologic descriptions of cores, Leach Hot Springs area, Grass Valley, Nevada (continued)

Hole No.	Cored interval (m)	Sample depth (m)	Thermal conductivity mcal/cm sec °C		Lithology
			K	<K>	
Q-7	57.91 - 59.44	58.51	4.30[a]		Sandy silty clay
		58.56	4.54		
		58.72	4.25		
				4.17	
				± .16	
Q-8	28.96 - 32.00	28.96	1.87[a]		Light bluish-grey tuff with clear flat glass shards -- stratified.
		29.05	1.84		
		29.16	2.04		
		29.21	2.01[a]		
		29.39	2.07		
		29.54	2.07[a]		
		29.54	1.50[a]		
		29.84	1.75		
		29.97	2.25		
		30.56	2.15[a]		
		30.73	2.15		
		30.84	2.34		
		31.03	1.42		
		31.17	1.92[a]		
		31.17	1.43[a]		

Table B-1. Thermal conductivity and lithologic descriptions of cores, Leach Hot Springs area, Grass Valley, Nevada (continued)

Hole No.	Cored interval (m)	Sample depth (m)	Thermal conductivity mcal/cm sec °C		Lithology
			K	<K>	
Q-8	28.96 - 32.00	31.36	1.84		Light bluish-grey tuff with clear flat glass shards -- stratified.
		31.48	1.61[a]		
				1.86	
				± .07	
	64.62 - 66.14	64.77	3.39		Yellowish-buff sandy,? tuffaceous clay, some quartz grains.
		64.85	3.10[a]		
		64.95	3.92		
		65.03	2.85		
		65.14	2.66		
		65.36	3.06[a]		
		65.47	3.24		
		65.65	3.23[a]		
		65.76	2.54		
		65.90	2.62[a]		
				3.01	
				± .13	
Q-9	32.61 - 33.53	32.72	6.14		Sandy clay and gravel.
		32.79	3.81		
		32.85	4.64		
				4.68	
				± .63	

Table B-1. Thermal conductivity and lithologic descriptions of cores, Leach Hot Springs area, Grass Valley, Nevada (continued)

Hole No.	Cored interval (m)	Sample depth (m)	Thermal conductivity mcal/cm sec °C		Lithology
			K	<K>	
Q-9	48.77 - 50.29	48.77	3.97		Silty gravel, gravel, sandy clay.
		48.83	3.27		
		48.95	3.42		
		49.24	3.39[a]		
				3.49	
				± .14	
Q-10	33.53 - 35.02	33.77	2.81		Reddish-brown clayey siltstone, very few pebbles.
		33.85	2.72[a]		
		33.85	2.66[a]		
		33.96	2.88		
		34.14	2.73[a]		
		34.20	2.90		
		34.33	3.28		
		34.47	3.36[a]		
				2.90	
				± .09	
	48.77 - 50.29	49.01	4.27		Sandy claystone.
		49.10	3.92[a]		
				4.09	
				± .18	

Table B-1. Thermal conductivity and lithologic descriptions of cores, Leach Hot Springs area, Grass Valley, Nevada (continued)

Hole No.	Cored interval (m)	Sample depth (m)	Thermal conductivity mcal/cm sec °C		Lithology
			K	<K>	
Q-11	76.20 - 77.72	76.37	3.96		Clay and sandy clay with gravel.
		76.44	5.93		
		76.54	5.12		
				4.87	
				± .59	
Q-12	46.33 - 47.85	46.37	3.07		Grit, clay, angular gravel.
		46.42	3.78		
		46.57	5.12		
		46.67	5.07		
		46.85	4.83		
		46.88	5.67		
				4.39	
				± .45	
	57.91 - 59.44	58.02	2.92		Gritty, sandy clay.
		58.12	3.42[a]		
		58.18	3.84		
				3.35	
				± .27	

Table B-1. Thermal conductivity and lithologic descriptions of cores, Leach Hot Springs area, Grass Valley, Nevada (continued)

Hole No.	Cored interval (m)	Sample depth (m)	Thermal conductivity mcal/cm sec °C		Lithology
			K	<K>	
Q-13	85.34 - 86.87	85.40	3.66		Gravelly clay.
		85.57	3.54		
		85.66	3.89[a]		
		85.73	4.60		
		85.82	5.41[a]		
		85.86	4.94		
		85.96	5.52		
				4.38	
				± .31	
Q-14	29.26 - 30.78	29.33	4.08		Gravelly, gritty, clayey.
		29.37	6.24[a]		
				4.93	
				±1.03	
	46.63 - 47.55	46.66	5.21		Gravelly, sandy clay.

Q-15	28.96 - 30.48	28.96	2.26[a]		Clay.
		29.01	2.41		
		29.09	2.47		
		29.10	2.57[a]		
		29.15	1.90[a]		
		29.20	4.23		
		29.25	2.44		

Table B-1. Thermal conductivity and lithologic descriptions of cores, Leach Hot Springs area, Grass Valley, Nevada (continued)

Hole No.	Cored interval (m)	Sample depth (m)	Thermal conductivity mcal/cm sec °C		Lithology
			K	<K>	
Q-15	28.96 - 30.48	29.30	2.34		Clay
		29.34	2.41		
		29.37	1.86[a]		
		29.42	2.54		
		29.50	2.67		
		29.53	2.46[a]		
		29.53	2.45[a]		
		29.57	3.15		
		29.62	2.46		
		29.69	2.33		
				2.58 ± .09	
	42.67 - 44.20	42.86	3.14[a]		White siliceous tuff.
		42.91	2.99		
		43.00	2.75[a]		
		43.08	3.10		
		43.13	3.09		
		43.66	2.98		
		43.70	2.77		
				2.97 ± .06	

Table B-1. Thermal conductivity and lithologic descriptions of cores, Leach Hot Springs area, Grass Valley, Nevada (continued)

Hole No.	Cored interval (m)	Sample depth (m)	Thermal conductivity mcal/cm sec °C		Lithology
			K	<K>	
Q-16	48.77 - 50.29	48.33	3.10		Clayey silt with pebbles and gravel
		48.33	3.63		
		48.85	2.50		
		48.87	2.69		
		48.87	3.63		
		48.87	3.92		
				3.16	
				± .24	
	66.45 - 67.97	66.47	4.43		Well-sorted, medium-grained, moderately rounded sand (lithic fragments predominant).
		66.50	3.03		
		66.57	2.78[a]		
		66.57	4.74		
		66.60	3.64		
				3.57	
				± .37	
	75.29 - 76.81	75.35	4.72		0.5' gritty clay with pebbles -- remainder gravel with no matrix.
		75.36	4.27		
		75.41	4.64		
		75.46	4.21[a]		
		75.54	5.01		
		75.56	4.54		

Table B-1. Thermal conductivity and lithologic descriptions of cores, Leach Hot Springs area, Grass Valley, Nevada (continued)

Hole No.	Cored interval (m)	Sample depth (m)	Thermal conductivity mcal/cm sec °C		Lithology
			K	<K>	
Q-16	75.29 - 76.81	75.56	5.22		0.5' gritty clay with pebbles -- remainder gravel with no matrix.
				4.63	
				± .14	
Q-17	33.53 - 35.05	33.63	3.55		Brown clay with sand and pebbles.
		33.70	3.48		
		33.71	4.39		
		33.85	5.29		
				4.06	
				± .39	
	65.53 - 67.06	65.59	4.61		Gravelly, cobbly, clay

Q-18	28.35 - 29.87	28.46	3.30		Brown clayey sand
		28.62	4.38		
		28.69	4.04[a]		
		28.73	3.99		
				3.89	
				± .24	

Table B-1. Thermal conductivity and lithologic descriptions of cores, Leach Hot Springs area, Grass Valley, Nevada (continued)

Hole No.	Cored interval (m)	Sample depth (m)	Thermal conductivity mcal/cm sec °C		Lithology
			K	<K>	
Q-18	54.86 - 56.39	54.93	3.95		Brown, sandy clay
		54.93	4.17		
		55.01	3.76		
		55.07	4.32		
		55.11	4.47		
				4.12	
				± .13	
Q-19	24.38 - 25.91	24.38	3.57[a]		Clay with fine to medium gravel.
		24.51	4.39		
		24.62	4.70[a]		
		24.72	3.95		
		24.82	2.89[a]		
		24.91	3.00		
		25.07	3.91		
		25.26	5.19		
		25.37	3.54[a]		
		25.45	5.74		
		25.50	5.79[a]		
				4.03	
				± .29	

Table B-1. Thermal conductivity and lithologic descriptions of cores, Leach Hot Springs area, Grass Valley, Nevada (continued)

Hole No.	Cored interval (m)	Sample depth (m)	Thermal conductivity mcal/cm sec °C		Lithology
			K	<K>	
Q-21	24.69 - 25.91	24.77	4.09		Silty sandstone, abundant pebbles.
		24.86	6.14		
		25.01	4.16		
				4.63	
				± .57	
Q-22	24.38 - 25.91	24.46	3.15		Brown silty clay, scattered pebbles.
		24.55	3.44		
		24.63	3.11[a]		
		24.68	3.70		
		24.88	3.64		
		24.98	3.51[a]		
				3.41	
				± .10	
QH-6	27.43 - 28.96	27.43	3.10[a]		Brown, sandy, silty clay.
		27.54	3.53		
		27.70	4.19		
		27.79	3.75[a]		
		27.79	4.54[a]		
		27.91	4.77		

Table B-1. Thermal conductivity and lithologic descriptions of cores, Leach Hot Springs area, Grass Valley, Nevada (continued)

Hole No.	Cored interval (m)	Sample depth (m)	Thermal conductivity mcal/cm sec °C		Lithology
			K	<K>	
QH-6	27.43 - 28.96	28.07	4.02[a]		Brown, sandy, silty clay.
		28.13	4.73		
		28.19	5.10		
		28.40	4.58[a]		
		28.40	5.29[a]		
		28.50	4.00		
		28.61	3.65[a]		
				4.16	
				± .19	
	41.15 - 42.67	41.21	3.22		Sandy clay with fine gravel.
		41.26	3.75		
		41.35	4.57		
		41.39	4.14		
		41.44	4.19		
				3.92	
				± .24	
QH-7	34.44 - 35.97	34.55	2.97		Clay, fine-grained sand.
		34.82	2.89[a]		
		34.93	3.16		
		35.03	3.04[a]		
		35.08	4.39		

Table B-1. Thermal conductivity and lithologic descriptions of cores, Leach Hot Springs area, Grass Valley, Nevada (continued)

Hole No.	Cored interval (m)	Sample depth (m)	Thermal conductivity mcal/cm sec °C		Lithology
			K	<K>	
QH-7	34.44 - 35.97	35.21	3.95		Clay, fine-grained sand.
		35.31	4.66[a]		
		35.37	3.38		
		35.55	3.27[a]		
				3.43	
				± .19	
	60.96 - 62.48	61.06	3.02		Clay with coarse sand.
		61.26	2.73[a]		
		61.37	3.02		
		61.57	2.82[a]		
		61.68	2.83		
		61.93	2.68[a]		
		62.04	3.72		
		62.22	3.47		
		62.31	3.73		
				3.07	
				± .13	

Table B-1. Thermal conductivity and lithologic descriptions of cores, Leach Hot Springs area, Grass Valley, Nevada (continued)

Hole No.	Cored interval (m)	Sample depth (m)	Thermal conductivity mcal/cm sec °C		Lithology
			K	<K>	
QH-8	34.44 - 35.97	34.54	3.68		Medium-brown pebbly clay, sub-angular fragments of greenstone.
		34.62	4.23[a]		
		34.62	3.26[a]		
		34.81	4.19		
		34.90	2.80		
		35.08	2.83[a]		
		35.08	2.83[a]		
		35.17	3.48		
		35.28	3.50[a]		
				3.35	
				± .18	
	44.20 - 45.72	44.25	3.13		Brown clay with pebbles and gravel.
		44.32	3.08		
		44.44	2.71[a]		
		44.50	3.00		
		44.63	2.98		
		44.77	2.24[a]		
		44.77	2.74[a]		
		44.92	3.07		
		45.02	3.01[a]		
		45.08	3.00		

Table B-1. Thermal conductivity and lithologic descriptions of cores, Leach Hot Springs area, Grass Valley, Nevada (continued)

Hole No.	Cored interval (m)	Sample depth (m)	Thermal conductivity mcal/cm sec °C		Lithology
			K	<K>	
QH-8	44.20 - 45.72	45.21	3.32		Brown clay with pebbles and gravel.
		45.36	2.80[a]		
				2.90	
				± .09	
QH-9	48.77 - 50.29	48.77	3.22[a]		Brown gritty clay with pebbles and gravel.
		48.79	3.89		
		48.83	3.47		
				3.51	
				± .19	
QH-11	27.43 - 28.96	27.46	3.42		Mostly gravel, very wet and soft
		27.52	4.45		
				3.87	
				± .51	
	39.62 - 41.15	39.62	2.40[a]		Brown and bluish gray layered clayey sand.
		39.70	2.56		
		39.77	2.25[a]		
		39.98	2.16[a]		
		40.08	2.30		
		40.17	2.21[a]		
				2.31	
				± .06	

Table B-1. Thermal conductivity and lithologic descriptions of cores, Leach Hot Springs area, Grass Valley, Nevada (continued)

Hole No.	Cored interval (m)	Sample depth (m)	Thermal conductivity mcal/cm sec °C		Lithology
			K	<K>	
QH-11	49.68 - 51.21	49.77	2.54		Brown clay
		49.91	2.52		
		50.02	2.26		
		50.15	2.55		
		50.25	2.35[a]		
		50.35	2.28		
		50.45	2.58		
		50.63	2.33[a]		
		50.75	2.46		
		50.87	2.56		
		51.02	2.23		
		51.08	2.23[a]		
		51.08	2.36		
		51.16	2.60		
				2.46 ± .07	
QH-12	39.62 - 41.15	39.67	2.26		Fine sandstone, pebbles, brown siltstone.
		39.79	2.46		
		39.95	3.39[a]		
		40.08	2.25		
		40.13	2.85		
		40.26	3.48[a]		

Table B-1. Thermal conductivity and lithologic descriptions of cores, Leach Hot Springs area, Grass Valley, Nevada (continued)

Hole No.	Cored interval (m)	Sample depth (m)	Thermal conductivity mcal/cm sec °C		Lithology
			K	<K>	
QH-12	39.62 - 41.15	40.28	3.76		Fine sandstone, pebbles, brown siltstone.
		40.51	2.81		
		40.61	2.69[a]		
		40.64	2.81		
		40.76	2.91		
		40.84	2.63[a]		
		40.89	2.83		
		41.02	2.54[a]		
				2.77 ± .11	
QH-13	35.05 - 36.58	35.11	4.88		Reddish-brown claystone with abundant angular rock fragments.
		35.19	3.51		
		35.34	4.28		
		34.44	5.79[a]		
				4.46 ± .47	
	48.77 - 50.29	48.82	5.31		Brown silty clay with abundant angular pebbles.
		48.94	6.37		
		49.02	4.09		
				5.09 ± .66	

[a]Conductivity measured with probe along axis of core.

APPENDIX C

Heat-flow calculations, Q and QH holes.

Heat flows were calculated over the depth intervals indicated (Table C-1) by multiplying the interval temperature gradients by the appropriate thermal conductivities. The basic data for holes Q-1 through Q-3 and QH-1 through QH-4 were presented by Sass and others (1976). Basic data for the other holes are graphed and tabulated in Appendices A and B.

For the 1976 work, heat flows were calculated using both needle probe and chip conductivities. For the former, the gradient over ∿3 meters centered on the core was calculated and combined with the harmonic mean conductivity K_1 to calculate q_1 (Table C-1). The harmonic mean chip conductivity K_2 calculated assuming a porosity of 40%, see discussion of conductivity and porosity above) over linear sections of the temperature profiles was combined with the least-squares temperature gradient to determine q_2 (Table C-1). The value adopted for a given hole (q_3, Table C-1) was usually the rounded mean of all the determinations, but in some instances, one or more of the individual estimates was excluded from the mean. This was most often done because of an obvious disturbance (usually hydrologic) to the temperature profile. Values of q_3 flagged with superscript "c" are from holes in which convective disturbances have been inferred from curvature or abrupt irregularities in the temperature profile.

Table C-1. Calculations of heat flow for Q and QH holes, Grass Valley, Nevada

Hole	Depth interval (m)	Gradient (°C/km)	N*	Conductivity† (mcal/cm sec °C)		Heat flow†† (μcal/cm² sec)		
				K_1	K_2	q_1	q_2	q_3
Q-1	50 - 200	65.5	12	3.42		2.24		2.2
Q-2	50 - 160	55.5	10	3.68		2.04		2.0
Q-3	50 - 170	120	16	4.06		4.87		4.9
Q-4	15 - 53	57.1	7	4.09			2.33	
	53 - 65	32.8	3	3.39			1.11	
	51.8 - 53.3	50.9	12	3.49		1.77		
								2±[c]
Q-5	38 - 107	40.8	18		4.04		1.65	
	61.9 - 62.5	33.2	1	4.52		1.5		
	76.2 - 77.7	35.2	2	3.69		1.3		
								1.6
Q-6	12 - 27	90.2	3		4.30		3.9	
	30 - 53	48.6	6		4.05		2.0	
	33.5 - 35.1	61.3	2	4.33		2.66		
	57.0 - 58.5	29.5	3	4.12		1.21		
								3±[c]
Q-7	24 - 73	33.7	12		3.76		1.27	
	32.9 - 34.1	45.4	6	3.37		1.53		
	57.9 - 59.4	36.8	8	4.17		1.53		
								1.5
Q-8	17 - 38	139.2	4		2.83		3.94	
	46 - 66	61.6	5		4.09		2.52	
	29.0 - 30.5	152.1	9	1.91		2.91		
	30.5 - 32.0	143.4	8	1.80		2.58		
	64.6 - 66.1	22.6	10	3.01		0.68		
								3±[c]
Q-9	27 - 55	32.6	8		4.54		1.48	
	32.6 - 33.5	39.2	3	4.68		1.83		
	48.8 - 50.3	26.0	4	3.49		.91		
								1.5
Q-10	15 - 30	38.3	4		4.36		1.67	
	30 - 52	48.3	4		3.76		1.81	
	33.5 - 35.1	42.2	8	2.90		1.22		
	48.8 - 50.3	48.5	2	4.09		1.98		
								1.7
Q-11	46 - 78	37.08	8		4.21		1.56	
	76.2 - 77.7	34.66	3	4.87		1.69		
								1.6

Table C-1. Calculations of heat flow for Q and QH holes, Grass Valley, Nevada (continued)

Hole	Depth interval (m)	Gradient (°C/km)	N*	Conductivity† (mcal/cm sec °C)		Heat flow†† (μcal/cm²sec)		
				K_1	K_2	q_1	q_2	q_3
Q-12	35 - 62	44.5	7		3.74		1.67	
	46.3 - 47.8	38.2	6	4.39		1.68		
	57.9 - 59.4	41.9	3	3.35	1.40			
								1.7
Q-13	30 - 91	40.0	12		4.43		1.77	
	85.3 - 86.9	56.9	7	4.38		2.49		
								1.8[C]
Q-14	47 - 116	22.4	19		4.52		1.01	
	29.3 - 30.5	40.0	2	4.93		1.97		
	46.6 - 47.5	35.3	1	5.21		1.84		1.5±
Q-15	18 - 43	94.8	6		3.07		2.91	
	28.9 - 30.5	91.4	17	2.45		2.24		
	42.7 - 44.2	126.2	7	2.97		3.75		
								3.0[C]
Q-16	23 - 81	82.4	13		3.89		3.21	
	48.8 - 50.3	75.7	6	3.16		2.39		
	66.4 - 68.0	81.7	5	3.57		2.92		
	75.3 - 76.8	80.0	7	4.63		3.70		
								3.0
Q-17	15 - 41	174.7	5		3.79		6.62	
	44 - 75	134.4	8		4.30		5.78	
	33.5 - 35.0	174.0	4	4.06		7.06		
	65.5 - 67.0	135.3	1	4.61		6.24		
								6.5
Q-18	14 - 23	98.4	2		3.12		3.07	
	38 - 53	71.0	8		3.39		2.41	
	28.3 - 29.9	59.6	4	3.89		2.32		
	54.9 - 56.4	68.9	5	4.12		2.84		
								2.7
Q-19	13 - 27	67.2	3		3.61		2.42	
	32 - 55	45.2	6		3.50		1.58	
	24.4 - 25.9	56.2	11	4.03		2.27		
								2.3
Q-20	12 - 30	72.2	5		4.56		3.29	
	30 - 69	43.0	9		4.49		1.93	
								2.5
Q-21	18 - 61	36.4	11		4.31		1.57	
	24.7 - 25.9	38.4	3	4.63		1.78		
								1.7

Table C-1. Calculations of heat flow for Q and QH holes, Grass Valley, Nevada (continued)

Hole	Depth interval (m)	Gradient (°C/km)	N*	Conductivity† (mcal/cm sec °C)		Heat flow†† (μcal/cm²sec)		
				K_1	K_2	q_1	q_2	q_3
Q-22	12 - 24	33.6	4		3.50		1.18	
	27 - 49	20.0	5		4.27		0.84	
	24.4 - 25.9	25.9	6		3.41	0.86		
								1.0
QH-1	80 - 155	224	12	4.03		9.03		9.0
QH-2	25 - 130	52	17	2.88		1.50		1.5
QH-3	80 - 155	118	9	4.33		5.11		5.1
QH-4	125 - 155	42	11	3.25		1.36		1.4
QH-5	55 - 85	44	7	3.89			1.71	
	85 - 128	30.7	9	4.57			1.40	
								1.6
QH-6	15 - 50	51.4	7		4.15		2.13	
	27.4 - 29.0	47.1	13	4.16		1.96		
	41.1 - 42.7	54.3	5	3.92		2.13		
								2.1
QH-7	15 - 30	98.4	3		3.23		3.18	
	30 - 73	45.4	6		3.74		1.70	
	34.4 - 36.0	48.2	9	3.43		1.65		
	61.0 - 62.5	45.8	9	3.07		1.41		
								1.6
QH-8	19 - 49	66.2	6		3.48		2.30	
	34.4 - 36.0	54.2	9	3.35		1.82		
	42.7 - 44.2	68.5	12	2.90		1.98		
								2.0
QH-9	30 - 75	55.8	9		3.98		2.22	
	48.8 - 50.3	62.6	3	3.51		2.20		
								2.2
QH-11	29 - 55	42.0	6		2.86		1.20	
	27.4 - 29.0	35.7	2	3.87		1.38		
	39.6 - 41.1	63.1	6	2.31		1.46		
	49.7 - 51.2	48.4	14	2.41		1.17		
								1.3
QH-12	12 - 26	109.4	4		3.73		4.08	
	26 - 38	71.0	7		4.27		3.03	
	38 - 52	105.3	3		3.50		3.68	
	39.6 - 41.1	102.4	14	2.77		2.84		
								3.5

Table C-1. Calculations of heat flow for Q and QH holes, Grass Valley, Nevada (continued)

Hole	Depth interval (m)	Gradient (°C/km)	N*	Conductivity† (mcal/cm sec °C)		Heat flow†† (μcal/cm²sec)		
				K_1	K_2	q_1	q_2	q_3
QH-13	30 - 50	120.0	5		3.90		4.67	
	35.1 - 36.6	125.0	4	4.46		5.57		
	48.8 - 50.3	120.0	3	5.09		6.10		
								5.5
QH-14	23 - 73	29.6	10		3.92		1.16	
								1.20

APPENDIX D

The relation between T_{15_m} and heat flow for Q and QH holes

In an attempt to calculate representative heat flows for the T holes, numerous approaches and associated statistical schemes were tried. The criteria finally adopted were:

1) forcing the data to fit a linear function between heat flow and T_{15_m}. This theoretically should be the case, but statistically does not always represent the function that best fits the data.

2) selecting groups of holes that were not obviously disturbed by water flow for each regional analysis rather than all the holes within the region.

This appendix presents plots of heat flow versus temperature at 15 meters using Q and QH holes in three regions (Figures D-1, D-2, and D-3) along with their calculated linear least-squares fits and the 95% confidence bands (dashed lines). The confidence bands for three Q-18 regions (Figure D-1) are too large to be shown on the graph (because only three points were used in the calculation). Obviously some subjectivity is involved in this approach and we emphasize that the "T" heat flows were only used to help fill in the details of the heat-flow picture and should not be assigned the same status as values obtained from deeper holes.

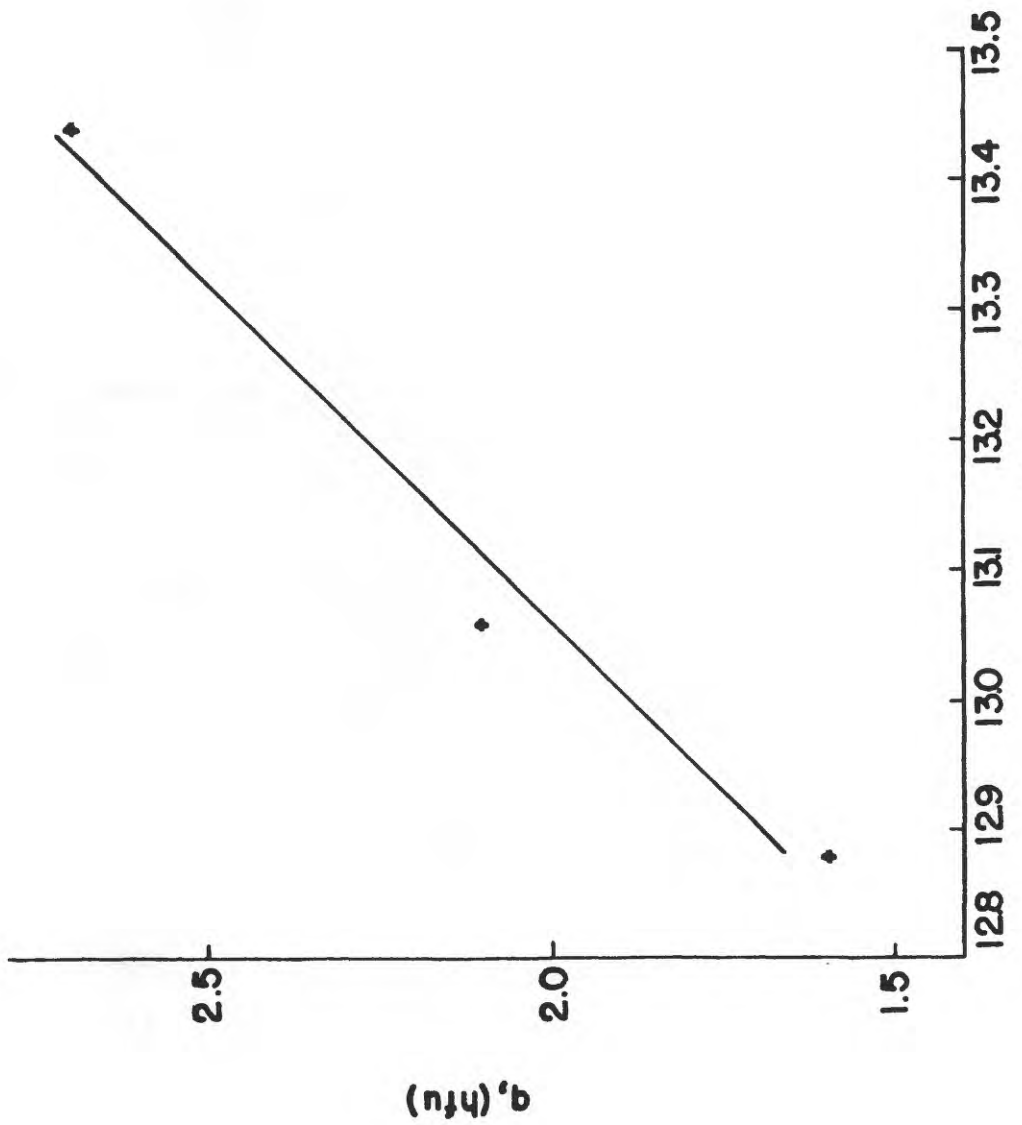

Figure D-1. Heat flow versus temperature at 15 meters for Q and QH holes in the vicinity of Q-18 (Figure 2).

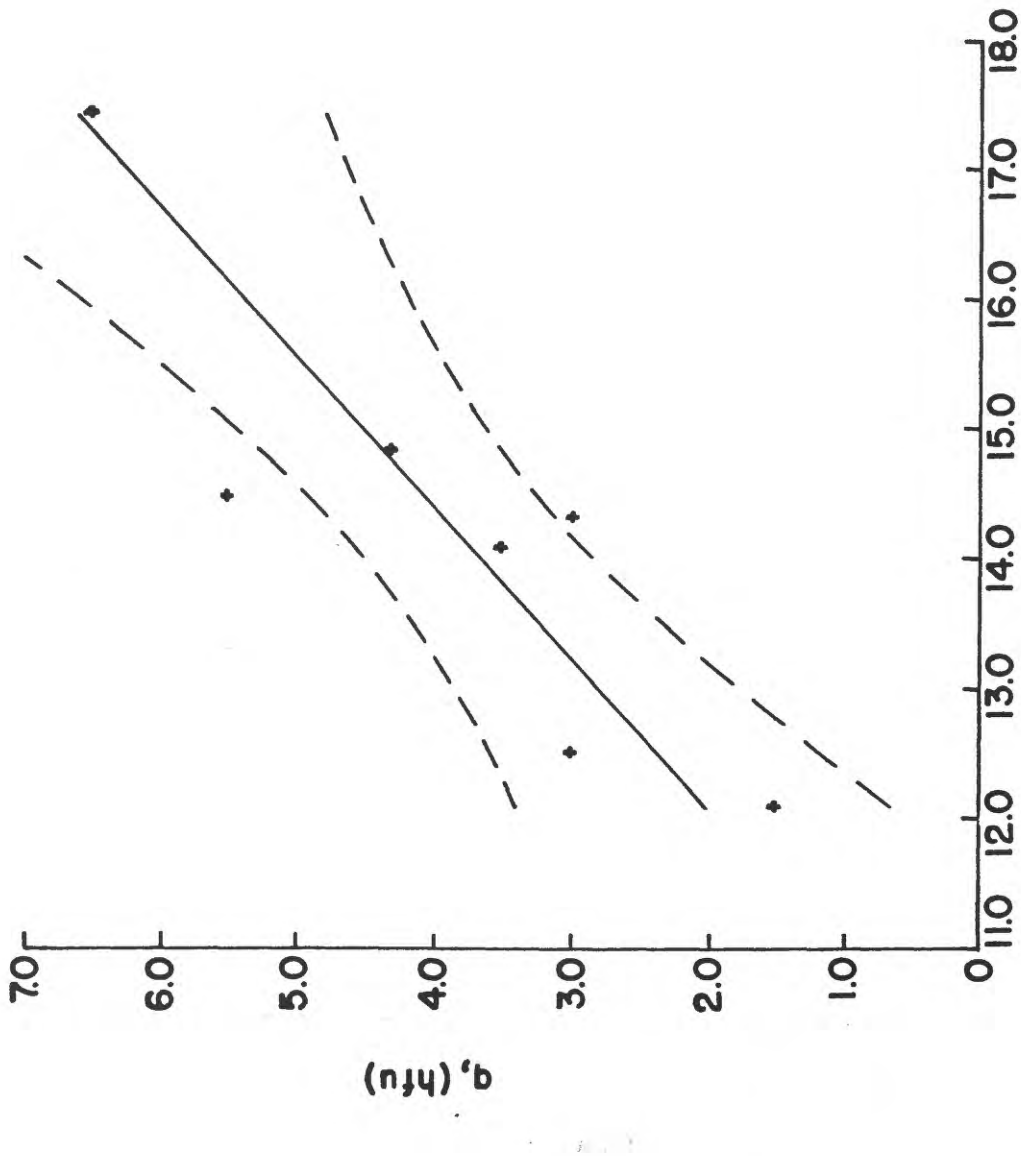

Figure D-2. Heat flow versus temperature at 15 meters for Q and QH holes in the vicinity of QH-3 (Figure 2). Dashed curves enclose the 95% confidence band.

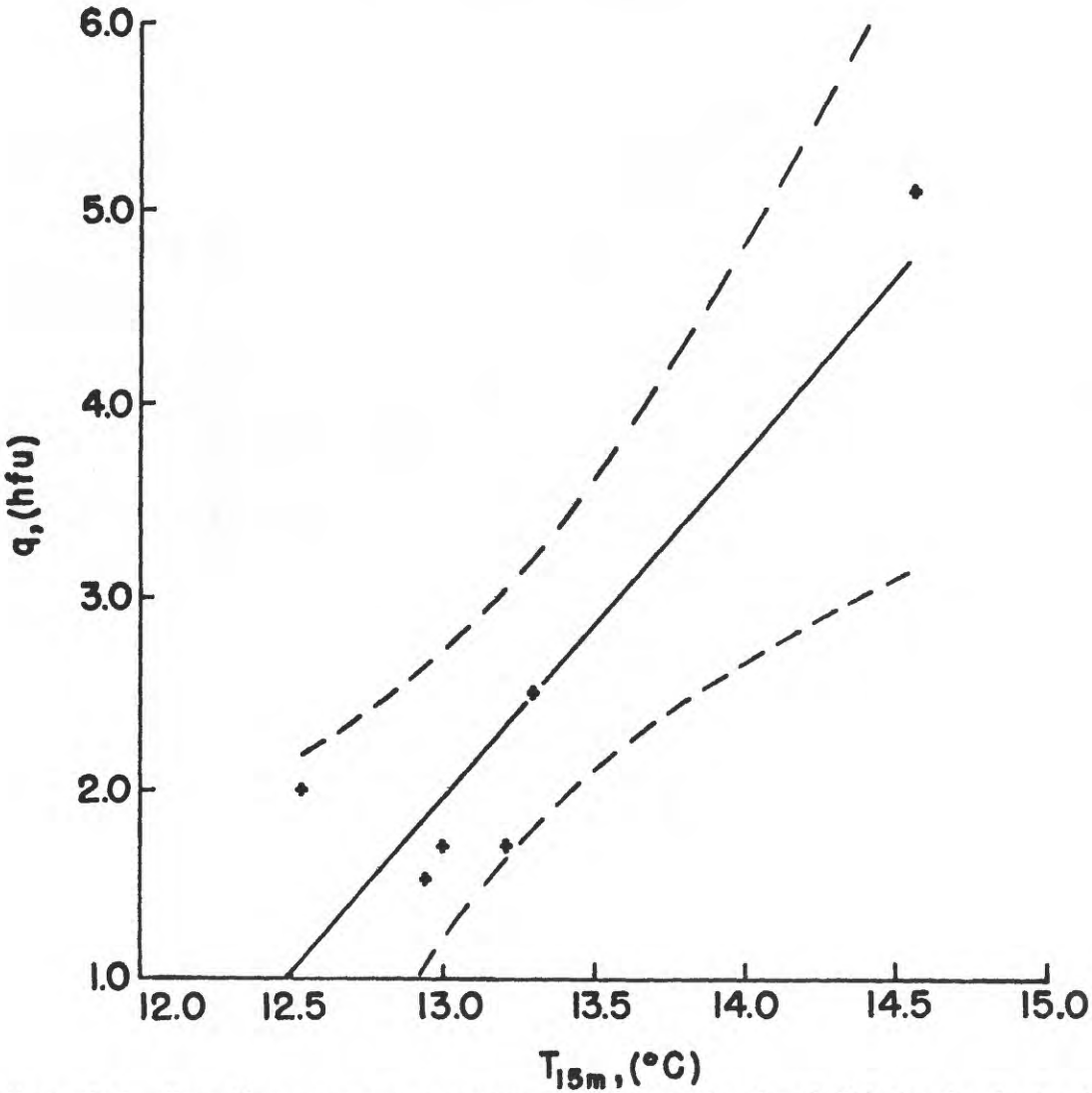

Figure D-3. Heat flow versus temperature at 15 meters for Q and QH holes in the Panther Canyon area (Figure 2). Dashed curves enclose the 95% confidence band.

APPENDIX E

Contouring software

Contour plots appearing in Figures 7, 22, 25, 26, 28, and 29 were made using the California Computer Products (CalComp) General Purpose Contour Program (GPCP).

The program is divided into three parts:

1) Gradient (tangent plane) generation,

2) Grid value generation,

3) Contour generation.

In part 1) a tangent plane is calculated at each randomly spaced data point that must satisfy these requirements:

1) The plane must pass through the data at each point, and

2) The angles this plane makes with vectors to all of the various neighborhood points must be minimized.

Grid value generation (part 2) begins by selecting the n neighboring data points closest to the grid value in question. The program assigns weights to the data points on the basis of the distance from the grid value and then proceeds to calculate the grid value. This process is repeated for all the grid values.

Finally, in part 3, GPCP uses this discrete surface to generate the contour lines.

The variable that influences the final contour map most is the number of neighboring points used to construct the grid and tangent surface. Generally, the larger the number of neighboring points used in gridding, the smoother the contour features; few points produce a contour

map emphasizing local features. For all contour maps but one (Figure 25) 10 points were used to construct each grid element. Figure 25 includes the heat-flow data from the T holes as well as the H, Q, and QH holes. As the T holes tend to be clustered around the Q or QH holes, the number of neighboring points used in the first two parts of the program were reduced from 10 to 5 to highlight the local effects of the "T" data points.